THE ROLE OF VAB-3 IN THE CAENORHABDITIS ELEGANS OXIDATIVE STRESS RESPONSE

JOONYEOB YEO

A THESIS SUBMITTED TO
THE FACULTY OF GRADUATE STUDIES
IN PARTIAL FULFILLMENT OF THE REQUIREMENTS
FOR THE DEGREE OF
MASTER OF SCIENCE

GRADUATE PROGRAM IN BIOLOGY
YORK UNIVERSITY
TORONTO, ONTARIO

DECEMBER 2020

Abstract

The oxidative stress response protects the cell by balancing the number of free radicals inside the cell. BRAP2 is a Ras effector with ubiquitin ligase activity and conserved in *C. elegans*. Our lab has previously shown that *C. elegans* BRAP-2 is a negative regulator of SKN-1/Nrf2 that activates ROS detoxifying enzymes, and *vab-3/PAX6* RNAi induction in *brap-2* mutants reduced basal expression levels of *gst-4*. Based on the link between SKN-1 and BRAP-2, I examined the role of VAB-3 in the oxidative stress response. I found that a loss of *vab-3* caused decreased basal expression levels of *gst-4* in *brap-2; vab-3* double mutants, decreased expression levels of *gst-4, sdz-8, ugt-13* and *ctl-1* and increased mortality rates toward oxidative stress in *C. elegans*. Moreover, I found that VAB-3 together with SKN-1 synergistically enhanced activities of *gst-4* and *skn-1c* promoters. Thus, VAB-3 contributes to the oxidative stress response through the SKN-1/Nrf2 pathway.

Acknowledgement

First and foremost, I would like to thank my supervisor, Dr. Kubiseski. The opportunity and guide that you provided to me helped me a lot to understand what real research is. I am very grateful for your dedication to my project. Through the project, I have gained valuable research experience and skills. I am and will always be proud of the fact that I was a part of your lab.

Next, I would like to thank my advisor, Dr. Rosonina. I am very grateful that you spent time helping me on how to train myself to be a good scientific writer and presenter. Both your class and progress meetings gave me exceptional knowledge and tips on being an effective writer and presenter.

I also would like to thank other people who have made my graduate school experience enjoyable:

Vu: You are a great teacher and exceptional researcher. I have learned a lot from you. Thank you for giving me all the great advice and tips.

Mohamed: I learned all the important laboratory knowledge and skills from you. Up to these days, I use what I learned from you. So, thank you so much for everything you shared with me.

Marjan: Thank you for giving me tips on lab work. You always provided me possible answers that I could try to solve problems. Additionally, I will never forget the fun we had whenever we talk about politics. You made my graduate school experience fun.

Farnaz: Thank you for giving me tips on lab work. You always provided me possible answers that I could try to solve problems. I will never forget the nights that we were the only people left in the LSB. You are a very hardworking and dedicated researcher. I really respect that.

Gaby, Vikki, Helen, Anna, Cindy, David, Nick, Vijay, and Kyra: Thank you guys for the fun times, and helping me whenever I needed help, and for being fantastic friends.

Lastly, I would like to express my gratitude to my family: Thank you for giving me all the support during my school years. I will always be grateful for what you have done for me.

Table of Contents

List of Tables

List of Figures

List of Mammalian Homologs of *C. elegans*. The *C. elegans* genes and its counterparts in vertebrates used and investigated in this work. A major source of references for *C. elegans* genomic information is Wormbase which is cited in this paper accordingly.

C. elegans (N2- Wild Type) gene name	Mammalian	Function/ Expression in *C. elegans*
act-1	Actin Beta **(ACTB)**	Animal motility, body wall and pharyngeal muscle
age-1	Phosphatidylinositol-4,5-bisphosphate 3-kinase catalytic subunit alpha **(PIK33CA)**	Involved in development, dauer and longevity
akt-1/2	Serine/threonine kinase **(AKT1/2)**	Involved in cellular protein modification process, insulin receptor signaling pathway and intrinsic apoptotic signaling pathway.
brap-2	Brca1 associated protein 2 **(BRAP2)**	A *brap-2* gene mutated worm is vulnerable to oxidative stress
cdc-42	Cell Division Cycle 42 **(CDC42)**.	A positive regulator of male tail tip morphogenesis.
ctl-1/2	Catalase **(CAT1)**	Antioxidant enzyme that protects against ROS. Activity contributes to lifespan extension. Negatively regulated by IIS pathway.
daf-2	Insulin like growth factor 1 receptor **(IGF1R)**	Receptor tyrosine kinase. Involved in development, dauer, longevity, reproduction, and fat storage.
daf-16	Forkhead box O1 **(FOXO)**	Transcription factor that is negatively regulated by IIS. Regulates dauer, longevity, stress responses and metabolism.
daf-18	Phosphatase and tensin homolog **(PTEN)**	Involved in longevity, dauer, larval development and importing proteins into nucleus.

dhs-8	WW domain containing oxidoreductase **(WWOX)**	Antioxidant enzyme that protects against ROS.
gst-4	Glutathione-S-transferase **(GST)**	Catalyzes redox reactions to neutralize free radical oxygen species
gsto-2	Glutathione-S-transferase omega 1/2 **(GSTO1/2)**	Catalyzes redox reactions to detoxify xenobiotics
him-5	N/A	Involved in X chromosome segregation
ksr-1/2	Kinase suppressor of Ras **(KSR)**	A positive modifier of vulva induction
let-60	Ras protooncogene family **(RAS)**	A GTP-binding Ras proto-oncogene family member
lin-45	A-Raf proto-oncogene, serine/threonine kinase **(ARAF)**	Ras GTPase binding proteins. Involved in defense response against Gram-positive bacterium, signal transduction and vulval development.
mek-1/2	MAP kinase kinase **(MKK7)**	Phosphorylates downstream factors during the Ras signal pathway
mpk-1	Extracellular signal-regulated kinases **(ERK)**	MAP kinase involved in several cellular processes including cell migration, immunity, vulva development and germline progression for oogenesis.
nsy-1	Mitogen-activated protein kinase kinase kinase 15 **(MAP3K15)**	Involved in defense response against other organism, p38MAPK cascade and MAP kinase activity.
pdk-1	3-phosphoinositide dependent protein kinase 1 **(PDPK1)**	Involved in dauer larval development and regulation of synaptic growth at neuromuscular junction.

pmk-1	p38 Kinase **(MAPK)**	Phosphorylate SKN-1 and induces nuclear localization for SKN-1
sdz-8	Carbonyl reductase 1 **(CBR1)**	Antioxidant enzyme that protects against ROS.
sek-1	Mitogen-activated protein kinase kinase 6 **(MAP2K6)**	Involved in defense response against other organism, p38MAPK cascade and regulation of oviposition.
skn-1	Nuclear factor erythroid-2-related factor 2 **(Nrf2)**	Involved in the endoderm specification. Enhances expressions of phase II enzymes
ugt-13	UDP glucuronosyltransferase family 1 member A10 **(UGT1A10)**	Antioxidant enzyme that protects against ROS.
vab-3	Paired box protein **(PAX6)**	Involved in epidermal morphogenesis, gonad cell migration and male tail specific sensory structure formation

List of Abbreviations

ACT	Actin
AKT	Protein Kinase B (PKB)
ARE	Antioxidant Response Element
BRAP2	Brca1 Associated Binding Protein 2
BRCA	Breast Cancer susceptibility gene
CAT	CATalase
CDC	Cell Division Cycle related
cDNA	Complementary DNA
C. elegans	*Caenorhabditis elegans*
DAF	Abnormal Dauer Formation
DHS	DeHydrogenases Short chain
DNA	Deoxyribonucleic Acid
E3	Ubiquitin ligase
E. coli	*Escherichia coli*
ERK	Extracellular signal-regulated kinases
FOXO	FOrkhead boX O
GEF	Guanine Nucleotide Exchange Factor
GFP	Green Fluorescent Protein
GRB2	Growth factor receptor-bound protein 2
GST	Glutathione-S-Transferase
GSTO	Glutathione-S-Transferase Omega
GTP	Guanine Triphosphate
HIM	High Incidence of Males
IGF	Insulin Growth Factor
IIS	Insulin/Insulin-like growth factor Signaling
IMP	Impedes Mitogenic Signal Propagation
KEAP1	Kelch-like ECH-Associated Protein 1
KSR	Kinase Suppressor of Activated Ras

LET	Lethal
LIN	Abnormal cell LINeage
MAPK-MPK	Mitogen-Activated Protein Kinase
MAPKK	Mitogen-Activated Protein Kinase Kinase
MAPKKK	Mitogen-Activated Protein Kinase Kinase Kinase
MEK	Erk Kinase
mRNA	messenger RNA
NGM	Nematode Growth Media
NLS	Nuclear Localization Signal
NSY	Neuronal SYmmetry
NRF2	NucleaR Factor (erythroid-derived 2)-like 2
PCR	Polymerase Chain Reaction
P38	Protein 38 MAPK
PAX	PAired boX
PDK	Phosphoinositide dependent kinase
PHLPP	PH domain and Leucine rich repeat Protein Phosphatase
PHLP	PH domain and Leucine rich repeat Protein phosphatase homolog
PI3K	PhosphatIdylinositol 3-Kinase
PMK	P38 Map Kinase Family
PTEN	Phosphatase and TENsin homolog
qPCR	Quantitative Polymerase Chain Reaction
RT-PCR	Reverse Transcriptase Polymerase Chain Reaction
RAF	Rapidly Accelerated Fibrosarcoma
RAS	Rat Sarcoma Oncogene
RNA	Ribonucleic Acid
RNAi	RNA Interference
ROS	Reactive Oxygen Species
RTK	Receptor Tyrosine Kinase
SDZ	SKN-1 Dependent Zygotic transcript
SKN	Skinhead

SOD3	Superoxide Dismutase 3
SOS	Son of Sevenless
SW-PCR	Single Worm PCR
TF	Transcription Factor
UGT	UDP-Glucuronosyl Transferase
VAB-3	Variable ABnormal morphology 3
WDR	WD Repeat-containing protein
WT	Wild Type
YF	Kubiseski Lab Strain

Introduction

1.1 Aging

Aging is closely associated with various diseases. For instance, the risk of receiving a cancer diagnosis increases as a person's age approaches their 60s (1). Similar trends are observed in the onset of Parkinson's and Alzheimer's disease (2,3). Revealing mechanisms of aging is essential to promote longevity and improve human health. Thus, studying and understanding the mechanisms of aging is crucial to advance research on human health. In simple terms, aging is a process that starts with the rapid development of an organism and ends with its slow degeneration. However, understanding how exactly aging proceeds has not been an easy task.

In 1956, Denham Harman proposed the free radical theory that explains how aging proceeds. Essentially, Denham states that metabolic processes, such as biologic oxidation and reduction reactions naturally generate free radicals. These radicals then attack the organism, which results in aging (4). Denham reported that the accumulation of ROS (Reactive Oxygen Species) is due to mitochondrial damage which, ultimately contributes to aging (5). Although his theory has been supported by many studies (6–8), others have contradicted the theory (9,10). The contradiction has been demonstrated by studies on the lifespan of *Caenorhabditis elegans* where high levels of ROS are correlated with a long lifespan, while antioxidant treatments on *C. elegans* shorten their lifespan (10). Interestingly, the elevated levels of ROS in mitochondria of *C. elegans* promotes extended lifespan. However, the increase in the cytoplasmic ROS levels in the worm has shown to reduce lifespan (9). Such findings support that the ROS is positively correlated with aging in *C. elegans.* Yet, the fact that ROS attacks and damages cellular elements

such as DNA, RNA, or proteins are still relevant to aging. All in all, research based on the free radical theory has shown insight into the mechanisms of aging and elucidated aging-related biological processes.

1.2 The Oxidative Stress Response

In the cell, superoxide anion ($O^{\bullet}_{2}^{-}$), the hydroxyl radical ($OH^{\bullet}$), and hydrogen peroxide (H_2O_2) are sources of oxidative stress (11). These free radicals can be generated by endogenous (i.e., metabolic by-products) or exogenous causes (i.e., ionizing radiation) in the cell (12). ROS contributes to various cellular processes at a low dosage like cell cycle progression, proliferation, differentiation, and immune response, and redox balance within the cell (13,14). On the other hand, the elevation in ROS levels in the cell results in oxidative stress. This stress can then activate an apoptotic pathway or induce cellular senescence to accelerate aging (Figure 1.1) (15,16).

Eukaryotic cells have evolved to defend themselves against foreign substances. For example, xenobiotics are metabolized by the innate detoxification process to be secreted from the cell (17). Neutralization of ROS is also part of the detoxification process. Any process that metabolizes xenobiotics can generate ROS. Thus, the process itself needs to take care of its own ROS by-products. The cell takes care of the ROS using special transcription factors that monitor levels of the ROS (18,19). This surveillance system, upon detecting the surged levels of ROS, activates specialized enzymes to counteract unbalanced ROS levels (20–22).

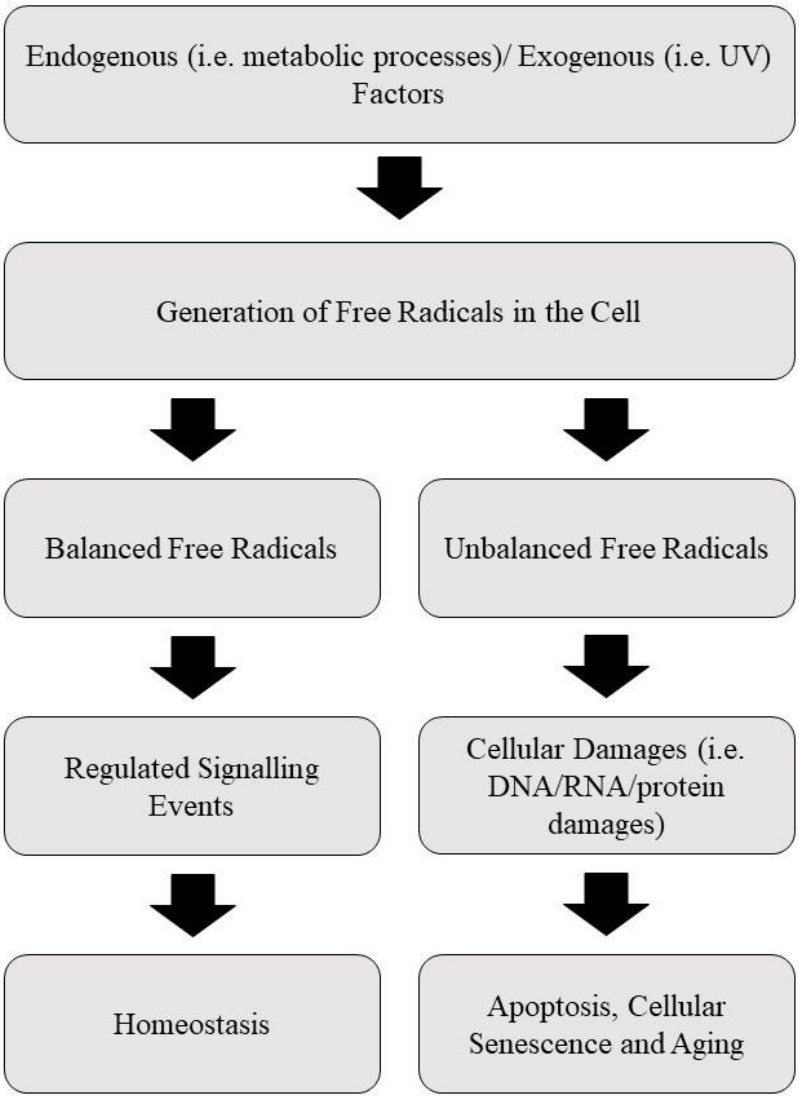

Figure 1. 1 The cellular response to free radicals.

While the figure presents a simplified version of how the cell responses to free radicals, the response depends on a massive network of cellular signaling pathways to execute the proper response against free radical species. Based on the status of free radical balance, the cell can either promote homeostasis or defence mechanisms such as apoptosis or cellular senescence, resulting in aging. Figure adapted from (12).

1.2.1 Superoxide Dismutase, Catalase, and FOXO

Two types of enzymes involved in neutralizing ROS are SODs (Super Oxide Dismutases) and CATs (CATalases). SODs, which are part of phase I detoxification, decrease ROS levels by their catalytic activity on transforming superoxide anion into hydrogen peroxide and oxygen ($2O_2^{\bullet-}+2H^+ \rightarrow H_2O_2+O_2$) (23,24). Hydrogen peroxide is relatively stable and can diffuse through different cellular compartments. As superoxide anions become hydrogen peroxide, ROS levels are reduced within the cell (25). Along with SODs, CATs contribute to the reduction of ROS as well. Whereas SODs focus on generating hydrogen peroxide, CATs breakdown hydrogen peroxide into water and oxygen molecules. The breakdown involves electron transfer based oxidation resulting in the removal of ROS (21). Expression levels of these enzymes are determined by the insulin-responsive transcription factor: FOXO (Forkhead box transcription factor) (26,27). Upon activation of the insulin signaling pathway by growth factors, FOXO proteins are phosphorylated by AKT (protein kinase B), and sequestered in the cytoplasm by 14-3-3 proteins. The phosphorylation then leads to the nuclear exclusion of FOXO proteins. Consequently, FOXO becomes the target for ubiquitin-mediated proteasomal degradation, resulting in the downregulation of the target genes, including SODs and CATs (Figure 1.2) (28–30).

1.2.2 Phases II Enzymes and Nrf2

Different phases of detoxification are employed to process xenobiotics. Phase I enzymes focus on solubilizing targets by oxygen molecule transfer. Phase II enzymes then catalyze the conjugation on the targets to neutralize their reactivities. Lastly, phase III detoxification involves transporters that pump out the targets, thus achieving detoxification (22,31).

Due to the nature of the phase I reaction, regulating the oxygen transfer can result in the production of ROS (31). For example, monooxygenase cytochrome P450 is responsible for oxidizing its substrates. Before cytochrome P450 oxidizes its substrates, it needs to be reduced by one electron. The result of the reduction leads to the release of superoxide anion, which can act as ROS if not managed properly (32). Hence, phase II enzymes such as GSTs (glutathione-S-transferases) are used to neutralize ROS generated from phase I reactions or other sources in the cell. The GSTs conjugate a reduced form of GSH (glutathione) to ROS and remove ROS reactivities. The abundance of GSH in the cell enables such a detoxification system, allowing GSTs to reduce the amount of ROS (33). Another example of the phase II enzymes is UGTs (uridine diphosphate glucuronosyltransferases). Like GSTs, UGTs conjugate UDP (glucuronic acid from uridine diphosphate glucuronic acid) to ROS that results in the formation of glucuronides. Such a reaction allows ROS levels to be reduced (34). Thus, the expression of phase II enzymes is essential for the cell to protect itself from oxidative stress.

To activate phase II enzymes, AREs (Antioxidant Response Elements), which are in promoter regions of cytoprotective genes, are needed to be recognized and bound by Nrf2 (nuclear factor erythroid 2 [NF-E2]-related factor 2) (35). Nrf2 is from the CNC (Cap ‘n’ Collar) family and is a basic region-leucine zipper-type transcription factor (36). The Neh1 (Nrf2–Erythroid cell-derived protein with CNC Homology 1) domain on Nrf2 recognizes the sMaf (small musculoaponeurotic fibrosarcoma) to form a dimer. Consequently, dimerization allows the nuclear-translocated Nrf2 to bind AREs of its downstream target genes leading to activation (37–39).

Since Nrf2 is a cellular entity, the abundance of Nrf2 is determined by a regulatory mechanism. When the cell is not under stress, the negative regulation on Nrf2 is achieved by the

ubiquitylation mediated protein degradation mechanism. For the Nrf2 to be ubiquitinylated, Keap1 (thiol-rich kelch-like ECH-associated protein 1) needs to bind to Neh2 domain of the Nrf2 to form the Keap1/Nrf2 complex. The binding, then, allows Cul3 (cullin-3)/Rbx1 (RING box protein1) E3 ubiquitin ligase complex to ubiquitinylate Nrf2. As a result, Nrf2 undergoes proteasomal degradation (40). When the cell is under stress, the stress inducers facilitate the conformational change of a Keap1/Nrf2 complex from open to closed conformation. The amount of Keap1 is not infinite. In other words, Keap1 can bind to only a fixed number of Nrf2. As a result, when the inducers trigger the Keap1/Nrf2 complex to be in the closed state, no Keap1 is available for newly synthesized Nrf2 molecules. Thus, the Nrf2 is free to be nuclear localized and activates its downstream target genes (41).

Once Nrf2 bypasses the Keap1 binding system, Nrf2 is imported into the nucleus. Nrf2 has NLS (nuclear localization signal) motifs that allow the Nrf2 to be nuclear-localized. Nrf2 has multiple NLS motifs, including the one located at the Neh2 domain. The NLS at the inhibitory sequence suggests that Nrf2 is a highly active transcription factor (42). One residue involved in both Keap1 interaction and phosphorylation by PKC (protein kinase C) is Serine 40 at the Neh2 domain. According to Huang and colleagues, the phosphorylation at Ser 40 by PKC leads to the activation of AREs containing genes. Additionally, phosphorylation discourages Keap1 from interacting with Nrf2 (43). Aside from PKC, other kinases such as ERK (extracellular-signal-regulated kinase), PKB (p38 kinase, and protein kinase B) have been shown to influence the activation of AREs as well (44–47). Taken together, Nrf2 is a crucial transcription factor as its regulation dictates levels of AREs related genes expressions, including phase II detoxifying enzymes. The presence of multiple mechanisms regulating multiple enzymes indicates that the cell must regulate the ROS levels.

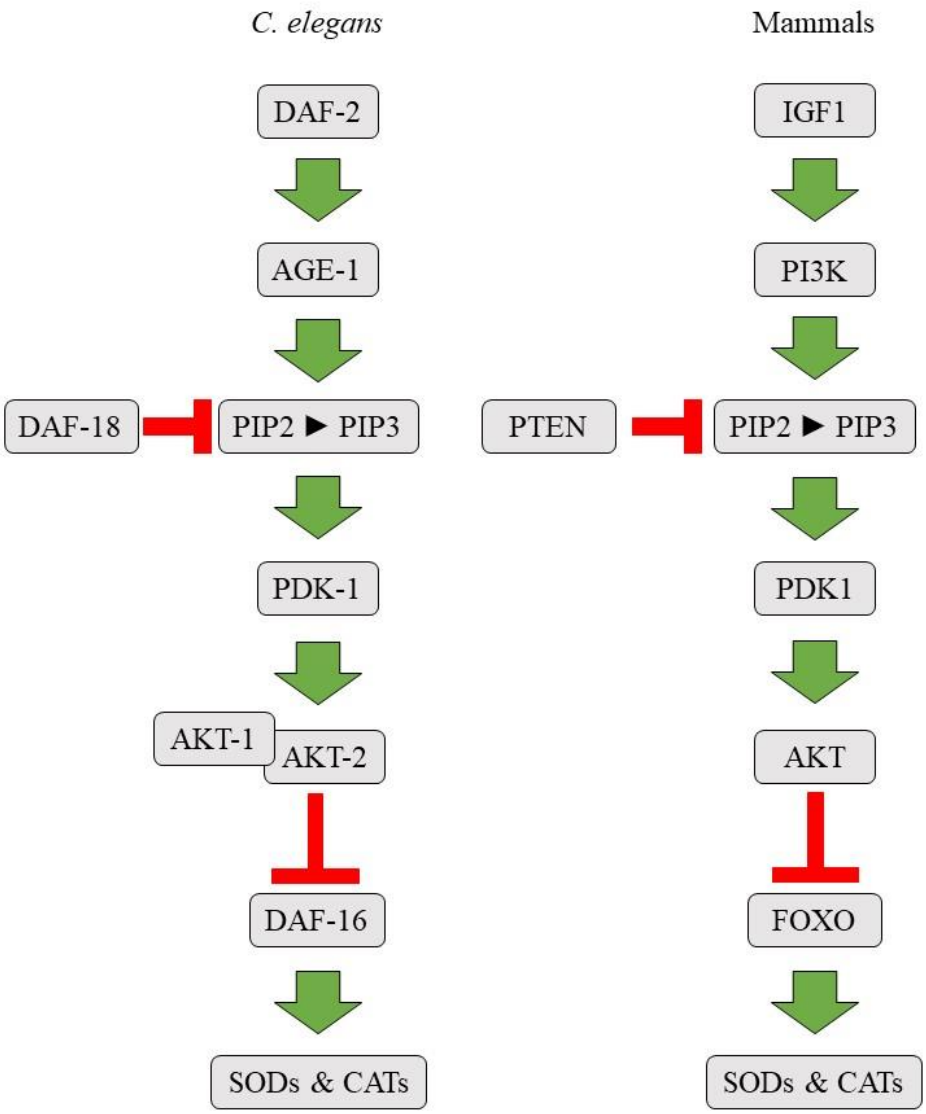

Figure 1. 2 Conserved regulation on activation of SODs and CATs that depend on the DAF-2/IIS pathway in C. elegans and the IGF/Insulin signaling pathway in mammals.

An increase in SODs and CATs levels are negatively regulated by the IGF/Insulin pathway in mammals and DAF-2/IS pathway in *C. elegans*. In addition to regulating the expression of SODS and CATs, the DAF-2/IIS pathways and mammalian IGF/Insulin pathway are also responsible for regulating metabolism and lifespan. Figure adapted from (28–30).

1.3 *C. elegans* as a Stress Response Model Organism

As a model organism, the free-living and non-parasitic nematode *Caenorhabditis elegans* have advanced research on molecular aspects of biological processes such as development, aging, innate immune response, neurological disorders, and stress responses (48,49). The genome sequencing on *C. elegans* has revealed that the model organism has human orthologs that count for 40% of human genes. Additionally, these orthologs are regulated and have roles in conserved signal pathways like their human counterparts (50). Such benefits offered by *C. elegans* provide opportunities to find and determine mechanisms on how the signal pathways influence the orthologs and vice versa.

Research using forward and reverse genetics in *C. elegans* can be easily conducted by involving a direct induction of mutations by IR (ionizing radiation) or EMS (ethyl-methanesulfonate). Furthermore, the gene silencing achieved by RNAi (RNA interference) is a viable option for studying lethal genes (51). Another fascinating aspect of *C. elegans* is that the generation of double mutants is possible by crossing two different strains (52). Such an advantage can be a valuable source for investigating and establishing a genetic link between two genes. Recent advancement in gene-editing technology like CRISPR (clustered regularly interspaced short palindromic repeats) has helped *C. elegans* genetics to reach its full potential by enhancing the efficiency of generating transgenic worms (53).

1.3.1 Aging in *C.elegans*

Aging in *C. elegans* has been extensively studied ever since discovering a relationship between the *age-1* (the *C. elegans* PI3K ortholog) gene and lifespan of *C. elegans*; worms with *age-1* mutations have shown extended lifespan compared to wild type worms (54). It has greatly

contributed to finding that IIS (Insulin and IGF-1 signaling) pathway is closely related to aging. Further research has shown that the IIS pathway involves *daf-2* (the *C. elegans* IGF1R ortholog), which impacts the development and metabolism of *C. elegans* (55). *daf-2* mutants under a permissive temperature show a longer lifespan than that of the wild type, while *daf-2* mutants under a non-permissive temperature show dauer form, which involves morphological changes such as a formation of thickened cuticles, elongation of the body, and slow metabolism in the worm to protect the worms against harsh conditions such as low nutrition availability or temperature changes (56). Such a finding has identified a *daf*-2 gene as a gene that influences aging in *C. elegans* along with *age-1* (55). *C. elegans* is not the only animal using the IIS to regulate development and metabolism since the IIS pathway is highly conserved among many species, including humans (57). In other words, a conserved IIS pathway influences lifespan of animals. Thus, research on the aging of *C. elegans* provides insight into mechanisms of aging in other species.

1.3.2 Oxidative Stress Response in *C. elegans*

As a eukaryote member, *C. elegans* exhibits high similarities in detoxifying ROS with mammalian ROS detoxification by having orthologs. The ROS detoxification in *C. elegans* involves a SOD group (SOD-1, SOD-2, and SOD-3, SOD orthologs), CTL group (CTL-1, and CTL-2, CAT orthologs), and phase II group. Each group is controlled by conserved pathways and responding transcription factors (58–60). Thus, studies on *C. elegans* ROS detoxification processes are useful to determine the role of genes and proteins and their involvement in ROS detoxification of mammals.

1.3.2.1 *C. elegans* Superoxide Dismutase, Catalase, and DAF-16

ROS in *C. elegans* is processed by SODs and CTLs that results in reduced oxidative stress. *C. elegans* uses SOD-1, SOD-2, and SOD-3 to produce hydrogen peroxide (H_2O_2). Hydrogen peroxide undergoes molecular breakdown to be split into water and oxygen molecules by CTL-1/2 (the *C. elegans* CAT orthologs). Both ROS detoxification systems are under the control of DAF-16 (the *C. elegans* FOXO ortholog) (59,60). The DNA binding domain of DAF-16 recognizes and binds to DBE (DAF-16 binding element) of its downstream target genes (30,61). Like the mammalian FOXO, DAF-16 activity depends on the IIS pathway (62). The growth factor triggered activation of the IIS pathway promotes the phosphorylation of DAF-16 by AKT-1/2 (AKT1/2 orthologs). The phosphorylation then promotes FTT-2 (the *C. elegans* 14-3-3 ortholog) proteins to bind and sequester DAF-16 in the cytoplasm to prevent the nuclear-localization of DAF-16 (63). Consequently, DAF-16 becomes a target for ubiquitination and subsequently undergoes ubiquitin-mediated proteasomal degradation (59,60).

1.3.2.2 *C. elegans* Nrf2 homolog SKN-1

In *C. elegans*, orthologs of mammalian phase II enzymes such as GST-4 (GST ortholog) or UGT-13 (UGT ortholog) process phase I processed reactive electrophiles or ROS by the conjugation that results in stable compounds (58). Regulation on these types of enzymes is achieved by SKN-1 (the *C. elegans* Nrf2 ortholog). Originally, SKN-1 was found to be involved in the endoderm specification during embryogenesis in *C. elegans*. The specification leads to the development of the body wall and pharynx. Hence, mutations in *skn-1* have been determined to be lethal (64). The function of SKN-1 is not limited to embryogenesis. Adult worms have shown to depend on SKN-1 expressions in amphid chemosensory neurons for longevity (65). Additionally, SKN-1 is a crucial member of the intestine detoxification system where high levels

of ROS are detoxified (66). SKN-1 has three isoforms, and each isoform is expressed in different tissues with specific functions: SKN-1A, SKN-1B, and SKN-1C (58). SKN-1A and SKN-1B are highly expressed in the nervous system, while SKN-1C is highly expressed in the intestine and hypothesized to correspond to mammalian Nrf2 (58).

The Nrf2 uses its CNC domain to bind its target DNA along with the dimerization with the sMaf (38,39). However, SKN-1 does not require dimerization like Nrf2. In other words, SKN-1 by itself can activate its downstream targets. The SKN-1 has a relatively more stable version of the helical structure in the CNC domain than Nrf2. Furthermore, the SKN-1 binds to the DNA minor groove of its targets (67–70). Taken all together, SKN-1 regulates its downstream targets as Nrf2 without dimerization. Additionally, both transcription factors have a highly conserved DIDLID domain, which consists of a 14-residues motif. The domain is characterized as a unique feature of the CNC protein family. The domain in SKN-1 is involved in transcriptional activation and inhibitory regulation (71).

Unlike mammalian Nrf2, SKN-1 does not appear to have an antagonist like Keap1. The regulation of SKN-1 is achieved by ubiquitin-mediated proteasomal degradation. WDR-23 (the *C. elegans* DCAF11 ortholog), an E3 ubiquitin ligase substrate adaptor, simultaneously interacts with the DIDLID domain of SKN-1 and DDB-1 (the *C. elegans* CUL4 ortholog) (72). The interaction has been predicted to encourage the degradation of SKN-1 through the ubiquitylation as the RNAi knockdown on *wdr-23* in worms results in an elevated amount of SKN-1 and increased expression levels of SKN-1 target genes (72). Interestingly, the WDR-23 is not the only regulatory mechanism on the SKN-1 activity. Kinases influence the activity of SKN-1 through phosphorylation triggered localization.

Based on where SKN-1 is phosphorylated, SKN-1 can be nuclear excluded or localized. The phosphorylation by kinases such as PMK-1 (the *C. elegans* MAPK 14 ortholog) or MPK-1 (the *C. elegans* ERK ortholog), which is under the control of the Ras/LET-60/MAPK pathway, triggers the nuclear localization of SKN-1. On the other hand, the IIS pathway uses AKT-1/2 to phosphorylate SKN-1 and inhibit nuclear localization (58,66,73–75). Once the phosphorylation determines the fate of SKN-1, nuclear-localized SKN-1 can activate and enhance expression levels of its downstream targets, including phase II detoxifying enzymes (Figure 1.3) (76,77). Interestingly, SKN-1 transactivates itself through a binding *skn-1c* promoter (78). Thus, along with the phase II enzymes, expression levels of SKN-1 itself also become upregulated.

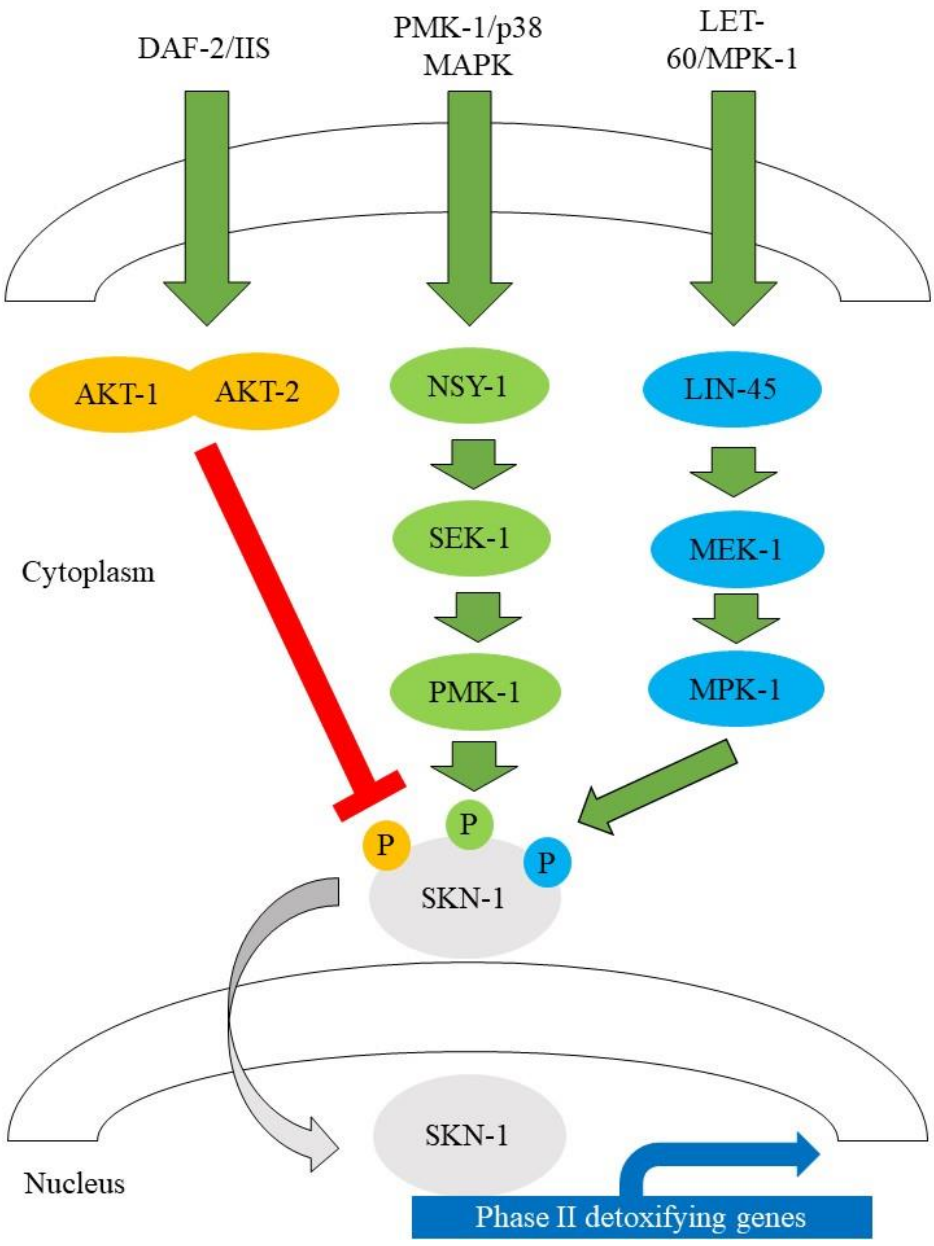

Figure 1. 3 Regulation of nuclear localization of SKN-1 by DAF-2/IIS, PMK-1/p38 MAPK, and MPK-1/ERK.

Activation of SKN-1 to induce expressions of phase II detoxifying genes require nuclear localization of SKN-1. The phosphorylation of SKN-1 is achieved by PMK-1 or MPK-1 and triggers the nuclear localization of SKN-1. On the other hand, phosphorylation of SKN-1 by the DAF-2/IIS pathway prevents nuclear localization of SKN-1. Adapted and modified from (58,66,73–75).

1.4 BRAP2: A Cytoplasmic Retention Protein

The cellular regulation of the nuclear localization of proteins is essential for the cell to produce a proper response to given environmental cues. For instance, Keap1 regulates nuclear localization of Nrf2 by sequestering Nrf2 in the cytoplasm through the direct binding to the Neh2 domain on Nrf2 (40). The interaction is an example of signal-based regulation on nuclear localization. The majority of proteins with a size greater than 40 kDa require NLS for their nuclear import (79). In other words, cytoplasmic retention proteins can sequester their targets by directly binding NLS motifs to prevent nuclear localization. The mechanism in which BRAP2 (Brca1 associated binding protein 2) prevents nuclear localization of BRCA1 (Breast Cancer) is an example. The BRAP2 binds NLS motifs on BRCA1 and retains the BRCA1 in the cytoplasm (80). Further research finds that it also binds the NLS of cell cycle inhibitor p21 and sequesters p21 in the cytoplasm (81). These findings have characterized BRAP2 as a cytoplasmic retention protein. Interestingly, BRAP2 recognizes and binds to SV40 large T antigen and human papillomavirus proteins (80). Such discovery strongly supports that the major function of BRAP2 depends on its ability to bind its targets. All in all, BRAP2 has proven itself to be an important regulator for nuclear localization.

1.4.1 Mammalian BRAP2

In a mammalian cell, BRAP2 uses its sequestering ability to regulate signaling pathways. For example, BRAP2 has a role as a negative regulator of the Ras (Rat sarcoma) signaling pathway; hence, it was also called IMP (Impedes Mitogenic Propagation). The role of BRAP2 in the pathway is to bind and sequester KSR (Kinase Suppressor of Ras) to prevent the Raf (Rapidly accelerated fibrosarcoma) – MEK (Mitogen-Activated Protein Kinase Kinase) complex formation under GDP bound Ras state. The KSR is a scaffold protein responsible for bringing all

elements of Raf/MEK/ERK cascade by encouraging the formation of Raf-MEK complex and promoting the phosphorylation cascade. Upon activation of the pathway, GTP bound Ras physically contacts BRAP2, which causes BRAP2 to use its E3-ligase ability to auto-ubiquitylate. The autoubiquitylation leads to ubiquitin-mediated proteolysis of BRAP2 (82). As a result, KSR can promote the cascade, and the phosphorylated ERK can phosphorylate its downstream factors to either promote or repress their activities (Figure 1.4) (83).

Recent research on BRAP2 has shown a possibility of BRAP2 influencing the IIS signal pathway involving the interaction with PHLPP1 (PH domain and Leucine-rich repeat Protein Phosphatase 1) in human testis. During the spermatogenesis, BRAP2 binds and sequesters PHLPP1 in the cytoplasm (84). The fact that AKT is the IIS terminal kinase and PHLPP1 is the antagonist of PDK1 (Phosphoinositide-Dependent Kinase-1) suggests that BRAP2 may regulate the IIS pathway indirectly. However, further research is required to determine whether the BRAP2 modifies signal transduction in the IIS pathway. In summary, the abilities of BRAP2 to recognize and sequester its target proteins control signaling pathways that ultimately result in cellular responses for the cell to defend itself against environmental stresses.

1.4.2 *C.elegans* BRAP-2

C. elegans has a BRAP2 ortholog called BRAP-2 (the *C. elegans* BRAP2 ortholog). Our lab has demonstrated that worms with *brap-2(ok1492)* mutations, which delete ZnF UBP (Zinc-Finger Ubiquitin Binding Domain) and leucine heptad repeats of BRAP-2, exhibit L1 larval growth arrest that involves the increased expression of CKI-1 (the *C. elegans* CKI ortholog) under oxidative stress-inducing conditions. Additionally, the expression has been shown to depend on *brc-1* (the *C. elegans* BRCA homolog) as the *brc-1* deletion mutation abolishes the

cki-1 expression. The discovery has provided insight on the genetic link between *brap-2* and *brc-1*, but it is not clear whether they physically interact (85).

Further research on BRAP-2 from our lab has found that worms with *brap-2(ok1492)* deletion mutations have increased expression levels of genes encoding for phase II detoxifying enzymes such as GST-4 compared to the wild type under non-oxidative stress-inducing conditions. The increase in the expression levels of phase II detoxifying enzymes in the *brap-2(ok1492)* mutants has been determined to be due to the increased nuclear localization of SKN-1. The regulation of BRAP-2 on the nuclear localization is hypothesized to be achieved through the p38 pathway. The *brap-2(ok1492)* mutants have exhibited increased phosphorylation levels of PMK-1 and increased expression levels of PMK-1 target genes, including the phase II detoxifying genes. Such a finding indicates that BRAP-2 may have a role in regulating the p38 pathway and its downstream transcription factor: SKN-1. Additionally, the investigation on mRNA levels of *skn-1c* in *brap-2(ok1492)* mutants has revealed that BRAP-2 inhibits expression levels of *skn-1c* (78). These findings strongly suggest that BRAP-2 negatively regulates the SKN-1 through controlling both the expression and nuclear localization levels.

Since *brap-2(ok1492)* mutants show elevated expression levels of phase II detoxifying genes and the elevation is related to a transcription factor SKN-1, our lab decided to performed a transcription factor specific RNAi screening on *brap-2(ok1492)* mutants to find potential candidates that may influence the expression levels of the phase II genes like SKN-1. Among the candidates, RNAi of a *vab-3* (the *C. elegans* PAX6 ortholog) gene decreased the expression levels of GST-4 in the *brap-2(ok1492)* mutants.

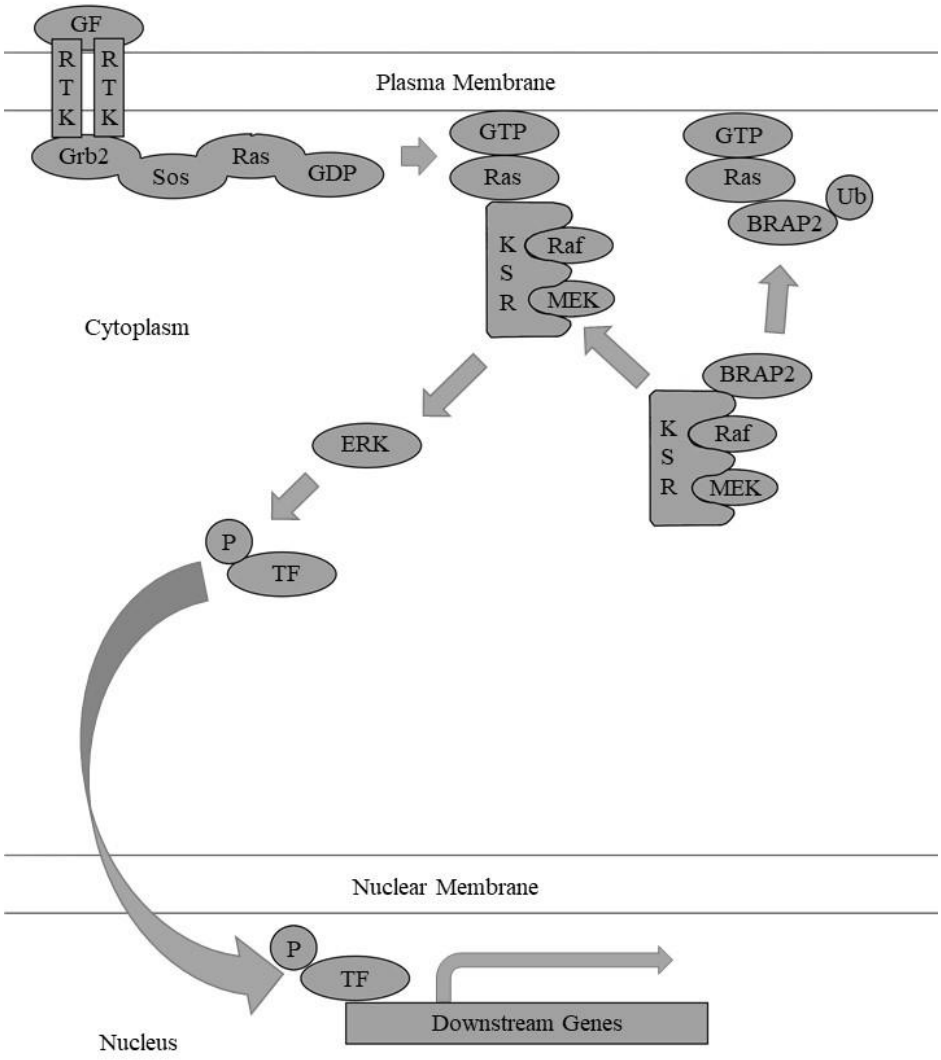

Figure 1. 4 The hypothesized role of BRAP2 in the mammalian Ras signaling pathway.

Under the condition where Ras is bound to GDP, BRAP2 binds and sequesters KSR and prevents the formation of Raf-MEK-ERK. The binding of growth factors to RTKs triggers the signal cascade, promoting Ras to be bound to GTP instead of GDP. The GTP bound Ras can directly bind BRAP2, causing dissociation of BRAP2 and KSR. The BRAP2 that interacts with GTP-bound Ras auto-ubiquitinylates itself and becomes a target for ubiquitinoylation and undergoes proteasomal degradation. The dissociation allows KSR to translocate to the plasma membrane to promote the formation of Raf-MEK-ERK. The phosphorylated ERK can phosphorylate its downstream targets, which result in activation of the downstream genes. Image adapted and modified from (82,83).

1.5 PAX6: a Potential Oxidative Stress Responsive Transcription Factor

Transcription factors contribute to determining cellular responses. In other words, the biological processes of an organism depend on transcription factors. One example is how the PAX6 (PAired boX protein) influences the development of an organism. PAX6 is a transcription factor that has a distinguishable characteristic: the presence of the DNA binding domain called the paired box domain. The domain was first identified from segmentation genes *paired, gooseberry,* and *gooseberry neuro* in *Drosophila melanogaster* (86). Further research found that the PAX6 gene is highly conserved throughout different species, including humans, mouse, zebrafish, quails, chickens, rat, and axolotl (87–93). A major role of PAX6 has been defined by its involvement in processes that determine development in the symmetry of an organism. In *D. melanogaster*, two PAX6 genes called *eyeless*, and *twin of eyeless* genes are essential components for eye development of the fly (94). In mammalian cells, PAX6 regulates the coordination of cell division of progenitors in the cerebral cortex to achieve proper symmetric or asymmetric cell division (95,96). PAX6 is also found to be expressed in the pancreas and developing central nervous system (92,97). These findings indicate that PAX6 is a crucial transcription factor for development.

The role of PAX6 is not limited to development. PAX6 has shown to be linked to the oxidative stress response of the cell as well. Studies from Hebert-Schuster *et al.* have demonstrated that overexpressed PAX6 in HepG2, a human lung cancer cell line, could enhance the CAT promoter activity (98). Additionally, in MIA-PaCa2 cells, a human pancreatic carcinoma cell line, PAX6 is highly localized in the nuclei upon exposure to oxidative stress induced by H_2O_2 (99). The fact that PAX6 recognizes and binds the CAT promoter and becomes

highly nuclear-localized under oxidative stress-inducing conditions suggests that PAX6 may have a regulatory role in the oxidative stress response of the cell.

1.5.1 Structure and Functions of PAX6

PAX6 in mammalian cells has three promoters: 5' P0, 5' P1, and internal Pα. Each promoter produces different isoforms of PAX6. The P0 produces the main PAX6 with a size of 46 kDa, while the P1 synthesizes an alternatively spliced version of the PAX6 called PAX6(5α) with the size of 48 kDa. Between these two isoforms, the difference is extra 14 amino acid residues on PAX6(5α). The extra amino acids are encoded in exon 5a in the *pax6* locus. Interestingly, the exon 5a has been found to abolish the DNA binding ability by PD (Paired Domain) of PAX6 (100). The PD is 128 amino acid long with a helix-turn-helix motif and encoded in a 384 base pair (bp) DNA sequence (86,100). The internal promoter Pα makes a truncated PAX6 that lacks the PD with the size of 33 kDa (87) (Figure 1.5). Regardless of the promoter, all PAX6 isoforms have a HD (HomeoDomain), which has a helix-turn-helix motif, at its N-terminal (101,102). Structural analysis on the PAX6 PD has revealed that it comprises 2 subunits: an N-terminal and C-terminal subdomain (103,104). With the help of crystallography, the DNA bound PAX6 structure has been resolved and has shown that the main PAX6 (the 46 kDa isoform) binds to DNA using the subunits and the HD (105).

As a transcription factor, PAX6 requires nuclear localization to bind and activate its downstream target genes. From the study on PAX-QNR, PAX6 in quails, two putative nuclear localization signal sites have been identified: one at the PD and the other at the beginning of the HD (97). The sequence (LKRKXXRXR) at the HD serves as a consensus nuclear localizing signal, while the nuclear localization sequence at the PD is hypothesized to reside in the range from 271 to 342 amino acids of the PAX-QNR (97,106). Furthermore, recent research on chick

PAX6 has identified the linker region that has 11 out of the 16 amino acids linking the N-terminal subdomain and C-terminal subdomain as the NLS. Along with the linker region, the N-terminal subdomain has the NLS at its C-terminus. Approximately half of the third α–helix of the N-terminal subdomain contains the NLS (107). The information on the NLS of PAX6 proteins is valuable since it provides insight into the regulation of the nuclear localization of PAX6 proteins. While the NLS on PAX6 has been identified, the upstream regulators of the PAX6 have not yet been determined.

Besides its downstream target genes, PAX6 transactivates itself. In other words, PAX6 binds its promoter to upregulate its expression levels. In zebrafish, the PST domain, which is rich in proline, serine, and threonine, can be phosphorylated by ERK and p38 kinase *in vitro*. The PST domain is located at the C-terminal region of the HD and has Ser at 413 as a highly conserved phosphorylation site, which can be phosphorylated by ERK or p38 kinase *in vivo* (108). Along with zebrafish PAX6, the p46 isoform of PAX-QNR in quails can activate the P0 promoter and transactivate (106).

1.5.2 Structure and Function of VAB-3 in *C.elegans*

In *C. elegans*, VAB-3 (the *C. elegans* ortholog of PAX6) has been identified as the PAX6 ortholog. The *vab-3* gene is located on the X chromosome and has a 1368 bp long coding DNA sequence. The transcription factor is involved in the development of *C. elegans.* For instance, mutations in a *vab-3* gene have resulted in abnormal alae, a protruding ridge, at the anterior hypodermal region of developing larvae (109). Furthermore, *vab-3* mutations have been shown to disrupt the gonad cell migration in a male worm resulting in sterility due to malformation of spicules at its tail (110). Additionally, a *vab-3* gene influences the asymmetrical development of embryonic B cells, which belong to one of *C. elegans* cell lineages (111). These findings

strongly suggest that *vab-3* is broadly involved in the development of *C. elegans* and is a crucial transcription factor for development.

Like the PAX6, VAB-3 proteins have PD and HD (Figure 1.5). The comparative analysis on the sequence of both domains of VAB-3 has revealed that the sequences have high similarity with human PAX6 HD and PD. The HD sequence of VAB-3 is 93% identical, while the PD sequence of VAB-3 is 79% identical. VAB-3 exists in 3 isoforms: a long VAB-3A and two short VAB-3B/C isoforms. The VAB-3A is 455 amino acid long and has HD and PD, hence called the PD isoform. VAB-3B/C are non-PD isoforms since they lack the PD. VAB-3B is 269 amino acids long, and VAB-3C is 296 amino acid long. Different promoters in *vab*-3 locus are used to express corresponding VAB-3 isoforms. Each isoform has been described to have different functions in different cell types. For example, VAB-3A represses expression of ETS-5 (the *C. elegans* FEV ortholog), which contributes to cellular differentiation in non-chemosensory neurons. VAB-3B/C isoforms are required to develop chemosensory neurons expressed in the anterior hypodermis and sensory ray cells of the male tail of *C. elegans* (109,112,113).

The regulation of nuclear localization of VAB-3 has been hypothesized to be influenced by the sequences nearby the HD. The N-terminal of the HD has the positively charged RMRLKRK sequence, which resembles the SV40 NLS and is hypothesized to be the NLS for the VAB-3 (114). Additionally, the non-PD form containing the PST domain is nuclear-localized. Such a finding indicates that the PST domain may serve as a cytoplasmic retention signal (113). Interestingly, the non-PD form has shown delayed nuclear localization that is affected by the developmental stages of the ray cells. In other words, the nuclear localization of the non-PD form is regulated temporally.

The transcriptional regulation by a transcription factor on its target genes can be achieved by direct binding of the transcription factor toward the genes. The discovery of direct interactions between VAB-3 with its target genes is an example. One of the VAB-3 target genes is *pat-2* (the *C. elegans* human Integrin subunit alpha5 ortholog) (115). Meighan and Schwarzbauer have found the effect of *vab-3* mutations on the promoter activity of *pat-2*, which was visualized by the GFP (Green Fluorescent Protein) fused to its promoter sequence in the DTCs (Distal Tip Cells). Through observing the GFP signals on DTCs, they found that the *pat-2p::gfp* reporter strains with *vab*-3 mutations showed lower GFP signals than *pat-2p::gfp* strains without the mutations. Furthermore, they confirmed the interaction between VAB-3 and the *pat-2* promoter by finding that a 420 bp of the promoter is where VAB-3 directly binds and upregulates the transcription of *pat-2* (115).

Interestingly, the *pat-2* promoter sequence has high similarity with the promoter sequence of *ceh-32* (the *C. elegans* human SIX homeobox 3 ortholog): another target gene of VAB-3 (116). Through a yeast one-hybrid system, Dozier and colleagues have identified the *ceh-32* promoter region where VAB-3 directly binds. Additionally, using gel shift assays, they have shown that VAB-3 binds the region with a specific sequence (ATCACTCAAGCGAGCT). Surprisingly, the sequence has up to 81% similarity with the PAX6 binding site consensus sequence (Figure 1.6) (103,116,117). In other words, the consensus sequence is conserved among different species. All in all, VAB-3 requires nuclear localization and the site-specific binding mechanisms to influence its downstream targets in *C. elegans*.

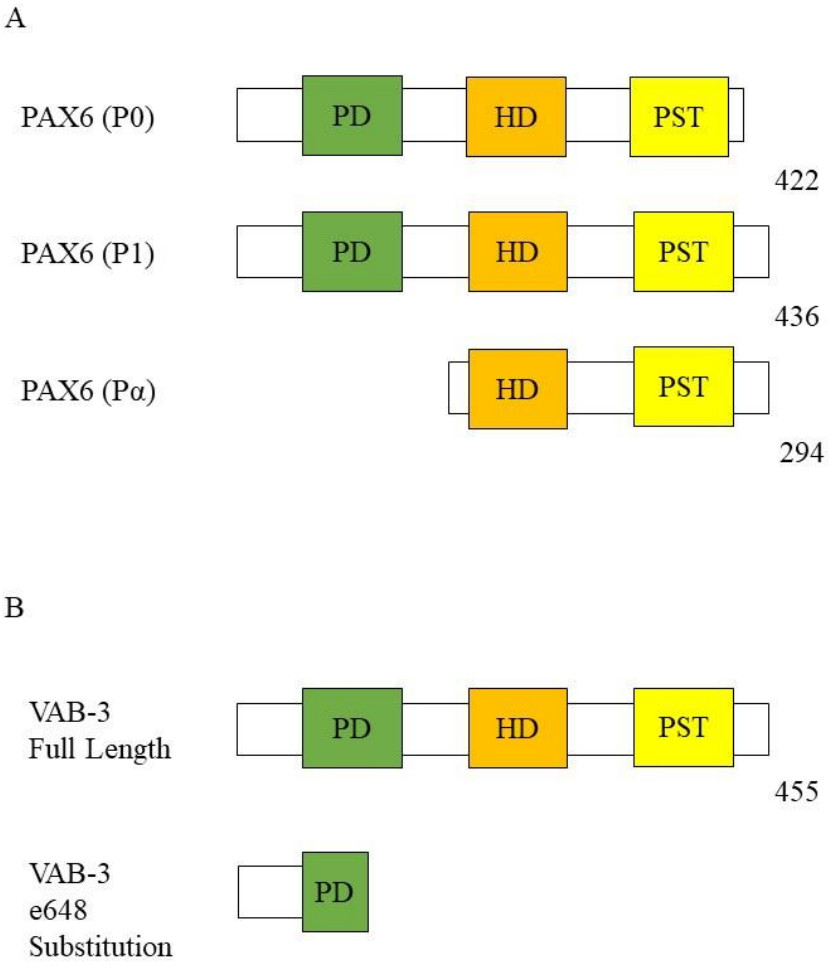

Figure 1. 5 Protein domain structures of mammalian PAX6 and *C. elegans* VAB-3.

(A) PAX6 (P0) is a 422 amino acid protein with a PD and HD that includes the PST region. These domains have been identified as DNA binding domains. Domain structure adapted from SMART and (84). PAX6 (P1) is an alternatively spliced version of PAX6 (P0) and has 14 extra amino acids. PAX6 (Pα) is another isoform that lacks the PD. (B) Full-length *C. elegans* VAB-3 is conserved and possesses a paired domain and homeodomain. It also retains the PST region. In this study, we focus on the *vab-3(e648)* gene product, where Tryptophan 101 is substituted by a opal stop codon in the *e648* allele, resulting in a nonsense mutation that causes the premature termination of VAB-3 proteins. Adapted and modified from (87,100–103,109,112,113).

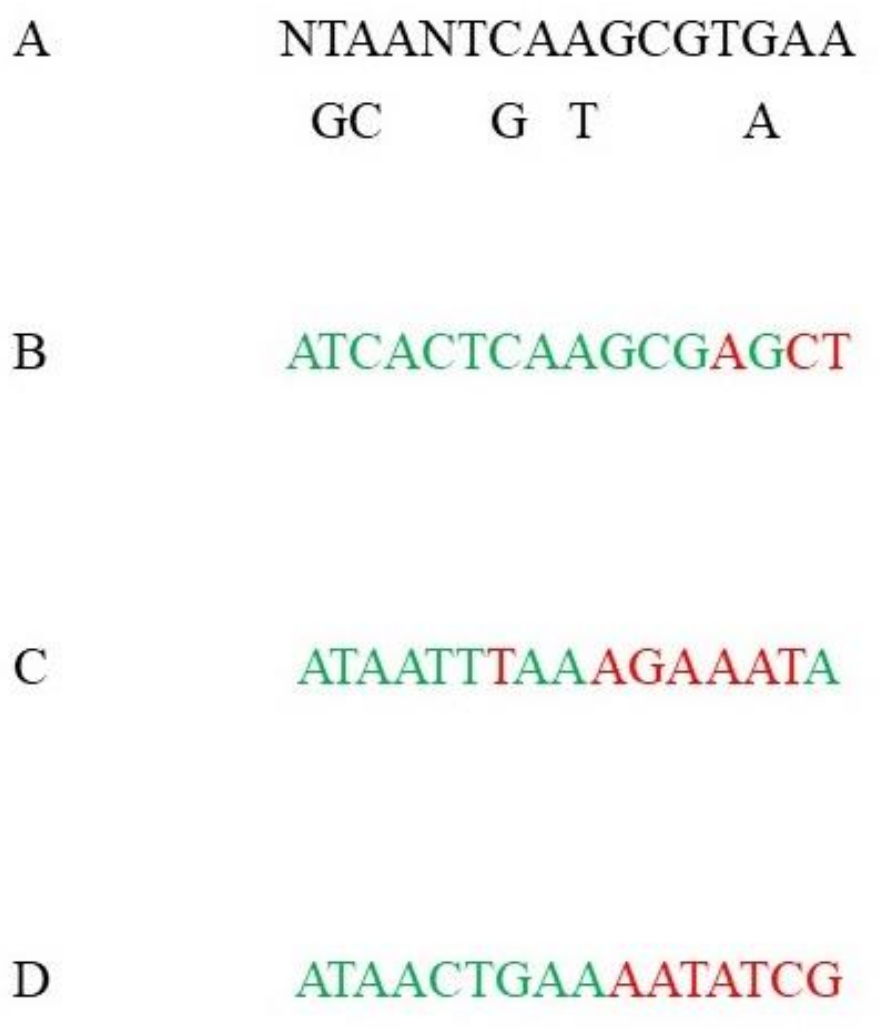

Figure 1. 6 Sequence similarity between PAX6 PD binding sequence and *C. elegans* VAB-3 binding sequence.

(A) The consensus PAX6 PD binding sequence, where 'N' can be any base. (B) A genomic fragment of the *ceh-32* where VAB-3 recognizes and binds. It has about 80% similarity with the consensus sequence. Green colours indicate the matching sequence base, while red indicates a non-matching sequence. (C) Upstream sequence of the *gst-4*. It has about 56% similarity with the consensus sequence. (D) Upstream sequence of the *skn-1*. It has about 56% similarity with the consensus sequence (103,116,117).

1.6 Conserved Pathways that are Relevant to the Study

1.6.1 The Ras pathway

For the cell to properly respond to surroundings, it is essential to relay signals from the outside to inside the cell; the cell uses MAPK (Mitogen-Activated Protein Kinase) pathways to achieve the proper relay. Based on the extracellular signals, the cell can determine whether it needs to grow, differentiate, or trigger apoptosis (118). The core component of the pathway is the phosphorylation cascade encouraged by three kinases: MAP3K, MAP2K, and MAPK. The ser/thr MAPK regulates nuclear localization or cytoplasmic retention of transcription factors to promote or repress cellular responses (119,120). Additionally, the pathway takes advantage of a scaffold protein that can bring the elements and enhance the cascade (121).

The Ras pathway is one of the well studied MAPK pathways. The RTK (Receptor Tyrosine Kinase)-Ras-ERK pathway is greatly influenced by a signal propagator called the small GTPase Ras. RTK dimerizes and phosphorylates its C-terminus as growth factors bind to the RTK (122). The phosphorylated tyrosine residues on the RTK attract adaptor proteins such as Grb2 (Growth factor receptor-bound protein 2) and result in activation of the small GTPase Ras via recruiting the GEF (guanine nucleotide exchange factor) Sos (Son of sevenless) (123). The activated Ras-GTP binds to Raf to promote Raf kinase activity (124). KSR scaffold proteins are involved in kinase activation, but their other roles include bringing together different elements of the Raf-MEK-ERK kinase cascade (124). The cascade enables the Raf to phosphorylate MEK, which phosphorylates ERK. As a result, the phosphorylated ERK can phosphorylate downstream factors to either promote or repress activities based on various cell types (83). For example, the activated ERK phosphorylates Nrf2 leading to the nuclear localization upregulation of phase II detoxifying enzymes (125,126).

In *C. elegans*, LET-23 (the *C. elegans* Epidermal Growth Factor Receptor ortholog) and EGL-15 (the *C. elegans* Fibroblast Growth Factor Receptor ortholog) are the RTKs that have been identified to directly influence LET-60 (the *C. elegans* Human Ras ortholog). The effector kinases that relay the signals from LET-60 to downstream targets are LIN-45 (the *C. elegans* Raf ortholog), MEK-2 (the *C. elegans* MAP2K1 ortholog), and MPK-1 (the *C. elegans* MAPK1 ortholog). The phosphorylation cascade operated by these kinases regulates the development of the germline and specification of cells for different tissues in *C. elegans* (127). For instance, *let-60* loss of function mutations interferes with the development of vulva resulting in worms without vulva, while the gain of function mutations in *let-60* induce the formation of multiple vulva in a worm (128). Additionally, the *let-60* mutations in a male worm cause malformation of the tail, preventing the sensory function of the tail (129,130). Furthermore, MPK-1 directly phosphorylates SKN-1 increasing the amount of nuclear-localized SKN-1 and upregulation of phase II detoxifying enzymes (66).

1.6.2 The p38 pathway

The cell must protect itself against UV, IR, or oxidative stress to survive. The pathway that is crucial for such a response is the SAPK (Stress Activated Protein Kinase) p38 MAPK pathway. The p38 kinase family has four members: p38α, p38β, p38γ, and p38δ MAPK isoforms (130). The p38 pathway starts with the activation of the TIR (Toll/IL-1 receptor) domain-containing IL-1RI (type-1 IL-1 receptor) by IL-1 (Interleukin-1), the pro-inflammatory cytokine. The activation then relays the signal to IL-1 receptor-associated kinases called IRAK and IRAK-2 through adaptor proteins such as MyD88 (MYD88 innate immune signal transduction adaptor) and Tollip (Toll Interacting Protein). These kinases directly activate downstream transcription factors or other kinases such as p38 kinase (131). Another mechanism for activating the p38

kinase is the MAPK cascade. The stress signal responsive MAP3Ks phosphorylate its downstream targets MAP2Ks. Then the MAP2Ks, such as MAP2K3 and MAP2K6, directly phosphorylate and activate the p38 kinase (129,132,133). Interestingly, protein kinases called TAOs (Thousands And One amino acids) have been identified to have MAP3K function and can also phosphorylate MAP2Ks leading to the activation of p38 kinase (129). The activated p38 kinase can then influence its downstream targets. For example, the p38α kinase can trigger the nuclear localization of Nrf2. The activated p38 kinase phosphorylates MAPKAPK-2 (MAP Kinase-Activated Protein Kinase 2), which phosphorylates Nrf2 directly. As a result, the phosphorylated Nrf2 is nuclear-localized and upregulates its downstream targets, such as phase II detoxifying enzymes (134).

In *C. elegans*, the p38 pathway is conserved. The pathway starts with the activation of TIR-1, which is the *C. elegans* SARM1 (Sterile Alpha and TIR Motif containing 1) ortholog. The receptor triggers the MAPK cascade that consists of MAPKs: NSY-1 (the *C. elegans* MAP3K15 ortholog) and SEK-1 (the *C. elegans* MAP2K6 ortholog). As a result, PMK-1 (the *C. elegans* p38 map kinase family ortholog) becomes activated (135). The TIR domain is involved in both mammalian and *C. elegans* p38 pathways. It indicates that the stress response triggered by cytokines is conserved. Like mammalian p38 kinase, PMK-1 can directly phosphorylate its downstream targets. Not surprisingly, PMK-1 has shown to phosphorylate SKN-1 and encourages its nuclear localization, resulting in the upregulation of phase II detoxifying enzymes (135).

1.6.3 The IIS pathway

The IIS pathway is highly conserved among different species and involved in the development and longevity of an organism (136). The mammalian IIS signaling begins with a

ligand binding to a membrane-bound IGF1 receptor. The consequence of the binding is an activation of the PI3K (PhosphoInositide 3-Kinase), which catalyzes the synthesis of PIP_3 ($PI(3,4,5)P_3$) from PIP_2 ($PI(3,4)P_2$). On the other hand, PTEN (Phosphatase and TENsin homolog) prevents the formation of PIP_3 by using its phosphatase function. PIP_3 encourages the PDK1 (Phosphoinositide-Dependent Kinase 1) to phosphorylate the AKT (Protein Kinase B), which exposes its Thr 308 to the PDK1 through a conformational change at the plasma membrane (136,137). The phosphorylated AKT can phosphorylate its major downstream target FOXO, leading to the sequestration of the FOXO in the cytoplasm (138). As a result, the FOXO cannot enter the nucleus and enhance expressions of its targets such as SOD or CAT (26,27).

Unlike humans, *C. elegans* has only one FOXO transcription factor: DAF-16 (139,140). The fact that *C. elegans* has only one FOXO makes the worm a perfect candidate to study the pathway. As a model organism, *C. elegans* has numerous mammalian counterparts and the FOXO in the IIS pathway. The pathway is activated by DAF-2 (the *C. elegans* IGF-1 ortholog). The stress or ligand binding induced activation of DAF-2 leads to the formation of PIP_3 by AGE-1. As a result, the PIP_3 responding kinase PDK-1 phosphorylates Thr 350 and Ser 517 on AKT-1 and AKT-2 at the plasma membrane. Thus, the phosphorylation of DAF-16 by AKT-1/2 can be achieved, resulting in the nuclear exclusion of DAF-16. Like mammalian IIS signaling, *C. elegans* has DAF-18, the *C. elegans* PTEN ortholog that reduces the levels of PIP_3 (141–144). The effect of the nuclear exclusion of DAF-16 directly influences expression levels of its downstream targets such as CTL-1/2 and SOD-2/3 (59,60).

1.7 Rationale, Hypotheses, and Objectives of the Project

Cumulated research has identified PAX6 as a transcription factor that determines the development of symmetry and oxidative stress response of an organism (95,96,98,99,145). The expression patterns of PAX6 have been observed in various tissues such as the endocrine pancreas and nervous system (92,97). Additionally, the facts, that PAX6 can bind the promoter of catalase and tend to be highly nuclear-localized under the oxidative stress-inducing conditions, suggest that PAX6 may positively regulate the oxidative stress response (95,96,98,99,145). However, its role as a positive regulator and mechanisms in which it undergoes has not yet been determined. Furthermore, it is unclear whether PAX6 influences other oxidative stress responding elements such as phase II detoxifying enzymes. These enzymes are essential components of the ROS detoxification that resolves oxidative stress derived from both endogenous and exogenous causes (12,34,146).

Our lab discovered that worms with *brap-2(ok1492)* mutations exhibit L1 development arrest and show elevated basal expression levels of phase II detoxifying enzymes such as GST-4. Furthermore, our lab found that elevation in expression levels of *gst-4* in *brap-2(ok1492)* mutants is linked to SKN-1 nuclear localization in the worms (78,85). Thus, our lab determined that BRAP-2 negatively regulates the phase II enzyme expressions via regulating SKN-1 nuclear localization. Based on the finding that SKN-1, as a transcription factor, is involved in elevating *gst-4* expression in these mutants, our lab conducted a transcription factor specific RNAi screening on *brap-2(ok1492)* mutants to find other candidates that influence expression levels of phase II enzymes. Our lab found that *brap-2(ok1492)* mutants with *vab-3*, the *C. elegans pax6* ortholog gene, RNAi (RNA interference) showed a decrease in the basal expression levels of

GST-4 in *brap-2(ok1492)* mutants. This observation suggests the possibility of VAB-3/PAX6 being involved in the oxidative stress response.

Studies on PAX6 in human cell lines have shown that PAX6 binds catalase promoter and PAX6 becomes highly nuclear-localized under oxidative stress-inducing conditions. Additionally, RNAi targeting a *vab-3/pax6* gene in *brap-2(ok1492)* mutants decreased the basal expression levels of GST-4 in the mutants. Based on these findings, I will test multiple hypotheses to verify a possible role of VAB-3 in the *C. elegans* oxidative stress response. The hypotheses include (1) *vab-3* is required for the elevated basal *gst-4* expression levels in *brap-2(ok1492)* mutated worms, (2) *vab-3* is required for survival under oxidative stress-inducing conditions, and (3) VAB-3 is involved in the SKN-1 mediated regulation on the *gst-4* and *skn-1c* promoter. This project aims to identify the role of VAB-3 in the oxidative stress response, especially the phase II detoxification, and determine mechanisms on how VAB-3 influences the signal cascade on the ROS detoxification.

Materials and Methods

2.1 *C. elegans* Strains

All worms were maintained and cultured under the standard condition following the protocol designed by Sydney Brenner (147). The *Caenorhabditis* Genetics Center (The University of Minnesota) and the National Bioresource Project (Tokyo, Japan) are the source for strains. All experiments involving worms had Bristol N2 as wild type. All experiments were carried at 20 degree Celsius otherwise noted in the corresponding sections. The strains used in the project are as followed: YF15 [*brap-2(ok1492)II*], YF211 [*brap-2(ok1492)II; vab-3(e648)*], YF67 [*brap-2(ok1492)II; dvIs19(gst-4p::gfp)*], CL2166 [*dvIs19(gst-4p::gfp)*], YF212 [*dvIs19(gst-4p::gfp); vab-3(e648)*], CB648 [*vab-3(e648)*], DR466 [*him-5(e1490)V*].

2.2 Generation of Double Mutants

Two types of double mutants were generated: *brap-2(ok1492)II; vab-3(e648)* and *dvIs19 (gst-4p::gfp); vab-3(e648)*. To generate *brap-2(ok1492)II; vab-3(e648)* double mutants, L3 hermaphrodites with homozygous *brap-2(ok1492)II* mutations were crossed with L3 male *him-5 (e1490)V* mutants. The L3 male progenies with heterozygous *brap-2(ok1492)II* mutations were then crossed with L3 hermaphrodites with homozygous *vab-3(e648)* mutations. The male progenies and hermaphrodites with *vab-3(e648)* mutations were denoted as P1 (Parental strains). Additionally, the progenies hatched from the eggs laid by the P1 hermaphrodites were denoted as F1. After allowing the F1 hermaphrodites to lay their eggs on NGM (Nematode Growth Medium) plates, SW-PCR (Single Worm Polymerase Chain Reaction) was performed on the F1 hermaphrodites to find the heterozygous mutations for *brap-2(ok1492)II*. The progenies with

heterozygous *brap-2(ok1492)II* mutations were denoted as F2 hermaphrodites. The F2 worms with notched heads were picked; the phenotype of a homozygous *vab-3(e648)* mutant is a notched head. After allowing the F2 worms to lay their eggs, another SW-PCR was performed to find the worms with homozygous *brap-2(ok1492)II* mutations. The progenies of the F2 worms with homozygous *brap-2(ok1492)II* mutations were denoted as F3 and were individually picked and placed on NGM plates.

To generate *dvIs19(gst-4p::gfp); vab-3(e648)* double mutants, fluorescence microscopy was used to detect the GFP. L3 hermaphrodites with homozygous *dvIs19(gst-4p::gfp)* mutations were crossed with L3 male *him-5 (e1490)V* mutants. The L3 male progenies with heterozygous *dvIs19(gst-4p::gfp)* mutations were then crossed with L3 hermaphrodites with homozygous *vab-3(e648)* mutations. The male progenies and hermaphrodites with *vab-3(e648)* mutations were denoted as P1 (Parental strains). Additionally, the progenies hatched from the eggs laid by the P1 hermaphrodites were denoted as F1.

After allowing the F1 hermaphrodites to lay their eggs on NGM plates, fluorescence microscopy was used to find the heterozygous mutations for *dvIs19(gst-4p::gfp)* from the F1 generation. A heterozygous mutation for *dvIs19(gst-4p::gfp)* can make worms show GFP expressions that can be observed by fluorescence microscopy. The progenies with heterozygous *dvIs19(gst-4p::gfp)* mutations were denoted as F2 hermaphrodites. The F2 worms with notched heads (homozygous *vab-3(e648)* mutant phenotype) were picked. After allowing the F2 worms to lay their eggs, fluorescence microscopy was used again to find the worms with homozygous *dvIs19(gst-4p::gfp)* mutations. The detection of homozygous mutations for *dvIs19(gst-4p::gfp)* were achieved by finding NGM plates containing GFP expressing worms only. The other plates containing both GFP expressing worms and worms without GFP expressions were excluded. The

progenies of the F2 worms with homozygous *dvIs19(gst-4p::gfp)* mutations were denoted as F3 and were individually picked and placed on NGM plates. After F4 worms hatched from the eggs laid by the F3, the F4 worms were observed under a fluorescence microscope to find plates containing the F4 worms with GFP only; the F4 worms with GFP, then, were individually picked and placed on NGM plates.

2.3 SW-PCR (Single Worm Polymerase Chain Reaction)

The SW-PCR was used to verify the genotype of double mutants. A single worm was picked and transferred to a 0.2 mL PCR tube (Diamed SSI3131-06) containing 5 uL of 10x Thermopol buffer (NEB E5000S) with 1mg/ml Proteinase K (NEB P8107S). The tube was then stored at a -80 °C overnight. After freezing, the tube was placed in a thermocycler machine (Biometra T Personal Thermocycler) for Proteinase K reaction. Subsequently, 500 uL of PCR master mix was prepared with the following materials: 394 uL of nuclease-free H_2O (Bioshop WAT222), 50 uL of 10x Thermopol buffer (NEB E5000S), 50 uL of 2 mM dNTP mix (NEB E5000S), 2 uL of 100 uM forward primer, 2 uL of 100 uM reverse primer and 2 uL of Taq polymerase (NEB E5000S). After the tube underwent the proteinase K reaction, 20 uL of the PCR mix was added to the tube. The tube was placed in the thermocycler for PCR reaction following a program with a cycle involving appropriate melting and annealing temperature according to primer sets used. The PCR products were verified by gel electrophoresis using Gel XL Ultra V-2 gel box (Labnet Interantional Inc). The 1% agarose gel was made with 0.4 g of agarose (Sigma A9539-50G) and 40 mL of 1x TAE (Tris(hydroxymethyl)aminomethane Acetic acid Ethylenediaminetetraacetic acid) buffer (Thermofisher B49). The PCR products captured in the gel were visualized by UV light (Alphaimager).

2.4 Worm Synchronization

Worms used for assays in this project were synchronized following egg-lay protocol described by the Morimoto Lab (http://groups.molbiosci.northwestern.edu/morimoto/research/Protocols).

2.5 Fluorescence Microscopy

Two percent agarose gel was used as a pad on a glass slide for worms to be placed. Anesthetization of worms was achieved by adding 2 mM Levamisole (Sigma L9756) to the pad. After preparing Levamisole on the pad, worms were mounted on the slide. Fluorescence from worms was captured and visualized by a Zeiss LSM 700 confocal laser-scanning microscope with Zen 2010 Software.

2.6 RNAi (RNA interference)

The RNAi was performed using a transcription factor RNAi library generated by the Walhout lab. NGM (Nematode Growth Media) plates for RNAi were prepared with the following extra ingredients: 0.4 mM IPTG, 100 µg/mL Ampicillin and 12.5 µg/mL Tetracycline. Worms were synchronized on the RNAi plates and fed with transformed *Escherichia coli* (*E. coli*) HT115 that expressed dsRNA (double-strand RNA) from pL4440 plasmids to target the homologous sequence. After allowing worms to grow for 48 hours, worms were treated or collected according to the project plan.

2.7 RNA Purification and qRT-PCR

Generally, 50 µL of mixed-stage worms were collected in a 1.5 mL microtube. The worms were washed with M9 buffer 3 times and stored in a -80 °C freezer overnight. Three

hundred µL of TRI Reagent (Sigma 93289) was added to the tube containing the frozen worms. The tube was vortexed for 20 minutes at 4°C. After the vortex, 300 µL of anhydrous ethanol was added to the tube, and the tube was vortexed for 4 seconds at room temperature. The vortexed solution was transferred to a Zymo column (Zymo R2060) for nucleic acid purification. The purification was proceeded with the protocol provided by the manufacturer. The concentration of the nucleic acid was measured using NanoDrop2000. The purified sample was treated with the DNA-Free Kit (Ambion AM1906). The concentration of the DNAse 1 treated RNA sample was measured with NanoDrop2000. The RNA sample was then used for cDNA synthesis (Applied Biological Materials G233). Quantification of mRNA levels was achieved by qRT-PCR using SYBR green master mix (Applied Biological Materials MasterMix-S) and the Qiagen Rotor-Gene Q System (Qiagen R0511133). A triplicate measurement from biological repeats was used to obtain data. Analysis of the data was performed using Applied Biosystems Comparative CT Method (CT Method). Expression levels of mRNA from each strain were normalized and compared relative to the wild type control. Unless noted, the internal endogenous control gene for the qRT-PCR was *act-1* (Actin).

2.8 Oxidative Stress Assays

Worms were raised and synchronized at 20 °C. The synchronized L4 worms were picked and transferred to a 12-well plate with 5 mM Sodium As (arsenite) in 9 wells and M9 buffer as a negative control in 3 wells. M9 buffer was prepared by mixing 3.0 g KH_2PO_4, 6.0 g Na_2HPO_4, 0.5 g NaCl, and 1.0 g NH_4Cl in 1 L of H_2O. After the worms were placed in the plate, numbers of live worms were scored every 2 hours for 6 hours. The worms that were not responsive to poking by a worm pick were considered dead.

2.9 cDNA Cloning

To construct 3xFLAG::VAB-3, the coding sequence for VAB-3 (1368bp) was amplified from worm cDNA using PCR. The amplified PCR product was cloned in-frame to a BamHI and EcoRI digested pCMV 7.1 (3xFLAG) vector using the HI-FI Assembly Mix (NEB M5520A) following the protocol given by the manufacturer. The assembled products were used to transform DH5α *E. coli* cells. After the transformation, the cells were grown on plates with 100 µg/mL Ampicillin for selection. After growing the cells in a 37 °C incubator overnight, individual colonies were picked and used for PCR with primers targeting both sequences of VAB-3 and the 3xFLAG vector. The colonies with PCR products were picked and transferred to 13 mL tubes containing 2 mL of LB with 100 µg/mL Ampicillin. The tubes were placed in a 37 °C shaker overnight. One mL of the 2 mL culture was used to purify the pCMV-7.1-3xFALG-VAB-3 constructs using PureLink™ Quick Plasmid Miniprep Kit (Thermofisher K210010) and sent for sequencing. Once the sample sequence was verified, the positive culture was transferred to a 250 mL Erlenmeyer flask with 50 mL of LB and 100 µg/mL Ampicillin and placed in a 37 °C shaker overnight. The 50 mL of the culture was used to purify the constructs with PuroSPIN™ Plasmid MIDIprep (Luna #NK112-20) by following the protocol given by the manufacturer. The quality and concentration of the constructs were measured and checked with NanoDrop2000.

2.10 Primer Design

The primers for the cloning VAB-3 were generated using Snapgene (https://www.snapgene.com/). The forward primer had 50 bp, which had the first 25 bp of VAB-3 sequence and 25 bp from the pCMV7.1-3xFLAG vector sequence containing an EcoRI restrictive digestion site. The reverse primer had 50 bp, which had the last 25 bp of VAB-3

sequence and 25 bp from the pCMV7.1-3xFLAG vector sequence containing a BamHI restrictive digestion site.

2.11 Luciferase Assay

The effects of *C. elegans* transcription factors on the luciferase activity of firefly luciferase, which is under control of *C. elegans* promoters, were assessed by using HEK293T (Human Embryonic Kidney) cells. The cells were cultured in DMEM (Dulbecco's Modified Eagle's Medium) (Fisher 11995065) supplemented with 10% FBS (Fetal Bovine Serum) (Thermofisher A3160401). The cells with 90% confluency in a 10 cm plate were transferred to a 24-well plate. The plate was placed in a 37 °C cell incubator for 16 hours. After the incubation, the cells were co-transfected with Lipofectamine 3000 (Thermofisher L3000001) in Opti-MEM, the low serum media for 4 hours. The amount of DNA used for the transfection was 1.5 μg per well in the plate. The transfected cells were recovered with DMEM with 10% FBS for 24 hours. After the recovery, the cells were lysed for 15 minutes with lysis buffer (Biotium #30085-1) and transferred to a 96-well plate. The plate was prepared to check the luminescence from the cells by following the protocol provided by the manufacturer. Subsequently, the plate was placed in Synergy™ H4 Hybrid Multi-Mode Microplate Reader (BioTek) to quantify the luminescence.

2.12 Statistical Analysis

GraphPad Prism 8 Software was employed to perform statistical analysis. Student T-test, One-way, and Two-way ANOVA were used to determine statistical significance of the data. The data with statistical analysis showing P values under 0.05 were determined to have statistical significance. Error bars represent +/- standard error of the mean.

Results

3.1 A loss of *vab-3* negatively influences basal expression levels of *gst-4* in *brap-2(ok1492)* strains

brap-2(ok1492) strains, which have a 1540 bp deletion in ZnF-UBP and leucine heptad repeats domains, have elevated basal expression levels of GST-4 under non-oxidative stress-inducing conditions (78). To determine whether the elevation in expression levels of GST-4 in *brap-2(ok1492)* mutants requires expression of a *vab*-3 gene, I decided to use confocal microscopy to observe GFP (Green Fluorescent Protein) expression levels in *brap-2(ok1492); dvIs19(gst-4p::gfp)* reporter strains that were fed with *vab-3* RNAi inducing HT115 *E. coli* cells under non-oxidative stress-inducing conditions. The *brap-2(ok1492); dvIs19(gst-4p::gfp)* reporter strains were generated by crossing *brap-2(ok1492)* mutants with *dvIs19(gst-4p::gfp)* mutants which have GFP fused *gst-4* promoter. Thus, expression levels of GFP are proportional to expression levels of GST-4 in *brap-2(ok1492); dvIs19(gst-4p::gfp)* reporter strains. This experiment allowed me to visualize expression levels of GST-4 in *brap-2(ok1492)* strains treated with *vab-3* RNAi.

I found that intensity of the GFP in *brap-2(ok1492); dvIs19(gst-4p::gfp)* strains fed with HT115 cells expressing control pL4440 vectors were stronger than intensity of the GFP in *brap-2(ok1492); dvIs19(gst-4p::gfp)* strains with *vab-3* RNAi induction. Interestingly, *dvIs19(gst-4p::gfp)* strains, which did not have elevated levels of GST-4 expression induced by *brap-2* mutations, with either the control vectors or *vab-3* RNAi showed no significant increase or decrease of expression levels of GFP (Figure 3.1A). Such a result indicates that *vab-3* RNAi impacts *brap-2* mutation-induced expression levels of GST-4 but does not influence basal GST-4

expression levels. Next, to quantify GFP fluorescence in the reporter strains, I measured the intensity of the fluorescence captured by confocal microscopy using the ImageJ software. The quantified values showed that GFP fluorescence levels in *brap-2(ok1492); dvIs19(gst-4p::gfp)* strains with the pL4440 vectors were higher than GFP fluorescence levels in *brap-2(ok1492); dvIs19(gst-4p::gfp)* strains with *vab-3* RNAi induction (Figure 3.1B).

To further investigate effects of *vab-3* loss in expression levels of *gst-4* in *brap-2(ok1492)* strains, I generated *brap-2(ok1492); vab-3(e648)* double mutants by crossing *brap-2(ok1492)* strains with *vab-3(e648)* strains. I then performed qRT-PCR to measure basal *gst-4* mRNA levels in the double mutants under non-oxidative stress-inducing conditions. I found that *brap-2(ok1492); vab-3(e648)* strains displayed lower expression levels of basal *gst-4* mRNA levels than basal *gst-4* mRNA levels in *brap-2(ok1492)* strains. However, basal *gst-4* mRNA levels in *vab-3(e648)* strains were not significantly different from basal *gst-4* mRNA levels in N2 worms (Figure 3.2). These results suggest that the effects of *vab-3* mutation on *gst-4* mRNA levels influenced *brap-2* mutation-induced increase in *gst-4* mRNA levels only. In other words, expression of *vab-3* gene is required for *brap-2* mutation-induced increase in expression levels of *gst-4* but not for basal *gst-4* expression levels. These results collectively indicate that expression of *vab-3* gene is specifically required for a *brap-2* mutation-induced increase in *gst-4* expression in *brap-2(ok1492)* strains.

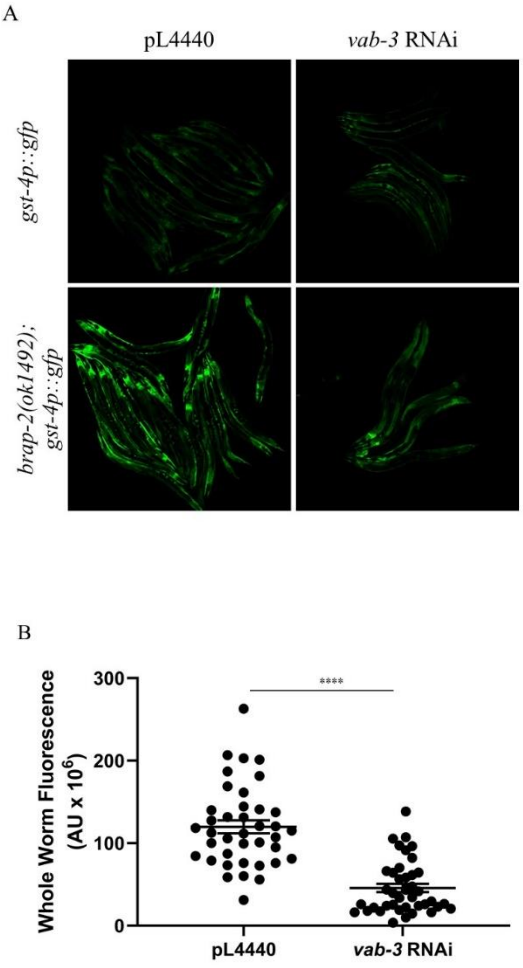

Figure 3. 1 *vab-3* RNAi reduces basal expression levels of *gst-4* in *brap-2(ok1492)* strains under non-oxidative stress-inducing conditions.

(A) Confocal images showing GFP fluorescence of *brap-2(ok1492); dvIs19(gst-4p::gfp)* and *dvIs19(gst-4p::gfp)* reporter strains. Both *brap-2(ok1492); dvIs19(gst-4p::gfp)* and *dvIs19(gst-4p::gfp)* strains were fed with HT115 *E.coli* cells that expressed either pL4440 vectors or dsRNA targeting *vab-3* mRNA for 48 hours. *brap-2(ok1492); dvIs19(gst-4p::gfp)* mutants with the pL4440 vector were used as positive controls, while the *dvIs19(gst-4p::gfp)* mutants were used as negative controls. The images were captured and rendered by Zen 2010 Software. (B) the *vab-3* knocked-down induced by *vab-3* RNAi significantly decreased intensity of the GFP fluorescence of *brap-2(ok1492); dvIs19(gst-4p::gfp)* mutants, while *dvIs19(gst-4p::gfp)* strains were not affected by *vab-3* RNAi induction under non-oxidative stress inducing conditions. For each strain under each condition, 39 worms were picked and used for the confocal microscopy and the quantification (n≈39). Statistical analysis was done using unpaired student t-test. $p<0.0001$****.

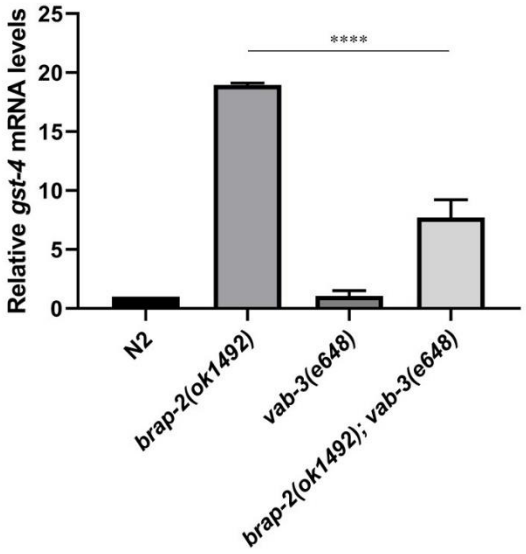

Figure 3. 2 *vab-3* mutation decreases basal *gst-4* mRNA levels in *brap-2(ok1492)* strains under non-oxidative stress-inducing conditions.

qRT-PCR was used to quantify mRNA levels of *gst-4*. Basal *gst-4* mRNA expression levels in *brap-2(ok1492); vab-3(e648)* double mutants were significantly lower than basal expression levels of *gst-4* mRNA in *brap-2(ok1492)* mutants. On the other hand, the difference between *vab-3(e648)* strains and N2, regarding basal expression levels of *gst-4* mRNA, was not statistically significant under non-oxidative stress-inducing conditions. Results were derived from 3 independent trials and normalized to *act-1* mRNA expression levels of the wild type (N2). Statistical analysis was done using one-way ANOVA. $p<0.0001$****.

3.2 *vab-3* is required for expression of *gst-4* of *C. elegans* under oxidative stress-inducing conditions

Both *vab-3* RNAi and *vab-3* mutations have shown their effects on a *brap-2(ok1492)* mutation-induced *gst-4* expression under non-oxidative stress-inducing conditions. To see whether the effects apply to the wild type (N2) with a loss of *vab-3* under either non-oxidative or oxidative stress-inducing conditions, I generated *dvIs19(gst-4p::gfp); vab-3(e648)* reporter strains by crossing *vab-3(e68)* strains with *dvIs19(gst-4p::gfp)* strains. I then assessed their responses to As (arsenite) treatment. Their fluorescence from GFP, which represents GST-4 expression due to its fusion to *gst-4* promoter, was captured and quantified. I found that *dvIs19(gst-4p::gfp); vab-3(e648)* strains treated with the As showed significantly lower fluorescence intensity than fluorescence captured from *dvIs19(gst-4p::gfp)* with the As treatment (Figure 3.3A). Furthermore, quantified fluorescence values of the *dvIs19(gst-4p::gfp); vab-3(e648)* strains were lower than the values of the *dvIs19(gst-4p::gfp)* (Figure 3.3B). Interestingly, the difference in GFP intensity between *dvIs19(gst-4p::gfp)* strains with M9 buffer, which was used as a negative control reagent, and *dvIs19(gst-4p::gfp); vab-3(e648)* strains with M9 buffer was not significant compared to the As treated groups. Such a result indicates that a loss of *vab-3* influenced the As induced GST-4 expression only. In other words, a loss of *vab-3* did not show any significant effect on baseline GST-4 expression levels (Figure 3.3A).

To ensure that the difference in the GFP intensity between *dvIs19(gst-4p::gfp)* and *dvIs19(gst-4p::gfp); vab-3(e648)* strains is due to *vab-3* mutations only, I performed confocal microscopy on *dvIs19(gst-4p::gfp)* reporter strains that were fed with *vab-3* RNAi inducing HT115 *E. coli* cells before the As treatment. The quantified values of fluorescence from the RNAi experiments showed that *dvIs19(gst-4p::gfp)* strains with *vab-3* RNAi displayed lower

GFP levels than *dvIs19(gst-4p::gfp)* strains without *vab-3* RNAi under oxidative stress-inducing conditions (Figure 3.3B). Such a result indicates that the GFP intensity difference was not from an unknown background mutation or RNAi off-target effects. In other words, only *vab-3* mutation or RNAi influenced the GST-4 expression levels.

To determine whether the GFP levels reflected expression levels of *gst-4* mRNA in worms, qRT-PCR was performed. I found that *vab-3(e648)* strains expressed lower levels of *gst-4* mRNA than *gst-4* expression levels of the wild type under As treatment, which provided oxidative stress-inducing conditions to the worms (Figure 3.4A). Like the previous experiments, *vab-3* mutations affected the worms under oxidative stress-inducing conditions only. To ensure that the results I observed from the mutation experiment were not due to an unknown background mutation, I performed qRT-PCR involving *vab-3* RNAi. I obtained the results which exhibited a similar trend as the results from the mutation experiments where the wild type with *vab-3* RNAi induction displayed reduced levels of *gst-4* mRNA expression than the wild type without the RNAi treatment under As treatment that induced oxidative stress response in the worms (Figure 3.5). However, while the trend showed that *gst-4* mRNA expression levels of the wild type without *vab-3* RNAi treatment were higher than the wild type without the RNAi treatment under the oxidative stress-inducing conditions, statistical analysis on the results showed no significance.

To test whether the difference was due to general oxidative stress or unique to the As treatment, other oxidative stress-inducing chemicals such as Ac (acrylamide) and PQ (paraquat) were used to induce the oxidative stress. Like the results derived from the As experiments, *vab-3(e648)* mutants showed decreased expression levels of *gst-4* mRNA levels than the wild type under AC (Figure 3.4B) or PQ treatment (Figure 3.4C). However, the experiment with PQ

treatment showed no statistical significance regarding the difference in *gst-4* mRNA expression levels between the wild type and *vab-3(e648)* strains. Such the difference suggests that *vab-3* may respond to the PQ induced oxidative stress differently compared to how *vab-3* responds to As or AC induced oxidative stress response. All in all, these results showed that *vab-3* is required for the expression of *gst-4* in *C. elegans* under oxidative stress-inducing conditions.

A

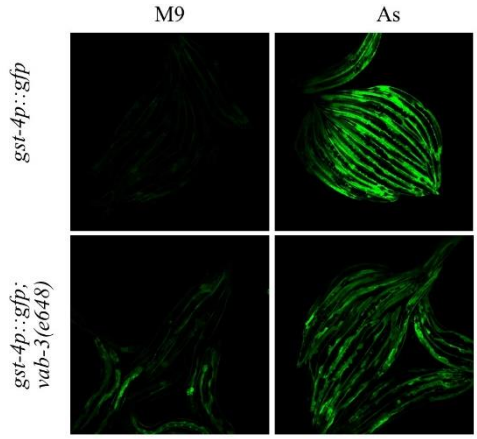

B

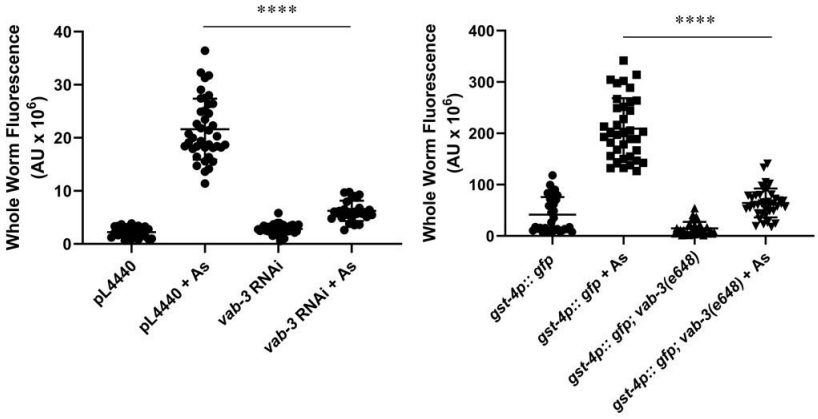

Figure 3. 3 *vab-3* is required for the expression of *gst-4* in *C. elegans* under oxidative stress-inducing conditions.

(A) Confocal images showing GFP fluorescence from *dvIs19(gst-4p::gfp)* and *dvIs19(gst-4p::gfp); vab-3(e648)* reporter strains. *dvIs19(gst-4p::gfp)* mutants treated with 5 mM As (arsenite) for 2 hours were used as positive controls, while *dvIs19(gst-4p::gfp)* and *dvIs19(gst-4p::gfp); vab-3(e648)* mutants treated with M9 buffer for 2 hours were used as negative controls. The images were captured and rendered by Zen 2010 Software. (B) Both *vab-3* RNAi and the *vab-3* mutation significantly decreased the GFP fluorescence intensity under the oxidative stress-inducing conditions. For the RNAi experiment, *dvIs19(gst-4p::gfp)* strains were fed with HT115 *E.coli* cells that expressed either pL4440 vectors or dsRNA targeting *vab-3* mRNA for 48 hours before being treated with either 5 mM As or M9 buffer for 2 hours. For each strain under each condition, 39 worms were picked and used for the confocal microscopy and the quantification (n≈39). Statistical analysis was done using one-way ANOVA. $p<0.0001$****.

A

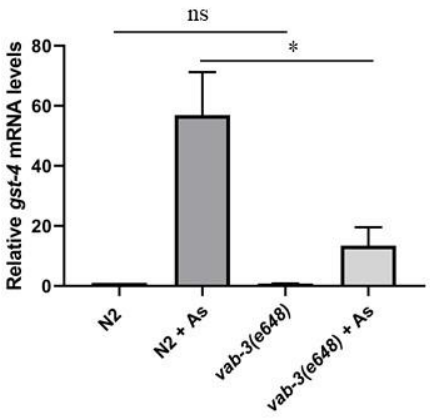

B

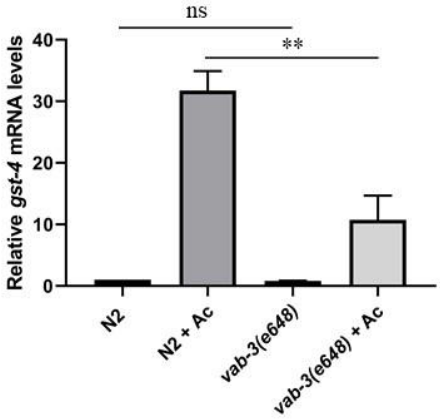

C

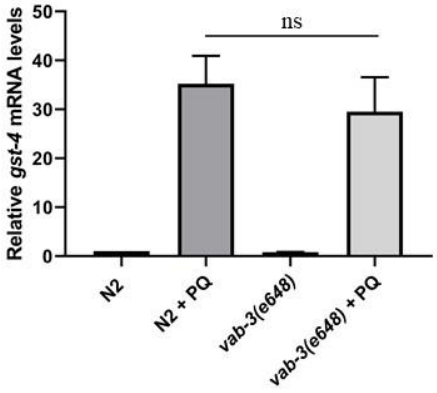

Figure 3. 4 *vab-3* mutations have decreased *gst-4* mRNA levels in *C. elegans* under oxidative stress-inducing conditions.

qRT-PCR was used to quantify mRNA levels of *gst-4. gst-4* mRNA expression levels of *vab-3(e648)* mutants were significantly lower than expression levels of *gst-4* mRNA in the wild type (N2). N2 worms treated with (A) 15 mM As (arsenite) or (B) 1g/L Ac (acrylamide) or (C) 200 mM PQ (paraquat) for 2 hours were used as positive controls, while the wild type and *vab-3(e648)* mutants treated with M9 buffer for 2 hours were used as negative controls. Results from each treatment were derived from 3 independent trials and normalized to *act-1* mRNA expression levels of the wild type. Statistical analysis was done using one-way ANOVA. $p<0.05$*, $p<0.01$**.

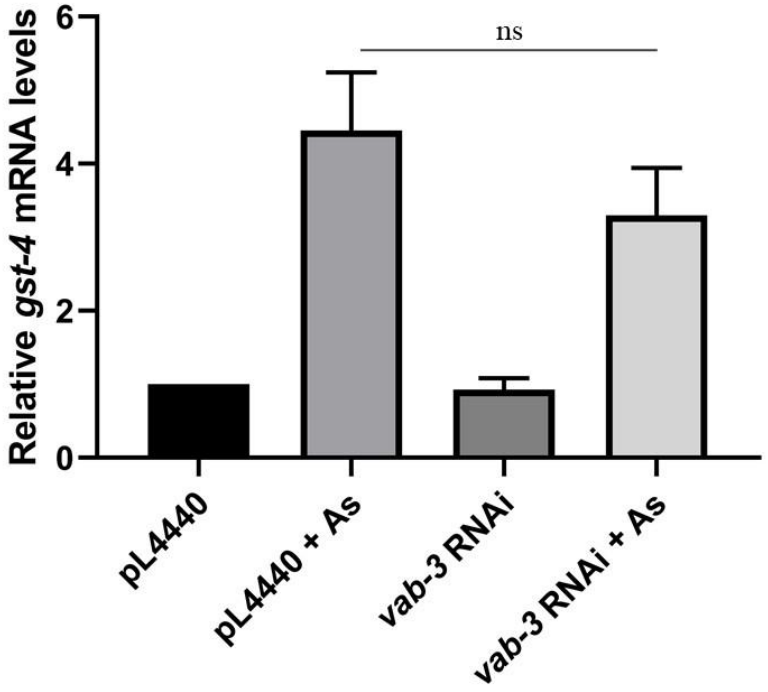

Figure 3. 5 *vab-3* RNAi downregulates *gst-4* mRNA levels in *C. elegans* under oxidative stress-inducing conditions.

qRT-PCR was used to quantify mRNA levels of *gst-4. gst-4* mRNA expression levels of the wild type (N2) with *vab-3* RNAi were lower than expression levels of *gst-4* mRNA in the wild type without the RNAi. The wild type was fed with HT115 *E.coli* cells that expressed either pL4440 vectors or dsRNA targeting *vab-3* mRNA for 48 hours before the treatment with either 15 mM As (arsenite) or M9 buffer for 2 hours. The wild type treated with 15 mM As was used as a positive control, while the wild type treated with M9 buffer for 2 hours was used as a negative control. Results were derived from 3 independent trials and normalized to *cdc-42* (the *C. elegans* CDC42 ortholog) mRNA expression levels of the wild type (148). Statistical analysis was done using one-way ANOVA.

3.3 *vab-3* is required for expression of ROS detoxifying genes of *C. elegans* under oxidative stress-inducing conditions

Besides GST-4 (GST ortholog), other phase II detoxifying enzymes also process ROS by the conjugation that results in stable compounds (58). As I found that a loss of *vab-3* has effects on *gst-4* mRNA expression levels in worms under oxidative stress-inducing conditions, I decided to determine whether a loss of *vab-3* affects mRNA expression levels of other phase II detoxifying genes in worms under oxidative stress-inducing conditions. Four genes were chosen to represent a phase II detoxifying enzyme group along with *gst-4*: *gsto-2* (the *C. elegans* GSTO1 ortholog), *dhs-8* (the *C. elegans* WWOX ortholog), *sdz-8* (the *C. elelgans* CBR3 ortholog), and *ugt-13* (the *C. elegans* UGT1A1 ortholog) (78). Using qRT-PCR, I found the difference in expression levels of these genes between *vab-3(e648)* mutants and the wild type (N2) under As treatment. Expression levels of the 4 genes in *vab-3(e648)* mutants were lower than the expression levels of the wild type. However, only the difference observed in *sdz-8,* and *ugt-13* mRNA levels were statically significant. In other words, the difference was seen in *gsto-2* and *dhs-8* mRNA levels between the wild type and *vab-3(e648)* strains were not statistically significant (Figure 3.6). Such results suggest that a loss of *vab-3* may not influence all phase II detoxifying genes.

Along with phase II detoxifying genes, CTL-1/2 (the *C. elegans* CAT orthologs) helps *C. elegans* to manage ROS levels by breaking down hydrogen peroxide into water and oxygen molecules (59,60). Additionally, overexpressed PAX6 (the human VAB-3 ortholog) in HepG2, a human lung cancer cell line, has shown to enhance the CAT promoter activity (98). Based on these findings, I measured mRNA levels of *ctl-1/2* to test whether a loss of *vab-3* affects these genes under oxidative stress-inducing conditions using PQ treatment. Like the phase II

detoxifying genes, both *ctl-1* and *ctl-2* mRNA expression levels were reduced by a loss of *vab-3* under oxidative stress-inducing conditions (Figure 3.7). However, only the experiment involving the *ctl-1* mRNA measure showed statistical significance. Such a result indicates that a loss of *vab-3* may influence *ctl-1* selectively but not *ctl-2*. All in all, the results obtained from these experiments suggest that a *vab-3* gene is required for the expression of ROS detoxifying enzymes under oxidative stress-inducing conditions in *C. elegans*.

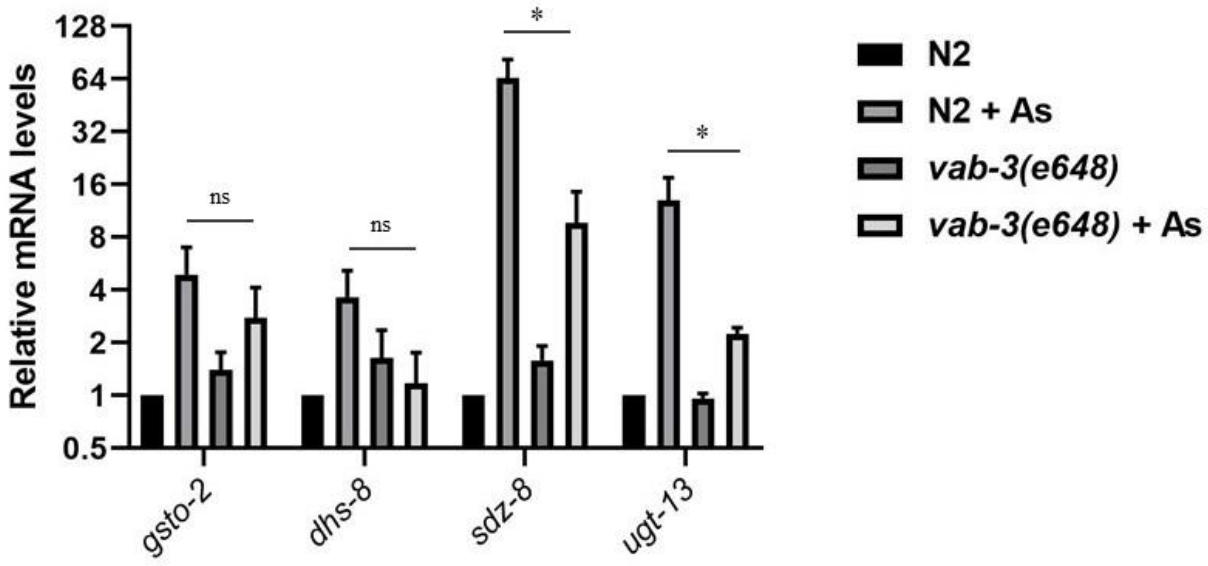

Figure 3. 6 *vab-3* is required for the expression of *sdz-8* and *ugt-13* genes of *C. elegans* under oxidative stress-inducing conditions.

qRT-PCR was used to quantify mRNA levels of phase II detoxifying genes: *gsto-2, dhs-8, sdz-8* and *ugt-13.* mRNA expression levels of phase II detoxifying genes of *vab-3(e648)* mutants were lower than mRNA expression levels of phase II detoxifying genes in the wild type (N2). The wild type treated with 15 mM As (arsenite) for 2 hours was used as a positive control, while the wild type and *vab-3(e648)* mutants treated with M9 buffer for 2 hours were used as negative controls. Results were derived from 3 independent trials and normalized to *act-1* mRNA expression levels of the wild type. Statistical analysis was done using one-way ANOVA. $p<0.05$*.

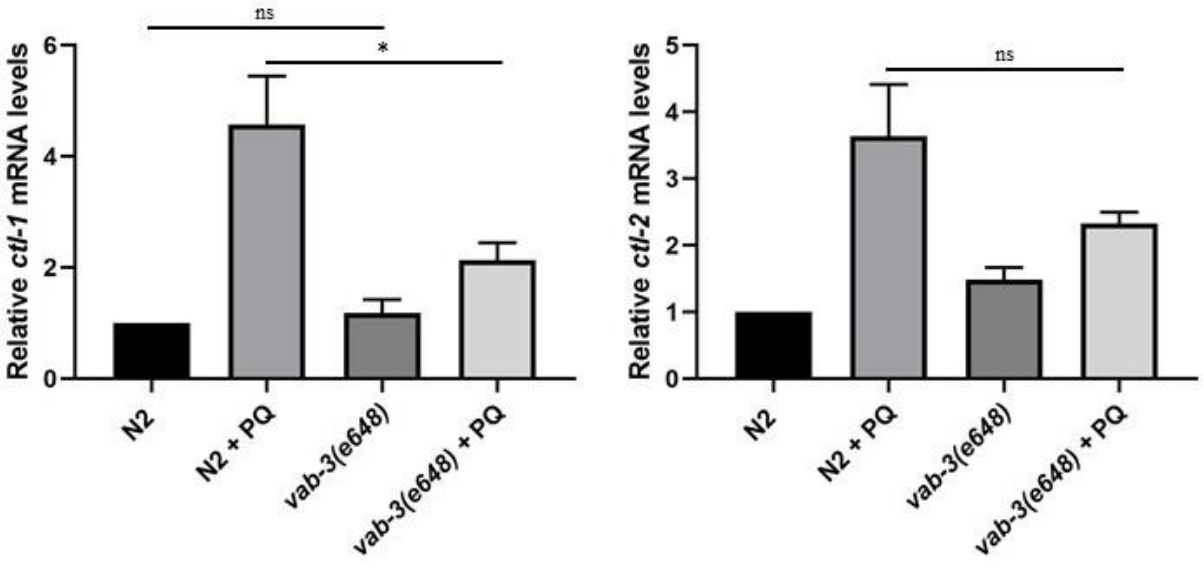

Figure 3. 7 *vab-3* is required for the expression of *ctl-1* of *C. elegans* under oxidative stress-inducing conditions.

qRT-PCR was used to quantify mRNA levels of *ctl-1* and *ctl-2*. mRNA expression levels of *ctl-1* and *ctl-2* of *vab-3(e648)* mutants were lower than mRNA expression levels of *ctl-1* and *ctl-2* in the wild type (N2) under the oxidative stress-inducing conditions. The wild type treated with 200 mM PQ (paraquat) for 2 hours was used as a positive control, while the wild type and *vab-3(e648)* mutants treated with M9 buffer for 2 hours were used as negative controls. Results were derived from 3 independent trials and normalized to *act-1* mRNA expression levels of the wild type. Statistical analysis was done using one-way ANOVA. $p<0.05$*.

3.4 a Loss of VAB-3 reduces survivability of *C. elegans* under oxidative stress-inducing conditions

Both catalase and phase II detoxifying enzymes are required for *C. elegans* to protect itself from ROS (59,60). Since a loss of *vab-3* showed its impact on mRNA levels of phase II detoxifying genes (*gst-4*, *sdz-8*, and *dhs-8*) and catalase (*ctl-1*) in worms under oxidative stress-inducing conditions, I sought to determine whether a loss of *vab-3* affects worm survival under oxidative stress-inducing conditions. I performed oxidative stress assays with *vab-3(e648)* mutants and found that the mutants were more susceptible to the oxidative stress-induced death than the wild type (N2). The difference between the mutants and wild type occurred as early as at 2 hours mark. Furthermore, the wild type with *vab-3* RNAi induction also showed their extreme sensitivity toward the oxidative stress. Therefore, both *vab-3* mutants and *vab-3* RNAi treated animals have dramatically decreased survivability of worms under oxidative stress (Figure 3.8).

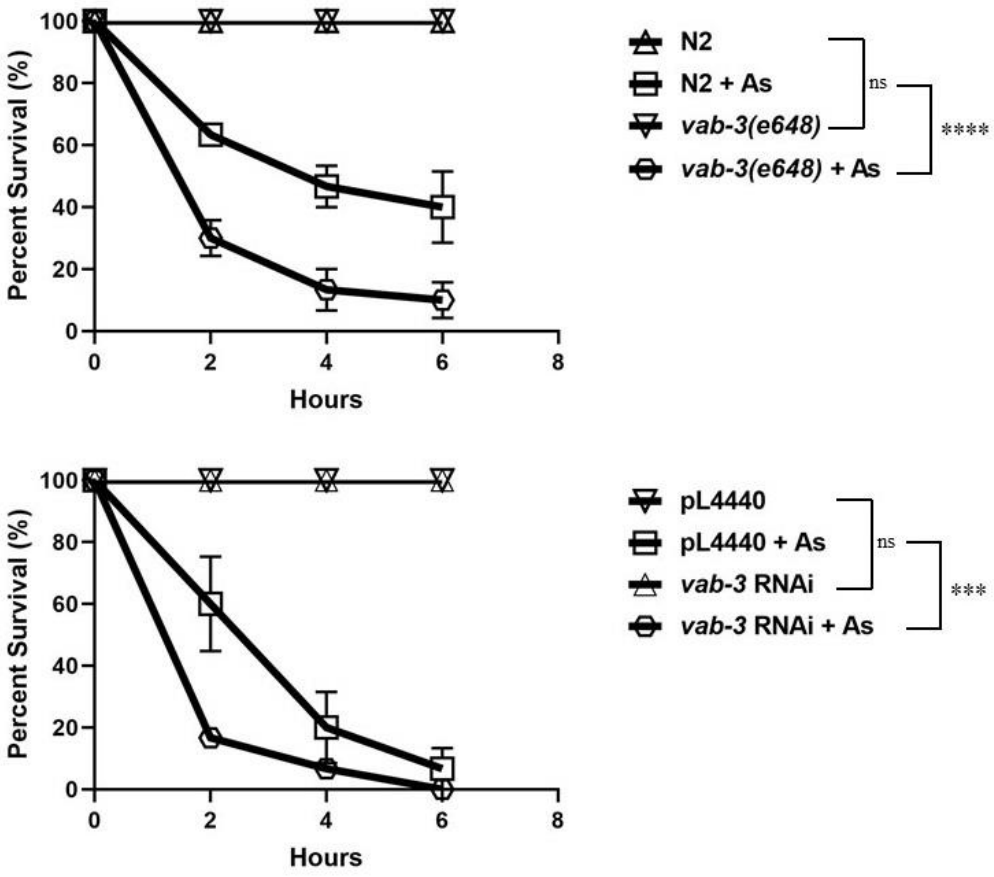

Figure 3. 8 The wild type has higher resistance against oxidative stress than worms with either *vab-3* mutation or *vab-3* RNAi.

Worms with *vab-3* mutation or *vab-3* RNAi showed high sensitivity toward the stress. Survival assays were performed to score the survivability of the worms in oxidative stress-inducing conditions. For the *vab-3* RNAi induction, the wild type (N2) was fed with HT115 *E.coli* cells that expressed either pL4440 vectors or dsRNA targeting *vab-3* mRNA for 48 hours before the treatment with 5 mM As (arsenite) or M9 buffer for 6 hours. For each strain under each condition, 30 worms were picked and used for the assay (n≈30). Statistical analysis was done by using two-way ANOVA. $p<0.0001$****, $p<0.001$***.

3.5 VAB-3 enhances SKN-1 mediated *gst-4* and *skn-1c* promoter activation

To understand how VAB-3 contributes to oxidative stress responses of worms, I tested whether VAB-3 influences SKN-1 activation of the *gst-4* promoter using HEK (Human Embryonic Kidney) 293T cells that were co-transfected with a luciferase reporter construct fused to the *gst-4* promoter along with SKN-1 and/or VAB-3. I found that the luciferase activity in the cells co-transfected with the reporter construct and VAB-3 or SKN-1 was higher than luciferase activities measured in cells transfected with the reporter construct only. Furthermore, the luminescence results from the luciferase assays showed a synergistic increase in the luciferase activity when the reporter construct was co-transfected with both SKN-1 and VAB-3 (Figure 3.9). These findings suggest that VAB-3 enhances SKN-1 activation of the *gst-4* promoter as a synergistic factor.

Based on the finding that SKN-1 transactivates itself through a binding *skn-1c* promoter, I performed another luciferase assays to determine whether VAB-3 affects the upstream of the *skn-1c* promoter as well (78). A luciferase reporter construct fused to the *skn-1c* promoter instead of the *gst-4* promoter was used for this assay. Like the assay results with the *gst-4* promoter, the HEK293T cells co-transfected with either SKN-1 or VAB-3 alone showed higher luminescence values than the cells with the reporter construct only. Additionally, the luminescence results showed the highest luciferase activity when HEK293T cells were co-transfected with both SKN-1 and VAB-3 (Figure 3.10). Such results indicate that SKN-1 and VAB-3 produce a synergistic effect on activating the *skn-1c* promoter.

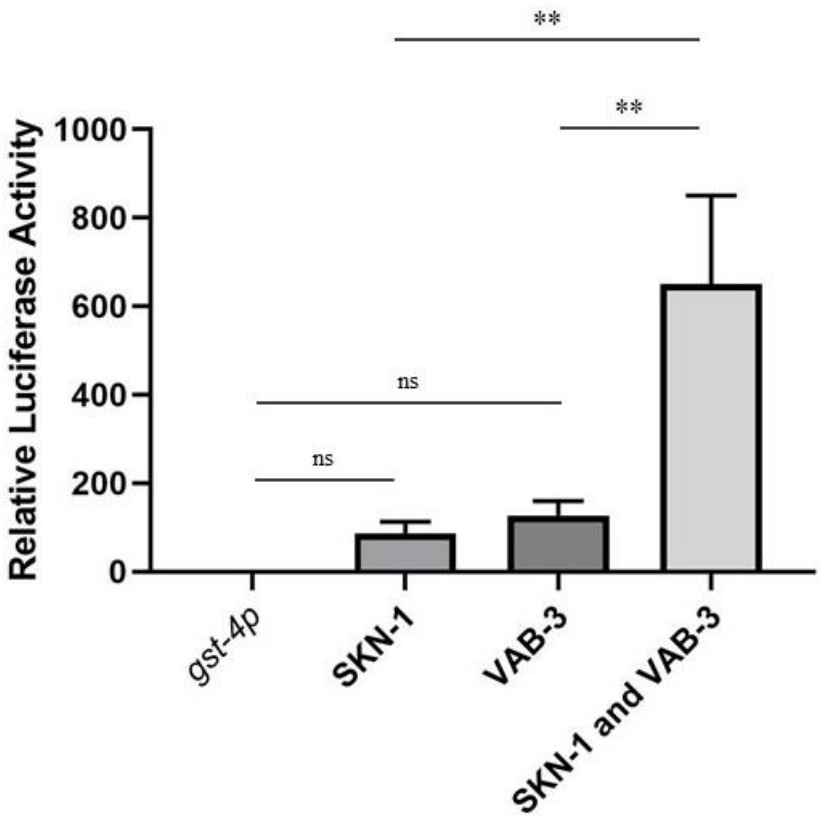

Figure 3. 9 VAB-3 enhances the SKN-1 mediated *gst-4* promoter activation.

The luminescence of firefly luciferases expressed from pGL4-*gst-4p* reporter vectors was dramatically elevated when SKN-1 and VAB-3 were co-expressed in HEK (Human Embryonic Kidney) 293T cells. The cells were co-transfected with one of the following combinations: (a) pGL4-*gst-4p* with the control EGFP vectors and 3xFLAG vectors, (b) pGL4-*gst-4p* with EGFP tagged SKN-1 and the control 3xFLAG vectors, (c) pGL4-*gst-4p* with the control EGFP vectors and 3xFLAG tagged VAB-3, or (d) pGL4-*gst-4p* with EGFP tagged SKN-1 and 3xFLAG tagged VAB-3. Results were derived from 7 independent trials and normalized to measured luminescence values from the cells transfected with (a) combination. Statistical analysis was done using one-way ANOVA. $p<0.01$**.

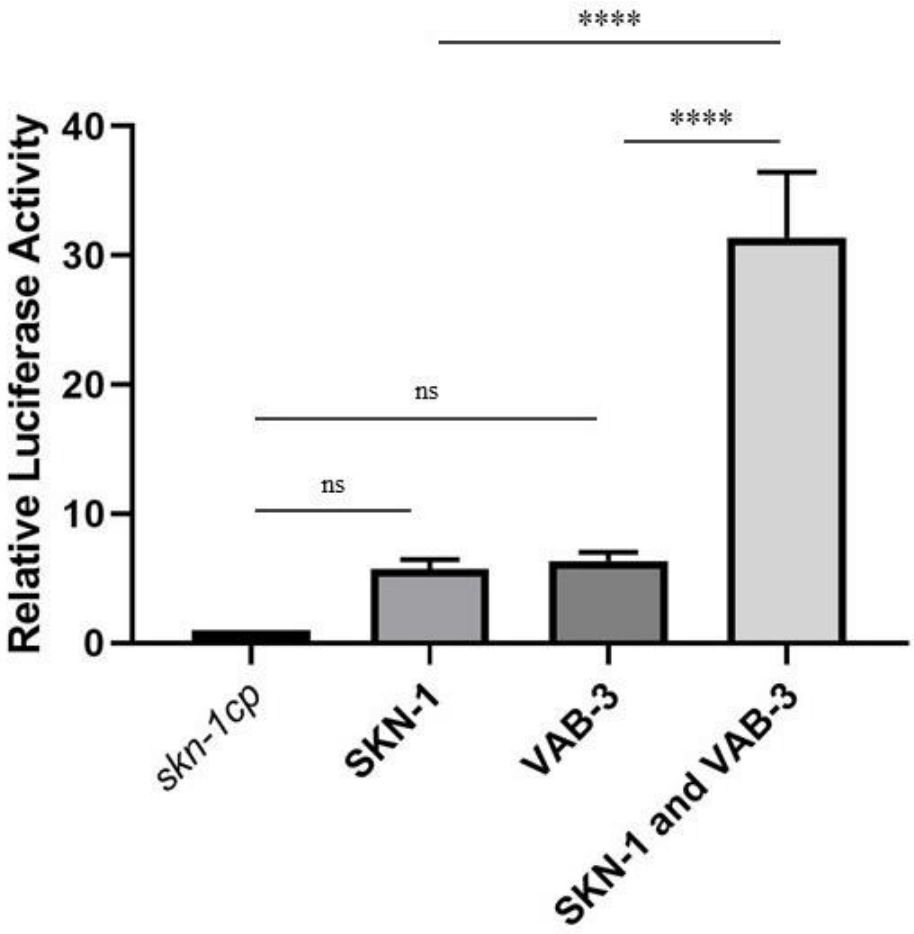

Figure 3. 10 VAB-3 enhances the SKN-1 mediated *skn-1c* promoter activation.

The luminescence of firefly luciferases expressed from pGL4-*skn-1cp* reporter vector was dramatically elevated when SKN-1 and VAB-3 were co-expressed in HEK (Human Embryonic Kidney) 293T cells. The cells were co-transfected with one of the following combinations: (a) pGL4-*skn-1cp* with the control EGFP vectors and 3xFLAG vectors, (b) pGL4-*skn-1cp* with EGFP tagged SKN-1 and the control 3xFLAG vectors, (c) pGL4 *skn-1cp* with the control EGFP vectors and 3xFLAG tagged VAB-3, or (d) pGL4-*skn-1cp* with EGFP tagged SKN-1 and 3xFLAG tagged VAB-3. Results were derived from 4 independent trials and normalized to measured luminescence values from the cells transfected with (a) combination. Statistical analysis was done using one-way ANOVA. $p<0.0001$****.

Discussion

4.1 Summary

This project aimed to define the role of VAB-3 in the oxidative stress response and report how vital VAB-3 is for *C. elegans* survival against oxidative stress. Through the project, I have identified VAB-3 as a positive regulator required for expressions of ROS detoxifying enzymes and demonstrated that VAB-3 is required for the oxidative stress response of *C. elegans.* I have found that (1) *vab-3* is required for the elevated basal *gst-4* expression levels in *brap-2(ok1492)* mutated worms, (2) *vab-3* is required for the oxidative stress response, and (3) VAB-3 is involved in the SKN-1 mediated regulation on the *gst-4* and *skn-1c* promoter.

4.2 Validation of *vab-3* as a gene that positively regulates basal expression levels of *gst-4* in *brap-2(ok1492)* mutants

The focus of our lab is to determine genetic links among *brap-2*, *skn-1*, and *vab-3* and the oxidative stress response of *C. elegans* in the context of signaling pathways. In mammals, BRAP2, a BRCA1 binding protein, and cytoplasmic retention protein, has been characterized as a Ras effector protein (80–82). Additionally, Nrf2 has been reported to regulate phase II detoxifying enzymes via nuclear localization under the control of the Ras signaling pathway (37–39,43). Since BRAP-2 is a *C. elegans* ortholog of mammalian BRAP2 and SKN-1 is a *C. elegans* ortholog of mammalian Nrf2 and a major activator of phase II detoxifying enzymes, it is hypothesized that BRAP-2 may regulate SKN-1 nuclear localization through the Ras signaling pathway. Previously, our lab has demonstrated a genetic interaction between *brap-2* and *skn-1*. The presence of highly nuclear-localized SKN-1 and elevated basal expression levels of SKN-1

target genes in *brap-2(ok1492)* mutants have illustrated that BRAP-2 down-regulates expression levels of SKN-1 target genes via negatively regulating SKN-1 nuclear localization (78).

Among the phase II detoxifying enzymes, the basal expression level of *gst-4* was affected most by *brap-2* mutations in *C. elegans*. Furthermore, a transcription factor specific RNAi screening on *brap-2(ok1492)* mutants has shown that the *brap-2* mutation mediated increase in *gst-4* expression levels was reduced by *vab-3* RNAi knockdown (78). Based on the facts that (1) *vab*-3 RNAi reduces basal *gst-4* expression levels in *brap-2(ok1492)* mutants, (2) VAB-3 is a *C. elegans* ortholog of mammalian PAX6, and (3) PAX6 has been reported to enhance oxidative stress response in mammalian cell lines, I sought to validate the genetic link between *brap-2* and *vab-3* regarding the basal *gst-4* expression levels and find out whether *vab-3* is required for the basal *gst-4* expression (78,101,111).

Using *brap-2(ok1492); dvIs19(gst-4p::gfp)* reporter strains and *brap-2(ok1492); vab-3(e648)* double mutants, the results in this project demonstrate a role for *vab-3* in the basal *gst-4* expression in the *brap-2(ok1492)* mutants. The *vab-3* is required for *brap-2(ok1492)* mutants to express higher basal expression levels of *gst-4* than the wild type (N2). Thus, I determined that *vab-3* promotes increased basal *gst-4* expressions in *brap-2(ok1492)* mutants. GSTs have been a major element for measuring oxidative stress responses in eukaryotic cells (33). Since *C. elegans* also belongs to eukaryotes, GSTs are conserved in worms (58). GSTs, as a member of phase II detoxifying enzymes, are required to resolve oxidative stress within the cell. They achieve a reduction in oxidative stress by conjugating reduced GSH to free radicals. Thus, elevated levels of GSTs in the cell indicates that the cell is under oxidative stress-inducing conditions such as exposures to chemicals or IR (33). In *brap-2(ok1492)* mutants, the worms express higher basal levels of *gst-4* than the wild type under non-oxidative stress-inducing conditions (78). However,

the degree of this increase in *brap-2(ok1492)* mutants was decreased by *vab-3* RNAi or mutation.

The results from the confocal microscopy has shown decreased GFP intensity in *brap-2(ok1492); dvIs19(gst-4p::gfp)* double mutants, that had GFP sequence fused to promoter of the *gst-4*, with *vab-3* RNAi than *brap-2(ok1492); dvIs19(gst-4p::gfp)* without the RNAi. Furthermore, the quantified values of the GFP intensity obtained from multiple numbers of *brap-2(ok1492); dvIs19(gst-4p::gfp)* mutants have shown a similar trend as the intensity comparison; the mutants with *vab-3* RNAi displayed lowered levels of the GFP than the mutants without the RNAi. These results indicate that *vab-3* was required for the *brap-2(ok1492)* mutants to keep their *gst-4* expression levels high.

Additionally, qRT-PCR performed on *brap-2(ok1492); vab-3(e648)* double mutants has shown a decrease in basal *gst-4* expression levels. Although *brap-2(ok1492); vab-3(e648)* double mutants expressed elevated basal levels of *gst-4* mRNA than the wild type, the levels were lower than *brap-2(ok1492)* mutants without *vab-3* mutations. Such a result agrees with the GFP experiment and illustrates that a *vab-3* gene is essential for *brap-2(ok1492)* mutants to express elevated basal levels of *gst-4* mRNA. Confocal microscopy and qRT-PCR performed by Hu also showed similar results. The microscopy involving *brap-2(ok1492); dvIs19(gst-4p::gfp)* with *elt-3* RNAi showed decreased basal expression levels of *gst-4*. Moreover, *brap-2(ok1492); elt-3(vp1)* double mutants exhibited reduced basal expression levels of *gst-4* (78). These findings indicate that *vab-3*, like *elt-3*, positively affects basal expression levels of *gst-4* in *brap-2(ok1492)* mutants.

One may assume that *brap-2(ok1492)* strains would survive better than the wild type under oxidative stress-inducing conditions due to elevated basal expression levels of phase II

detoxifying enzymes (78). However, *brap-2(ok1492)* strains would not survive better than the wild type under oxidative stress-inducing conditions. *brap-2* mutation affects the expression of phase II detoxifying enzymes and other stress responses of *C. elegans.* Recent dauer defective assays involving *brap-2(ok1492)* strains revealed that *brap-2(ok1492)* strains failed to enter dauer upon exposure to SDS (Sodium Dodecyl Sulphate-polyacrylamide) treatment, while the wild type could enter dauer (149). Such a finding indicates that a *brap-2* gene is required for other stress responses. Thus, although *brap-2(ok1492)* strains have elevated basal expression levels of phase II detoxifying enzymes, the strains may have defects in other responses required for the protection against oxidative stress. Hence, *brap-2(ok1492)* strains would not survive better than the wild type under oxidative stress-inducing conditions.

4.3 Validation of *vab-3* as an oxidative stress response gene in *C. elegans*

In human lung cancer cell lines, overexpressed PAX6 has been confirmed to enhance the promoter activity of catalase. Furthermore, PAX6 was highly nuclear localized in human pancreatic carcinoma cell line under the oxidative stress-inducing conditions (98,99). Since VAB-3 is the *C. elegans* ortholog of PAX6 and has been shown to influence basal expression levels of the *gst-4*, a ROS detoxifying enzyme, in *brap-2(ok1492)* mutants, I postulated that VAB-3 might contribute to general oxidative stress response in *C. elegans*. Using *dvIs19(gst-4p::gfp)* and *dvIs19(gst-4p::gfp); vab-3(e648)* reporter strains, I have found that both *vab-3* mutations and RNAi down-regulated the *gst-4* promoter activity in the strains that were stressed by As (arsenite). The fact that both mutations and RNAi experiments resulted in a similar effect indicates that these results were not obtained from background mutations or off-target RNAi effects. In other words, the downregulation of the promoter activity was due to the knocked down or knocked out only.

From the qRT-PCR experiments involving oxidative stress induced by As, both the *vab-3* RNAi induced wild type (N2) and *vab-3(e648)* mutants have shown decreased expression levels of *gst-4* mRNA compared to expression levels of *gst-4* mRNA in the wild type under the same oxidative stress-inducing conditions. However, unlike the experiments with *vab-3(e648)* mutants, the statistical analysis on the RNAi experiments showed no significance. While it is unclear why the RNAi experiments did not show the significance, one may explain through examining the effects of different diet given to the worms.

In molecular genetics research involving *C. elegans*, it is common to feed worms with bacteria expressing dsRNA to achieve gene knock-down (150). For RNAi experiments, worms are fed HT115 *E. coli* strains instead of OP50 *E, coli* strains. OP50 strains are standard diet used for maintaining *C. elegans* and have been used by researchers in *C. elegans* community. On the other hand, HT115 strains are used for RNAi experiments since OP50 strains cannot express dsRNA like HT115 strains (147,151,152). These 2 different strains have different effects on gene expressions, development, metabolism, behavior, and aging in *C. elegans* (153–159).

Recent research regarding the effects of *C. elegans* diet has shown that worms fed HT115 strains showed higher oxygen consumption than worms fed OP50 strains (160). Such finding suggests that HT115 strains induce oxidative stress in *C. elegans* more than OP50 strains induce the stress in *C. elegans*. An increase in oxygen consumption in organisms is an indication that oxidative stress is induced in the organisms. For instance, Tiwari and colleagues showed that Arabidopsis plant cells exhibited the accelerated oxygen consumption when the cells were incubated with GO (Glycine Oxidase), which catalyzed chemical reaction that resulted in the production of hydrogen peroxide. They determined that oxygen consumption was increased due

to the oxidative stress induced by GO treatment (161). Thus, these findings agree with the finding that HT115 strains can induce oxidative stress in *C. elegans*.

The fact that HT115 strains induce oxidative stress in worms may explain why the gap in expression levels of *gst-4* mRNA between the wild type under oxidative stress-inducing conditions and the wild type under non-oxidative stress-inducing conditions was not huge in the RNAi experiments. From the qPCR experiments, I found that expression levels of *gst-4* mRNA in the wild type fed OP50 with oxidative stress induced by As were about 60 times higher than the wild type fed OP50 under non-oxidative stress-inducing conditions. On the other hand, expression levels of *gst-4* mRNA in the wild type fed HT115 with oxidative stress induced by As were only 4 times higher than the wild type fed HT115 under non-oxidative stress-inducing conditions. Since the effect of As was consistent among all the worms, the results indicate that the negative control group fed HT115 had higher expression levels of *gst-4* mRNA than the negative control group fed OP50 due to the oxidative stress induced by HT115 strains. In other words, HT115 strains induced oxidative stress in worms and resulted in increased basal expression levels of *gst-4* mRNA in the worms in the RNAi experiments.

Another factor that might have contributed to determining the significance of the RNAi experiments is the difference between gene knock-down and gene knock-out. While mutations can permanently prevent the expression of target genes, RNAi can achieve complete silence of gene expression or partial reduction on gene expression (162–164). In the case of *vab-3* RNAi treatment, it induces a partial reduction in expression levels of *vab-3* in *C. elegans*. Worms with homozygous *vab-3(e648)* mutation exhibit phenotypes where they develop abnormal alae, a protruding ridge, at the anterior hypodermal region (109). However, *vab-3* RNAi did not cause the development of the abnormal alae in worms. In other words, the worms with *vab-3* RNAi

still had *vab-3* gene expressed. Such a difference might have been applied to expression levels of *gst-4* mRNA levels.

The qPCR results on *vab-3(e648)* mutants under the oxidative stress-inducing conditions showed greatly reduced expression levels of *gst-4* mRNA compared to the wild type under the oxidative stress-inducing conditions. On the other hand, worms treated with *vab-3* RNAi and oxidative stress induced by As did not show the decrease in expression levels of *gst-4* mRNA as much as the decrease observed in *vab-3(e648)* mutants under oxidative stress induced by As. These results suggest that the effects of complete knockout of a *vab-3* gene on *gst-4* mRNA expression were greater than the effects of *vab-3* RNAi on *gst-4* mRNA expression. On the whole, the combination of the facts that (1) HT115 strains increase basal expression levels of *gst-4* mRNA in worms by inducing oxidative stress and (2) *vab-3* RNAi has a relatively weaker impact on expression levels of *gst-4* mRNA than *vab-3* mutations as it only partially reduces *vab-3* gene expression in worms, may be the reason why the RNAi experiment did not show the significance.

A loss of *vab-3* has shown its effect on *gst-4* mRNA expression levels in worms under oxidative stress conditions induced by As. To investigate whether the effect of a loss of *vab-3* was specific to the As treatment, I induced oxidative stress in *vab-3(e648)* mutants by using different chemicals such as PQ (Paraquat) or Ac (Acrylamide) and measured *gst-4* mRNA expression levels in these mutants. I found that, regardless of the source of oxidative stress, *gst-4* mRNA expression levels of the wild type were increased upon exposure to oxidative stress-inducing chemicals. Additionally, *gst-4* mRNA expression levels were greatly reduced in *vab-3(e648)* strains under Ac treatment like the *vab-3(e648)* mutants with As treatment. However, *gst-4* mRNA expression levels in *vab-3(e648)* strains under PQ treatment were not greatly

reduced like the reduction observed in expression levels of *gst-4* mRNA in *vab-3(e648)* under either Ac or As treatment. These results suggest that PQ treatment may work differently compared to As or Ac treatment on *vab-3(e648)* mutants.

As causes oxidative stress by activating radicals producing systems such as NADH (Reduced form of Nicotinamide Adenine Dinucleotide) oxidase or plasma membrane NADPH (Reduced form of Nicotinamide Adenine Dinucleotide Phosphate) oxidase which then produces superoxide anions (165,166). On the other hand, PQ is known to produce hydrogen peroxide through NADPH mediated PQ redox cycle. The PQ redox cycle involves the reduction of PQ by NADPH-cytochrome c reductase and oxidation of the reduced PQ by NADPH-cytochrome P-450. The interaction between the reduced PQ and NADPH-cytochrome P-450 results in the production of hydrogen peroxide (167–169). Lastly, Ac induces oxidative stress by consuming GSH. Cytochrome P450 is responsible for metabolizing Ac and converts it into a reactive epoxide called GA (GlycidAmide). GA can then bind cellular nucleophiles with functional groups like -SH, -OH, or -NH_2 groups such as GSH (170–177). Since GSH is an essential element in the cell to balance free radical levels, consumption of GSH by GA contributes to the induction of oxidative stress (178–180).

While it is unclear why a loss of *vab-3* did not have much impact on expression levels of *gst-4* mRNA in *vab-3(e648)* strains under PQ treatment, one may be able to attempt to explain why the impact was not significant through exploring differences in how each chemical induces oxidative stress in cells. Among the 3 chemicals used to induce oxidative stress in worms, only PQ is known to be processed by NADPH-cytochrome c reductase. Cytochrome c reductase is part of ETC (Electron Transport Chain) in mitochondria and reduces Cytochrome C by

transferring electrons from ubiquinol (181). Additionally, under oxidative stress-inducing conditions, cytochrome c can be leaked into the cytosol from mitochondria (182).

Recent findings indicate that leaked cytochrome C is reduced in the cytosol (183). It is unclear whether Cytochrome c reductase is responsible for the reduction of cytosolic cytochrome c. Yet, since cytochrome c reductase is occupied with PQ and may not perform its work as part of ETC under PQ treatment, the PQ treatment may contribute to the leakage of cytochrome c into the cytosol. The leaked cytosolic cytochrome c can interact with other molecules such as 14-3-3 proteins. 14-3-3 proteins are responsible for binding AKT-phosphorylated proteins such as FOXO transcription factors. The FOXO bound by 14-3-3 proteins is then exported from the nucleus and cannot contribute to the activation of its downstream target genes (184). Recent findings on apoptosis have shown that 14-3-3 proteins can be bound by cytochrome c instead of Apaf-1 (Apoptotic protease activating factor 1) to activate the caspases cascade for apoptosis (185). Such findings suggest that cytochrome c can bind 14-3-3 proteins and make the 14-3-3 target proteins free from the sequester by 14-3-3 protein.

In *C. elegans,* FTT-2 and PAR-5 are the *C. elegans* 14-3-3 protein orthologs. FTT-2, like mammalian 14-3-3 proteins, binds DAF-16, the *C. elegans* FOXO ortholog, and sequesters it in the cytoplasm (186). While mammalian 14-3-3 proteins are known to be bound by cytochrome c, it is not known whether *C. elegans* cytochrome c binds FTT-2 or PAR-5. However, the discovery of the interaction between the mammalian cytochrome c and 14-3-3 proteins suggests the possibility that *C. elegans* cytochrome c may bind FTT-2 and let DAF-16 be free from the sequester by FTT-2. The DAF-16, free from the sequester, then can enter the nucleus and activates it downstream gene such as *gst-4* (75). Thus, PQ treatment in *C. elegans* may cause a malfunction in cytochrome c reductase, causing leakage of cytochrome c from mitochondria into

the cytoplasm. Such leakage then may encourage interaction between *C. elegans* cytochrome c and FTT-2. As a result, DAF-16 may be free from FTT-2 sequester and activate its downstream gene like *gst-4*.

Based on these findings and possibilities, it may be possible that *vab-3(3648)* strains might have had the series of events involving cytochrome c unlike other *vab-3(e648)* strains that were exposed to either As or AC. In other words, even though *vab-3(e648)* strains treated with PQ treatment did not have functional VAB-3 proteins, the strains might have increased expression levels of *gst-4* mRNA due to the increase in DAF-16 that were free from FTT-2 sequester, which was caused by the cytochrome c binding FTT-2. Thus, *vab-3(e648)* strains exposed to PQ treatment may have lower expression levels of *gst-4* mRNA than the wild type but have higher expression levels of *gst-4* mRNA than other *vab-3(e648)* strains that are exposed to either As or Ac.

brap-2(ok1492) mutants have shown increased basal expression levels of *gst-4*. Along with the *gst-4*, other phase II detoxifying genes such as *gsto-2, dhs-8, sdz-8,* and *ugt-13* are also upregulated in the mutants (78). Since a loss of *vab-3* downregulated expression levels of *gst-4* in *brap2(ok1492)* mutants and the wild type under oxidative stress-inducing conditions, I sought to test whether a loss of *vab-3* has effects on expression levels of other phase II detoxifying genes. Several genes were selected to represent a phase II detoxifying enzyme group: *gsto-2, dhs-8, sdz-8* and *ugt-13.* Using qRT-PCR, I have found that *vab-3(e648)* mutants displayed lower expression levels of *sdz-8* and *ugt-13* than the wild type under oxidative stress induced by As treatment. The results indicate that a loss of *vab-3* has a negative impact on expression levels of *sdz-8* and *ugt-13*. In other words, *vab-3* is required for *C. elegans* to express SDZ-8 and UGT-13 enzymes to protect themselves against oxidative stress.

While GST-4 and UGT-13 resolve oxidative stress by removing free radicals through conjugation, SDZ-8, the *C. elegans* CBR3 ortholog, may resolve oxidative stress induced by As in a different way. CBR3 (CarBonyl Reductase 3) is an NADPH (Reduced form of Nicotinamide Adenine Dinucleotide Phosphate) dependant reductase. In other words, CBR3 catalyzes the reduction of carbonyl substrates using NADPH and H^+ (187). Additionally, CRB3 is under the control of Nrf2, the master regulator of phase II detoxifying enzymes (188). Hence, upon oxidative stress induced by As, Nrf2 upregulates expression levels of CRB3 that may resolve oxidative stress by catalyzing the reduction of carbonyl substrates using free radicals produced by As. Thus, SDZ-8, as the *C. elegans* CBR3 ortholog, may resolve oxidative stress induced by As through catalyzing reduction of carbonyl substrates using NADPH and free radicals produced by As.

Unlike *gst-4* or *ugt-13* genes in *vab-3(e648)* strains under the As treatment, expression levels of *gsto-2* in the *vab-3(e648)* strains were not significantly lower than the expression levels of the wild type under the oxidative stress-inducing conditions. Furthermore, the statistical analysis of the results showed no significance. The difference in their roles in resolving oxidative stress induced by As may be the reason why a loss of *vab-3* did not influence *gsto-2* as much as it did to *gst-4* or *ugt-13* expression. GST-4 and UGT-13 work on the radicals through conjugation and remove the free radicals (34,58). GSTO-2 (the *C. elegans* GSTO1 ortholog), however, does not directly work on the radicals.

Detoxification of As in a human body demonstrates how GSTO1 detoxifies As. As is metabolized in a human body through a series of reduction events along with methylation. A job of GSTO1 in the detoxification is to reduce MMA^V (MonoMethylArsonic acid) to MMA^{III} (MonoMethylArsonous acid). These relatively weak toxic molecules can then be excreted

through urines (189–191). Thus, GSTO-2 resolves oxidative stress by reducing the amount of toxic MMA^V in *C. elegans*. In other words, GSTO-2 focuses on removing As itself rather than working on free radicals. Such the difference between GSTO-2 and GST-4 on a method to resolve oxidative stress may explain why they have such a huge gap regarding their expression levels in worms under oxidative stress conditions induced by As.

Since the amount of free radicals produced by As is far greater than the amount of As itself in worms, expression levels of phase II detoxifying enzymes that directly interact with free radicals such as GST-4 would be higher than expression levels of enzymes that interact with As itself like GSTO-2 (58,189–192). These findings lead me to formulate a possible explanation of why a loss of *vab-3* did not impact expression levels of *gsto-2* compared to *gst-4* expression levels under As treatment. A loss of *vab-3* has a huge impact on expression levels of *gst-4* because a *vab-3* gene may affect phase II enzymes that directly work on free radicals only.

The qPCR results showed that expression levels of *gst-4* mRNA in the wild type under As treatment were far greater than the expression levels of *gsto-2* mRNA in the wild type. Such a difference was expected since there were more free radicals than As molecules in worms. Other phase II detoxifying enzymes such as *sdz-8* and *ugt-13* also showed much greater expression levels than expression levels of *gsto-2* in the wild type. On the other hand, expression levels of *gst-4, sdz-8* and *ugt-13* in *vab-3(e648)* strains under As treatment were greatly reduced compared to the wild type. However, *gsto-2* mRNA expression levels in the *vab-3(e648)* strains were like *gsto-2* mRNA expression levels in the wild type. The only difference between GSTO-2 and the other phase II detoxifying enzymes such as GST-4 is that GSTO-2 works on As rather than free radicals. Thus, these findings suggest that a loss of *vab-3* may impact phase II detoxifying enzymes that directly work on free radicals only.

Another gene that was not greatly influenced by a loss of *vab-3* is *dhs-8*, the *C. elegans* WWOX ortholog (78). WWOX enzymes are WW domain-containing oxidoreductases that are related to mitochondria and ROS (193–195). Since WWOX is required to prevent mitochondrial dysfunction and remove free radicals, WWOX may be responsible for removing free radicals derived from mitochondrial dysfunction. Like *gsto-2* mRNA expression levels in the wild type under As treatment, expression levels of *dhs-8* mRNA in the wild type was much lower than expression levels of other phase II detoxifying genes such as *gst-4* or *sdz-8*. Additionally, expression levels of *dhs-8* mRNA in *vab-3(e648)* strains under As treatment were not significantly lower than the expression levels of *dhs-8* in the wild type under As treatment.

These findings leave me to hypothesize that DHS-8 works on free radicals derived from mitochondrial dysfuntion but not the radicals derived from As. The increase in expression levels of *dhs-8* mRNA in the wild type under As treatment may be due to the influence of free radicals derived from As, on mitochondria which may lead to the production of free radicals derived from mitochondrial dysfunction. Hence, DHS-8 may work on the free radicals derived from mitochondrial dysfunction only. Furthermore, such a statement leads me to form a hypothesis where a loss of *vab-3* may influence phase II detoxifying enzymes that work on free radicals in the cytosol but not the free radicals from mitochondrial dysfunction.

Besides phase II detoxifying enzymes, CATs (catalases) are other enzymes that resolve oxidative stress in the cell. CATs reduce ROS levels in the cell by breaking down the hydrogen peroxide into water and oxygen molecules. This process is achieved by electron transfer based oxidation. Like GSTs, expression levels of CATs in the cell have been measured to estimate the degree of oxidative stress and cell responses against the stress. Hence, increased expression levels of CATs in the cell indicates that the cell is under oxidative stress-inducing conditions.

Previously, Hebert-Schuster and *et al.* have reported that overexpressed PAX6 increased the CAT promoter activity (21,33,98). Since VAB-3 is the *C. elegans* ortholog of PAX6 and PAX6 influences the CAT promoter activity, I sought to test whether a loss of *vab-3* has effects on expression levels of human CAT orthologs in *C. elegans*: cytosolic catalase *ctl-1* and peroxisomal catalase *ctl-2* (196,197).

Catalase works on hydrogen peroxide to produce oxygen and water molecules. Thus, the use of chemicals that produce hydrogen peroxide inside worms was required. When the wild type was exposed to As, the worms did not show increased expression levels of *ctl-1* or *ctl-2* mRNA. Such results suggest that As treatment might not induce production of hydrogen peroxide through its known pathways to generate ROS: activating either NADH oxidase or NADPH oxidase in the worms. Thus, I used PQ instead of As to activate CTL-1 and CTL-2 in worms. Using qRT-PCR, I found that both *ctl-1* and *ctl-2* mRNA expression levels in the wild type were increased upon exposure to PQ treatment. As PQ undergoes NADPH mediated redox cycle in the cytosol, the cycle contributes to hydrogen peroxide production in the cytosol. CTL-1, as a cytosolic catalase, works on the hydrogen peroxide from the PQ redox cycle. CTL-2 may also work on the hydrogen peroxide produced from the PQ redox cycle. However, it may work on the hydrogen peroxide close to the cellular membrane only since CTL-2 is a membrane-bound peroxisomal catalase (167–169,196,197). Thus, the increase in *ctl-1* and *ctl-2* mRNA expression in the wild type under PQ treatment was due to the increase in the amount of hydrogen peroxide.

A human cell has both catalase and peroxisome (98,198). While PAX6 is determined to enhance the activity of the CAT promoter by binding the promoter, a relationship between peroxisomes and PAX6 has not been determined yet (98). Interestingly, a loss of *vab-3* decreased expression levels of *ctl-1* significantly under the PQ treatment, while the expression levels of *ctl-*

2 were not significantly reduced in *vab-3(e648)* strains under the PQ treatment. Such results indicate that a *vab-3* gene is required for the expression of *ctl-1* only. In other words, like PAX6, VAB-3 is required for the expression of cytosolic catalases. While we do not know whether PAX6 has any interaction with peroxisomes, the qPCR results suggest that VAB-3 may not be involved in the expression of peroxisomal catalases.

Since the goal of the project was to determine whether the expression of a *vab-3* gene protects *C. elegans* against oxidative stress-inducing conditions, I performed oxidative stress assays involving *vab-3(e648)* mutants and the wild type with *vab-3* RNAi induction. As expected, worms with either *vab-3* mutations or *vab-3* RNAi induction have shown decreased resistance than the wild type against the oxidative stress induced by As. These findings indicate that a *vab-3* gene contributes to the protection against oxidative stress by contributing to the expression of ROS detoxifying enzymes such as phase II detoxifying enzymes and catalases in *C. elegans*.

4.4 Identification of VAB-3 as a transcription factor that enhances the SKN-1 mediated *gst-4* and *skn-1c* promoter activities

SKN-1 has been identified as a master regulator for phase II detoxifying genes. As a transcription factor, SKN-1 recognizes, binds, and activates promoters of its downstream factors (58). For instance, Hu has revealed the effects of SKN-1 on the *gst-4* promoter. Using a luciferase assay, Hu has shown that SKN-1 recognizes the *gst-4* promoter and enhances the promoter activity. Furthermore, she found the transcription factor called ELT-3 that upregulates expression levels of the *gst-4* and dimerizes with SKN-1 to enhance the SKN-1 mediated activation of the *gst-4* promoter (78). Since a *vab-3* gene has shown to upregulate expression

levels of the *gst-4* and is known as a transcription factor, I sought to determine whether VAB-3 influences the *gst-4* promoter activity. I performed luciferase assays and found that VAB-3 could enhance the *gst-4* promoter activity. Additionally, like ELT-3, VAB-3 enhanced the SKN-1 mediated activation of the *gst-4* promoter as well. Interestingly, the relative luciferase activity values from the cells transfected with a combination of SKN-1 and VAB-3 were much greater than values calculated from the simple addition of relative luciferase activity values from the SKN-1 only transfected cells and VAB-3 only transfected cells. In other words, SKN-1 and VAB-3 have shown the synergistic effect not a simple additive effect on the *gst-4* promoter activity. Such a finding was also found with ELT-3 (78). Hence, I determined that VAB-3 is a transcription factor that upregulates the *gst-4* promoter activity and synergistic factor for the SKN-1 mediated activation of the *gst-4* promoter.

Among SKN-1 isoforms, SKN-1C is the main transcription factor that regulates the oxidative stress response. In other words, the activity levels of SKN-1C is directly related to the oxidative stress response. Recent findings on SKN-1C have shown that SKN-1 can transactivate its promoter activity (58,78). As I found that VAB-3 synergistically enhances the SKN-1 mediated activation of the *gst-4* promoter, I tested whether VAB-3 synergistically enhances the SKN-1 mediated activation of the *skn-1c* promoter. Using luciferase assays, I found that not only VAB-3 synergistically enhances the SKN-1 mediated *skn-1c* promoter activity, but also can enhance the *skn-1c* promoter activity without SKN-1. Such a finding indicates that VAB-3 is involved in regulating expressions of ROS detoxifying enzymes and SKN-1C.

4.5 Potential future studies for VAB-3 in *C. elegans*

This study has demonstrated how important VAB-3 is for the oxidative stress response and survival. I have also determined VAB-3 as a transcription factor that enhances the *gst-4* and *skn-1c* promoter activities. However, I have not determined whether VAB-3 directly interacts with the *gst-4* promoter or *skn*-1c promoter. Dozier and Epstein have reported that the consensus PAX6 PD binding sequence has high similarity with VAB-3 binding sequence. Furthermore, upstream sequences of both the *gst-4* and *skn-1* have shown about 50% similarity with the consensus sequence (103,116,117). Thus, direct interaction validation is important to construct a model to demonstrate how VAB-3 influences the promoters. If VAB-3 directly binds the promoters, specifying the sequences of VAB-3 that bind the promoters would be a crucial task to establish the model. One way to determine the interaction would be luciferase assays with either the truncated *gst-4* promoter fused luciferase constructs or truncated VAB-3.

Since VAB-3 has PD and HD for binding DNA, mutating sequences at either HD or PD would show whether these domains are required for the *gst-4* or *skn-1c* promoter interaction (109,112,113). On the other hand, I have tested whether VAB-3 and SKN-1 directly interact. I used Co-IP (Co-immunoprecipitation) mediated luciferase assays to test the interaction. Unfortunately, VAB-3 and SKN-1 did not show any interaction in HEK293T cells. I assume that the interaction between VAB-3 and SKN-1 may require the promoters as a platform to interact with each other. To test this, ChIP (Chromatin immunoprecipitation)-sequencing can be used to determine where on the promoters VAB-3 and SKN-1 interact with the promoters. Such a test would reveal whether the promoters are required for SKN-1 and VAB-3 to work together.

VAB-3 is hypothesized to possess NLS at the N-terminal of the HD for nuclear localization as the N-terminus resembles the SV40 NLS (58,66,74,74,75,114). To observe the

nuclear localization of VAB-3 *in vivo*, a *vab-3* gene can be fused with HaloTag sequences using a CRISPR/Cas9 method to generate *vab-3::halotag* reporter strains (199–201). The reporter strains will show whether VAB-3 is nuclear-localized under oxidative stress-inducing conditions. Moreover, to examine whether VAB-3 nuclear localization is influenced by phosphorylation, *pmk-1* (a human p38 kinase ortholog) or *mpk-1* (a human ERK ortholog) RNAi induction can be applied to *vab-3::halotag* reporter strains under oxidative stress-inducing conditions to test whether a loss of *pmk-1* or *mpk-1* affects nuclear localization of VAB-3.

The Ras and p38 pathways participate in the oxidative stress response through SKN-1 activation in *C. elegans*. Nuclear localization of SKN-1 is essential for the activation of phase II detoxifying enzymes. The regulation of nuclear localization is achieved by kinases like ERK or p38 kinases (58,66,73–75). Interestingly, studies on PAX6 in zebrafish have demonstrated that 413 Ser at the PST domains can be phosphorylated by ERK or p38 kinases. While VAB-3 does not have 413 Ser like zebrafish PAX6, it has 402 Ser and 404 Ser. Additionally, VAB-3 has shown a possibility of having cytoplasmic retention signals at its PST domains at the C-terminal region of the HD as VAB-3 without the PST domains was nuclear localized (108,113). Together, these findings suggest that nuclear localization of VAB-3 may be determined by phosphorylation.

To test whether the PST domains of VAB-3 have a phosphorylation site like zebrafish PAX6, site-directed mutations that target the PST domains, including 402 Ser and 404 Ser, would be applied to *vab-3::halotag* reporter strains. The reporter strains with mutations at the PST domains will be placed under oxidative stress-inducing conditions. After the stress treatment, expression patterns of VAB-3 would be observed. This experiment would reveal

whether VAB-3 with mutations at the PST domains is nuclear-localized during oxidative stress. These experiments will establish a link between VAB-3 and kinases.

The *C. elegans* hermaphrodites have 50 glial cells. Among these glia, 4 glial cells are categorized as CEPsh (CEPhalic sheath) glia that influence CEP dopaminergic sensory dendrites and a neuropil, which is viewed as a brain of the animal (202–204). VAB-3 is required for the development of dorsal and ventral CEPsh glia (205). While VAB-3 is expressed in the glia, SKN-1 is found to be expressed in neurons in lateral, ventral, and dorsal ganglia (206). It is unclear whether VAB-3 is expressed in neurons in these ganglia or SKN-1 is expressed in the glia. However, the synergistic effects observed from the luciferase assays involving *gst-4* and *skn-1c* promoter indicate that VAB-3 and SKN-1 work together *in vitro*. Thus, there is a possibility where VAB-3 and SKN-1 may be expressed in the same cell types.

To test whether VAB-3 and SKN-1 are expressed in same cell types, *ldIs7*[*skn-1b/c::gfp + rol-6*(*su1006*)] strains will be crossed with *vab-3::halotag* reporter strains to generated *ldIs7*[*skn-1b/c::gfp + rol-6*(*su1006*)]*; vab-3::halotag* double mutants (199–201). Observing the double mutants using confocal microscopy would verify whether SKN-1 and VAB-3 are expressed in same cell types. Furthermore, the double mutants can be used to determine whether SKN-1 and VAB-3 are co-localized into the nucleus upon exposure to oxidative-stress inducing conditions. These experiments will provide answers to the possibility of co-expression of SKN-1 and VAB-3 in the same cell types and co-nuclear localization of SKN-1 and VAB-3 under oxidative stress-inducing conditions.

The project presented here sought to determine the role of VAB-3 in the oxidative stress response under acute oxidative stress-inducing conditions. In other words, I did not expose *vab-3(e648)* mutants to chronic oxidative stress-inducing conditions. Recently, chronic acrylamide

exposures have been reported to induce oxidative stress and activate *gst-4* (207). Thus, it would be interesting to determine whether VAB-3 is required to provide resistance to chronic oxidative stress conditions or if the resistance is limited to the acute response.

Conclusion

BRAP2 is a cytoplasmic retention protein involved in regulating cell cycle and tumour suppressor. When its function is lost due to mutation, it results in the increased risk of developing cancer (80,81). In *C. elegans*, BRAP-2 is hypothesized to regulate nuclear localization of SKN-1 via signaling pathways. The upregulation of expressions of phase II detoxifying enzymes in *C. elegans* requires SKN-1 and other transcription factors such as ELT-3 (78). This project has revealed another transcription factor VAB-3 that is required for expressions of phase II detoxifying enzymes and other ROS detoxifying enzymes like catalases in *C. elegans*. A mutation in a *vab-3* gene negatively impacts expression levels of SKN-1 target genes such as *gst-4, sdz-8,* and *ugt-13* and other ROS detoxifying enzymes like *ctl-1,* which are necessary for *C. elegans* to defend itself against oxidative stress (Figure 4.1). While more research is required to determine mechanisms in which VAB-3 is regulated by signaling pathways, the work presented here has identified a new role of VAB-3 in *C. elegans* in the oxidative stress response. Since *C. elegans* has approximately 40% of the genes that are counterparts of human disease genes, findings in this project may provide insight on how PAX6 contributes to oxidative stress response in humans (50). The discovery of new roles of transcription factors allows us to understand how each transcription factor comes together to achieve profound effects in the cell. Learning and constructing models to describe how the massive network of transcription factors works to accomplish effective oxidative stress responses is essential for us to advance our knowledge of aging mechanisms.

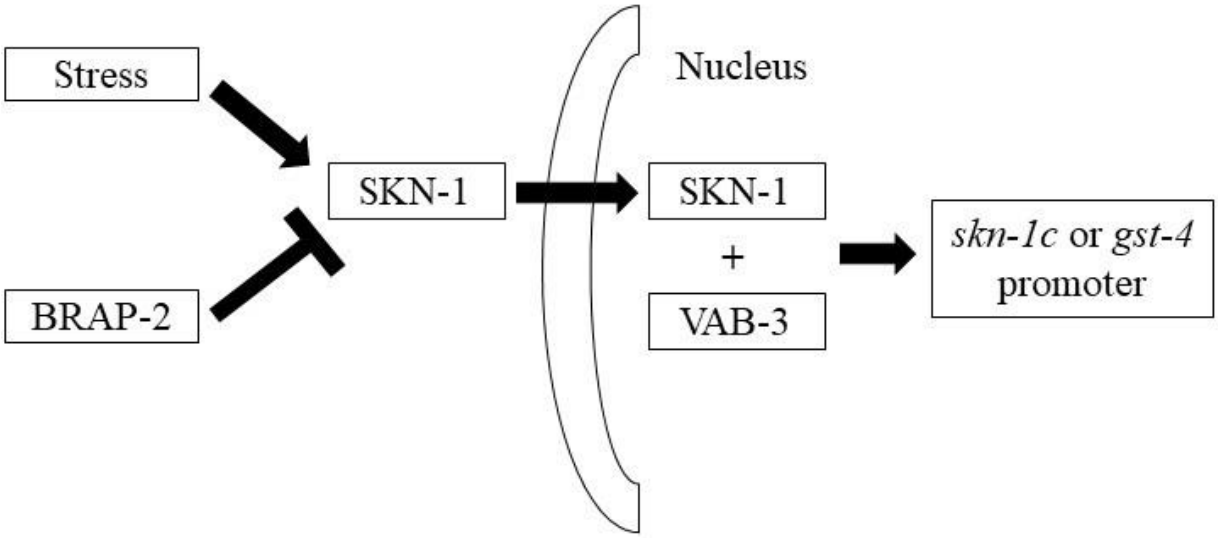

Figure 4. 1 Proposed model of VAB-3 in the regulation of phase II detoxification gene *gst-4*

Induction of oxidative stress promotes phosphorylation and nuclear localization of SKN-1, while BRAP-2 prevents the nuclear localization. Activated SKN-1 upregulates expression levels of *gst-4* or *skn-1c* with VAB-3 at the nucleus. The upregulated expression levels of GST-4 or SKN-1C contribute to the oxidative stress response of *C. elegans*.

References

1. White, M. C. *et al.* Age and Cancer Risk. *Am. J. Prev. Med.* **46,** S7-15 (2014).
2. Guerreiro, R. & Bras, J. The age factor in Alzheimer's disease. *Genome Med.* **7,** (2015).
3. Pagano, G., Ferrara, N., Brooks, D. J. & Pavese, N. Age at onset and Parkinson disease phenotype. *Neurology* **86,** 1400–1407 (2016).
4. Harman, D. Aging: A Theory Based on Free Radical and Radiation Chemistry. *J. Gerontol.* **11,** 298–300 (1956).
5. Harman, D. The Biologic Clock: The Mitochondria? *J. Am. Geriatr. Soc.* **20,** 145–147 (1972).
6. Larsen, P. L. Aging and resistance to oxidative damage in Caenorhabditis elegans. *Proc. Natl. Acad. Sci. U. S. A.* **90,** 8905–8909 (1993).
7. Montecino-Rodriguez, E., Berent-Maoz, B. & Dorshkind, K. Causes, consequences, and reversal of immune system aging. *J. Clin. Invest.* **123,** 958–965 (2013).
8. Van Raamsdonk, J. M. & Hekimi, S. Reactive Oxygen Species and Aging in Caenorhabditis elegans: Causal or Casual Relationship? *Antioxid. Redox Signal.* **13,** 1911–1953 (2010).
9. Schaar, C. E. *et al.* Mitochondrial and Cytoplasmic ROS Have Opposing Effects on Lifespan. *PLOS Genet.* **11,** e1004972 (2015).
10. Yang, W. & Hekimi, S. A Mitochondrial Superoxide Signal Triggers Increased Longevity in Caenorhabditis elegans. *PLOS Biol.* **8,** e1000556 (2010).
11. Halliwell, B. Free radicals and antioxidants: updating a personal view. *Nutr. Rev.* **70,** 257–265 (2012).

12. Finkel, T. & Holbrook, N. J. Oxidants, oxidative stress and the biology of ageing. *Nature* **408,** 239–247 (2000).

13. Covarrubias, L., Hernández-García, D., Schnabel, D., Salas-Vidal, E. & Castro-Obregón, S. Function of reactive oxygen species during animal development: Passive or active? *Dev. Biol.* **320,** 1–11 (2008).

14. Zhang, J. *et al.* ROS and ROS-Mediated Cellular Signaling. *Oxid. Med. Cell. Longev.* **2016,** (2016).

15. Chen, Q. M. *et al.* Molecular analysis of H2O2-induced senescent-like growth arrest in normal human fibroblasts: p53 and Rb control G1 arrest but not cell replication. *Biochem. J.* **332,** 43–50 (1998).

16. Redza-Dutordoir, M. & Averill-Bates, D. A. Activation of apoptosis signalling pathways by reactive oxygen species. *Biochim. Biophys. Acta BBA - Mol. Cell Res.* **1863,** 2977–2992 (2016).

17. Benedetti, M. S. *et al.* Drug metabolism and pharmacokinetics. *Drug Metab. Rev.* **41,** 344–390 (2009).

18. Klotz, L.-O. *et al.* Redox regulation of FoxO transcription factors. *Redox Biol.* **6,** 51–72 (2015).

19. Vomund, S., Schäfer, A., Parnham, M., Brüne, B. & von Knethen, A. Nrf2, the Master Regulator of Anti-Oxidative Responses. *Int. J. Mol. Sci.* **18,** 2772 (2017).

20. Fridovich, I. Superoxide Dismutases. *Annu. Rev. Biochem.* **44,** 147–159 (1975).

21. Glorieux, C. & Calderon, P. B. Catalase, a remarkable enzyme: targeting the oldest antioxidant enzyme to find a new cancer treatment approach. *Biol. Chem.* **398,** 1095–1108 (2017).

22. Xu, C., Li, C. Y.-T. & Kong, A.-N. T. Induction of phase I, II and III drug metabolism/transport by xenobiotics. *Arch. Pharm. Res.* **28,** 249–268 (2005).

23. Bienert, G. P., Schjoerring, J. K. & Jahn, T. P. Membrane transport of hydrogen peroxide. *Biochim. Biophys. Acta* **1758,** 994–1003 (2006).

24. McCord, J. M. & Fridovich, I. The utility of superoxide dismutase in studying free radical reactions. I. Radicals generated by the interaction of sulfite, dimethyl sulfoxide, and oxygen. *J. Biol. Chem.* **244,** 6056–6063 (1969).

25. Fridovich, I. Superoxide Anion Radical ($O_2^{\cdot-}$), Superoxide Dismutases, and Related Matters. *J. Biol. Chem.* **272,** 18515–18517 (1997).

26. Kops, G. J. P. L. *et al.* Forkhead transcription factor FOXO3a protects quiescent cells from oxidative stress. *Nature* **419,** 316–321 (2002).

27. Nemoto, S. & Finkel, T. Redox Regulation of Forkhead Proteins Through a p66shc-Dependent Signaling Pathway. *Science* **295,** 2450–2452 (2002).

28. Brunet, A. *et al.* 14-3-3 transits to the nucleus and participates in dynamic nucleocytoplasmic transport. *J. Cell Biol.* **156,** 817–828 (2002).

29. Guo, S. *et al.* Phosphorylation of serine 256 by protein kinase B disrupts transactivation by FKHR and mediates effects of insulin on insulin-like growth factor-binding protein-1 promoter activity through a conserved insulin response sequence. *J. Biol. Chem.* **274,** 17184–17192 (1999).

30. Murphy, C. T. *et al.* Genes that act downstream of DAF-16 to influence the lifespan of Caenorhabditis elegans. *Nature* **424,** 277–283 (2003).

31. Hrycay, E. G. & Bandiera, S. M. in *Adv. Pharmacol.* (ed. Hardwick, J. P.) **74,** 35–84 (Academic Press, 2015).

32. Zangar, R. C., Davydov, D. R. & Verma, S. Mechanisms that regulate production of reactive oxygen species by cytochrome P450. *Toxicol. Appl. Pharmacol.* **199,** 316–331 (2004).

33. Gonzalez, F. J., Coughtrie, M. & Tukey, R. H. in *Goodman Gilmans Pharmacol. Basis Ther.* (eds. Brunton, L. L., Chabner, B. A. & Knollmann, B. C.) (McGraw-Hill Education, 2015). at <accessmedicine.mhmedical.com/content.aspx?aid=1127865059>

34. Fisher, M. B., Paine, M. F., Strelevitz, T. J. & Wrighton, S. A. The role of hepatic and extrahepatic UDP-glucuronosyltransferases in human drug metabolism. *Drug Metab. Rev.* **33,** 273–297 (2001).

35. Primiano, T., Sutter, T. R. & Kensler, T. W. Antioxidant-inducible genes. *Adv. Pharmacol. San Diego Calif* **38,** 293–328 (1997).

36. Motohashi, H., O'Connor, T., Katsuoka, F., Engel, J. D. & Yamamoto, M. Integration and diversity of the regulatory network composed of Maf and CNC families of transcription factors. *Gene* **294,** 1–12 (2002).

37. Cho, H.-Y., Marzec, J. & Kleeberger, S. R. Functional polymorphisms in Nrf2: implications for human disease. *Free Radic. Biol. Med.* **88,** 362–372 (2015).

38. Katsuoka, F. & Yamamoto, M. Small Maf proteins (MafF, MafG, MafK): History, structure and function. *Gene* **586,** 197–205 (2016).

39. Tebay, L. E. *et al.* Mechanisms of activation of the transcription factor Nrf2 by redox stressors, nutrient cues, and energy status and the pathways through which it attenuates degenerative disease. *Free Radic. Biol. Med.* **88,** 108–146 (2015).

40. Eggler, A. L., Small, E., Hannink, M. & Mesecar, A. D. Cul3-mediated Nrf2 ubiquitination and ARE activation are dependent on the partial molar volume at position 151 of Keap1. *Biochem. J.* **422,** (2009).

41. Zhang, D. D. & Hannink, M. Distinct Cysteine Residues in Keap1 Are Required for Keap1-Dependent Ubiquitination of Nrf2 and for Stabilization of Nrf2 by Chemopreventive Agents and Oxidative Stress. *Mol. Cell. Biol.* **23,** 8137–8151 (2003).

42. Theodore, M. *et al.* Multiple Nuclear Localization Signals Function in the Nuclear Import of the Transcription Factor Nrf2. *J. Biol. Chem.* **283,** 8984–8994 (2008).

43. Huang, H.-C., Nguyen, T. & Pickett, C. B. Phosphorylation of Nrf2 at Ser-40 by Protein Kinase C Regulates Antioxidant Response Element-mediated Transcription. *J. Biol. Chem.* **277,** 42769–42774 (2002).

44. Reddy, N. M. *et al.* PI3K-AKT Signaling via Nrf2 Protects against Hyperoxia-Induced Acute Lung Injury, but Promotes Inflammation Post-Injury Independent of Nrf2 in Mice. *PLoS ONE* **10,** (2015).

45. Yu, R. *et al.* Role of a Mitogen-activated Protein Kinase Pathway in the Induction of Phase II Detoxifying Enzymes by Chemicals. *J. Biol. Chem.* **274,** 27545–27552 (1999).

46. Yu, R. *et al.* Activation of Mitogen-activated Protein Kinase Pathways Induces Antioxidant Response Element-mediated Gene Expression via a Nrf2-dependent Mechanism. *J. Biol. Chem.* **275,** 39907–39913 (2000).

47. Zipper, L. M. & Mulcahy, R. T. Inhibition of ERK and p38 MAP Kinases Inhibits Binding of Nrf2 and Induction of GCS Genes. *Biochem. Biophys. Res. Commun.* **278,** 484–492 (2000).

48. Corsi, A. K. A Biochemist's Guide to C. elegans. *Anal. Biochem.* **359,** 1–17 (2006).

49. Moreno-Arriola, E. *et al.* Caenorhabditis elegans: A Useful Model for Studying Metabolic Disorders in Which Oxidative Stress Is a Contributing Factor. *Oxid. Med. Cell. Longev.* **2014,** (2014).

50. Culetto, E. A role for Caenorhabditis elegans in understanding the function and interactions of human disease genes. *Hum. Mol. Genet.* **9,** 869–877 (2000).

51. Gami, M. S., Iser, W. B., Hanselman, K. B. & Wolkow, C. A. Activated AKT/PKB signaling in C. elegans uncouples temporally distinct outputs of DAF-2/insulin-like signaling. *BMC Dev. Biol.* **6,** 45 (2006).

52. Ahringer, J. Reverse genetics. *WormBook* (2006). doi:10.1895/wormbook.1.47.1

53. Dickinson, D. J. & Goldstein, B. CRISPR-Based Methods for Caenorhabditis elegans Genome Engineering. *Genetics* **202,** 885–901 (2016).

54. Dorman, J. B., Albinder, B., Shroyer, T. & Kenyon, C. The Age-1 and Daf-2 Genes Function in a Common Pathway to Control the Lifespan of Caenorhabditis Elegans. *Genetics* **141,** 1399–1406 (1995).

55. Kenyon, C. The first long-lived mutants: discovery of the insulin/IGF-1 pathway for ageing. *Philos. Trans. R. Soc. B Biol. Sci.* **366,** 9–16 (2011).

56. Hu, P. J. Dauer. *WormBook Online Rev. C Elegans Biol.* 1–19 (2007). doi:10.1895/wormbook.1.144.1

57. Barbieri, M., Bonafè, M., Franceschi, C. & Paolisso, G. Insulin/IGF-I-signaling pathway: an evolutionarily conserved mechanism of longevity from yeast to humans. *Am. J. Physiol.-Endocrinol. Metab.* **285,** E1064–E1071 (2003).

58. Blackwell, T. K., Steinbaugh, M. J., Hourihan, J. M., Ewald, C. Y. & Isik, M. SKN-1/Nrf, stress responses, and aging in Caenorhabditis elegans. *Free Radic. Biol. Med.* **88,** 290–301 (2015).

59. Chávez, V., Mohri-Shiomi, A., Maadani, A., Vega, L. A. & Garsin, D. A. Oxidative Stress Enzymes Are Required for DAF-16-Mediated Immunity Due to Generation of Reactive Oxygen Species by Caenorhabditis elegans. *Genetics* **176,** 1567–1577 (2007).

60. Sun, X., Chen, W.-D. & Wang, Y.-D. DAF-16/FOXO Transcription Factor in Aging and Longevity. *Front. Pharmacol.* **8,** 548 (2017).

61. Schuster, E. *et al.* DamID in C. elegans reveals longevity-associated targets of DAF-16/FoxO. *Mol. Syst. Biol.* **6,** 399 (2010).

62. Hesp, K., Smant, G. & Kammenga, J. E. Caenorhabditis elegans DAF-16/FOXO transcription factor and its mammalian homologs associate with age-related disease. *Exp. Gerontol.* **72,** 1–7 (2015).

63. Lee, M.-H. *et al.* Multiple Functions and Dynamic Activation of MPK-1 Extracellular Signal-Regulated Kinase Signaling in Caenorhabditis elegans Germline Development. *Genetics* **177,** 2039–2062 (2007).

64. Lin, K. T.-H., Broitman-Maduro, G., Hung, W. W. K., Cervantes, S. & Maduro, M. F. Knockdown of SKN-1 and the Wnt effector TCF/POP-1 reveals differences in endomesoderm specification in C. briggsae as compared with C. elegans. *Dev. Biol.* **325,** 296–306 (2009).

65. An, J. H. SKN-1 links C. elegans mesendodermal specification to a conserved oxidative stress response. *Genes Dev.* **17,** 1882–1893 (2003).

66. Okuyama, T. *et al.* The ERK-MAPK Pathway Regulates Longevity through SKN-1 and Insulin-like Signaling in Caenorhabditis elegans. *J. Biol. Chem.* **285,** 30274–30281 (2010).

67. Blackwell, T. K., Bowerman, B., Priess & Weintraub, H. Formation of a monomeric DNA binding domain by Skn-1 bZIP and homeodomain elements. *Science* **266,** 621–628 (1994).

68. Kophengnavong, T., Carroll, A. S. & Blackwell, T. K. The SKN-1 Amino-Terminal Arm Is a DNA Specificity Segment. *Mol. Cell. Biol.* **19,** 3039–3050 (1999).

69. Lo, M.-C., Ha, S., Pelczer, I., Pal, S. & Walker, S. The solution structure of the DNA-binding domain of Skn-1. *Proc. Natl. Acad. Sci. U. S. A.* **95,** 8455–8460 (1998).

70. Rupert, P. B., Daughdrill, G. W., Bowerman, B. & Matthews, B. W. A new DNA-binding motif in the Skn-1 binding domain-DNA complex. *Nat. Struct. Biol.* **5,** 484–491 (1998).

71. Walker, A. K. *et al.* A Conserved Transcription Motif Suggesting Functional Parallels between Caenorhabditis elegans SKN-1 and Cap‘n’Collar-related Basic Leucine Zipper Proteins. *J. Biol. Chem.* **275,** 22166–22171 (2000).

72. Choe, K. P., Przybysz, A. J. & Strange, K. The WD40 Repeat Protein WDR-23 Functions with the CUL4/DDB1 Ubiquitin Ligase To Regulate Nuclear Abundance and Activity of SKN-1 in Caenorhabditis elegans. *Mol. Cell. Biol.* **29,** 2704–2715 (2009).

73. An, J. H. *et al.* Regulation of the Caenorhabditis elegans oxidative stress defense protein SKN-1 by glycogen synthase kinase-3. *Proc. Natl. Acad. Sci. U. S. A.* **102,** 16275–16280 (2005).

74. Inoue, H. *et al.* The C. elegans p38 MAPK pathway regulates nuclear localization of the transcription factor SKN-1 in oxidative stress response. *Genes Dev.* **19,** 2278–2283 (2005).

75. Tullet, J. M. A. *et al.* Direct inhibition of the longevity promoting factor SKN-1 by Insulin-like signaling in C. elegans. *Cell* **132,** 1025–1038 (2008).

76. An, J. H. & Blackwell, T. K. SKN-1 links C. elegans mesendodermal specification to a conserved oxidative stress response. *Genes Dev.* **17,** 1882–1893 (2003).

77. Oliveira, R. P. *et al.* Condition-adapted stress and longevity gene regulation by Caenorhabditis elegans SKN-1/Nrf. *Aging Cell* **8,** 524–541 (2009).

78. Hu, Q., D'Amora, D. R., MacNeil, L. T., Walhout, A. J. M. & Kubiseski, T. J. The Oxidative Stress Response in Caenorhabditis elegans Requires the GATA Transcription Factor ELT-3 and SKN-1/Nrf2. *Genetics* **206,** 1909–1922 (2017).

79. Dingwall, C., Sharnick, S. V. & Laskey, R. A. A polypeptide domain that specifies migration of nucleoplasmin into the nucleus. *Cell* **30,** 449–458 (1982).

80. Fulcher, A. J., Roth, D. M., Fatima, S., Alvisi, G. & Jans, D. A. The BRCA-1 binding protein BRAP2 is a novel, negative regulator of nuclear import of viral proteins, dependent on phosphorylation flanking the nuclear localization signal. *FASEB J.* **24,** 1454–1466 (2010).

81. Asada, M. *et al.* Brap2 Functions as a Cytoplasmic Retention Protein for p21 during Monocyte Differentiation. *Mol. Cell. Biol.* **24,** 8236–8243 (2004).

82. Matheny, S. A. *et al.* Ras regulates assembly of mitogenic signalling complexes through the effector protein IMP. *Nature* **427,** 256–260 (2004).

83. Yoon, S. & Seger, R. The extracellular signal-regulated kinase: multiple substrates regulate diverse cellular functions. *Growth Factors Chur Switz.* **24,** 21–44 (2006).

84. Fatima, S., Wagstaff, K. M., Loveland, K. L. & Jans, D. A. Interactome of the negative regulator of nuclear import BRCA1-binding protein 2. *Sci. Rep.* **5,** (2015).

85. Koon, J. C. & Kubiseski, T. J. Developmental Arrest of Caenorhabditis elegans BRAP-2 Mutant Exposed to Oxidative Stress Is Dependent on BRC-1. *J. Biol. Chem.* **285,** 13437–13443 (2010).

86. Bopp, D., Burri, M., Baumgartner, S., Frigerio, G. & Noll, M. Conservation of a large protein domain in the segmentation gene paired and in functionally related genes of Drosophila. *Cell* **47,** 1033–1040 (1986).

87. Carriere, C. *et al.* Characterization of quail Pax-6 (Pax-QNR) proteins expressed in the neuroretina. *Mol. Cell. Biol.* **13,** 7257–7266 (1993).

88. Martha, A. D., Ferrell, R. E. & Saunders, G. F. Nonsense mutation in the homeobox region of the aniridia gene. *Hum. Mutat.* **3,** 297–300 (1994).

89. Matsuo, T. *et al.* A mutation in the Pax-6 gene in rat small eye is associated with impaired migration of midbrain crest cells. *Nat. Genet.* **3,** 299–304 (1993).

90. Mchedlishvili, L., Epperlein, H. H., Telzerow, A. & Tanaka, E. M. A clonal analysis of neural progenitors during axolotl spinal cord regeneration reveals evidence for both spatially restricted and multipotent progenitors. *Development* **134,** 2083–2093 (2007).

91. Nornes, S. *et al.* Zebrafish contains two Pax6 genes involved in eye development1The sequence reported in this paper has been deposited in the GenBank data base (accession no. AF061252).1. *Mech. Dev.* **77,** 185–196 (1998).

92. Walther, C. & Gruss, P. Pax-6, a murine paired box gene, is expressed in the developing CNS. *Development* **113,** 1435–1449 (1991).

93. Yamashita, W. *et al.* Conserved and divergent functions of Pax6 underlie species-specific neurogenic patterns in the developing amniote brain. *Development* **145,** dev159764 (2018).

94. Kumar, J. P. Retinal Determination: The Beginning of Eye Development. *Curr. Top. Dev. Biol.* **93,** 1–28 (2010).

95. Asami, M. *et al.* The role of Pax6 in regulating the orientation and mode of cell division of progenitors in the mouse cerebral cortex. *Development* **138,** 5067–5078 (2011).

96. Estivill-Torrus, G., Pearson, H., Heyningen, V. van, Price, D. J. & Rashbass, P. Pax6 is required to regulate the cell cycle and the rate of progression from symmetrical to asymmetrical division in mammalian cortical progenitors. *Development* **129,** 455–466 (2002).

97. Turque, N., Plaza, S., Radvanyi, F., Carriere, C. & Saule, S. Pax-QNR/Pax-6, a paired box- and homeobox-containing gene expressed in neurons, is also expressed in pancreatic endocrine cells. *Mol. Endocrinol. Baltim. Md* **8,** 929–938 (1994).

98. Hebert-Schuster, M. *et al.* Catalase rs769214 SNP in elderly malnutrition and during renutrition: Is glucagon to blame? *Free Radic. Biol. Med.* **51,** 1583–1588 (2011).

99. Shukla, S. & Mishra, R. Level of hydrogen peroxide affects expression and sub-cellular localization of Pax6. *Mol. Biol. Rep.* **45,** 533–540 (2018).

100. Xu, P. X. *et al.* Regulation of Pax6 expression is conserved between mice and flies. *Development* **126,** 383–395 (1999).

101. Cvekl, A. & Callaerts, P. PAX6: 25th anniversary and more to learn. *Exp. Eye Res.* **156,** 10–21 (2017).

102. Kissinger, C. R., Liu, B., Martin-Blanco, E., Kornberg, T. B. & Pabo, C. O. Crystal structure of an engrailed homeodomain-DNA complex at 2.8 Å resolution: A framework for understanding homeodomain-DNA interactions. *Cell* **63,** 579–590 (1990).

103. Epstein, J. A. *et al.* Two independent and interactive DNA-binding subdomains of the Pax6 paired domain are regulated by alternative splicing. *Genes Dev.* **8,** 2022–2034 (1994).

104. Jun, S. & Desplan, C. Cooperative interactions between paired domain and homeodomain. *Development* **122,** 2639–2650 (1996).

105. Xu, H. E. *et al.* Crystal structure of the human Pax6 paired domain–DNA complex reveals specific roles for the linker region and carboxy-terminal subdomain in DNA binding. *Genes Dev.* **13,** 1263–1275 (1999).

106. Carriere, C. *et al.* Nuclear localization signals, DNA binding, and transactivation properties of quail Pax-6 (Pax-QNR) isoforms. *Cell Growth Differ.* **6,** 1531 (1995).

107. Tabata, H., Koinui, A., Ogura, A., Nishihara, D. & Yamamoto, H. A novel nuclear localization signal spans the linker of the two DNA-binding subdomains in the conserved paired domain of Pax6. *Genes Genet. Syst.* **93,** 75–81 (2018).

108. Mikkola, I., Bruun, J.-A., Bjørkøy, G., Holm, T. & Johansen, T. Phosphorylation of the Transactivation Domain of Pax6 by Extracellular Signal-regulated Kinase and p38 Mitogen-activated Protein Kinase. *J. Biol. Chem.* **274,** 15115–15126 (1999).

109. Chisholm, A. D. & Horvitz, H. R. Patterning of the Caenorhabditis elegans head region by the Pax-6 family member vab-3. *Nature* **377,** 52 (1995).

110. Zhang, Y. & Emmons, S. W. Specification of sense-organ identity by a Caenorhabditis elegans Pax-6 homologue. *Nature* **377,** 55 (1995).

111. Chamberlin, H. M. & Sternberg, P. W. Mutations in the Caenorhabditis elegans Gene vab-3 Reveal Distinct Roles in Fate Specification and Unequal Cytokinesis in an Asymmetric Cell Division. *Dev. Biol.* **170,** 679–689 (1995).

112. Brandt, J. P. *et al.* Lineage context switches the function of a C. elegans Pax6 homolog in determining a neuronal fate. *Dev. Camb. Engl.* (2019). doi:10.1242/dev.168153

113. Zhang, Y., Ferreira, H. B., Greenstein, D., Chisholm, A. & Emmons, S. W. Regulated nuclear entry of the C. elegans Pax-6 transcription factor. *Mech. Dev.* **78,** 179–187 (1998).

114. Dingwall, C. & Laskey, R. A. Nuclear targeting sequences--a consensus? *Trends Biochem. Sci.* **16,** 478–481 (1991).

115. Meighan, C. M. & Schwarzbauer, J. E. Control of C. elegans hermaphrodite gonad size and shape by vab-3/Pax6-mediated regulation of integrin receptors. *Genes Dev.* **21,** 1615–1620 (2007).

116. Dozier, C., Kagoshima, H., Niklaus, G., Cassata, G. & Bürglin, T. R. The Caenorhabditis elegans Six/sine oculis Class Homeobox Gene ceh-32 Is Required for Head Morphogenesis. *Dev. Biol.* **236,** 289–303 (2001).

117. Cunningham, F. *et al.* Ensembl 2019. *Nucleic Acids Res.* **47,** D745–D751 (2019).

118. Dickinson, R. J. & Keyse, S. M. Diverse physiological functions for dual-specificity MAP kinase phosphatases. *J. Cell Sci.* **119,** 4607–4615 (2006).

119. Cargnello, M. & Roux, P. P. Activation and Function of the MAPKs and Their Substrates, the MAPK-Activated Protein Kinases. *Microbiol. Mol. Biol. Rev. MMBR* **75,** 50–83 (2011).

120. Krens, S. F. G., Spaink, H. P. & Snaar-Jagalska, B. E. Functions of the MAPK family in vertebrate-development. *FEBS Lett.* **580,** 4984–4990 (2006).

121. Brown, M. D. & Sacks, D. B. Protein Scaffolds in MAP Kinase Signalling. *Cell. Signal.* **21,** 462–469 (2009).

122. Lemmon, M. A. & Schlessinger, J. Cell signaling by receptor-tyrosine kinases. *Cell* **141,** 1117–1134 (2010).

123. Karnoub, A. E. & Weinberg, R. A. Ras oncogenes: split personalities. *Nat. Rev. Mol. Cell Biol.* **9,** 517–531 (2008).

124. Udell, C. M., Rajakulendran, T., Sicheri, F. & Therrien, M. Mechanistic principles of RAF kinase signaling. *Cell. Mol. Life Sci.* **68,** 553–565 (2011).

125. Cheung, K. L. *et al.* The Ras GTPase-activating-like Protein IQGAP1 Mediates Nrf2 Protein Activation via the Mitogen-activated Protein Kinase/Extracellular Signal-regulated Kinase (ERK) Kinase (MEK)-ERK Pathway. *J. Biol. Chem.* **288,** 22378–22386 (2013).

126. Tian, H. *et al.* MDA-7/IL-24 inhibits Nrf2-mediated antioxidant response through activation of p38 pathway and inhibition of ERK pathway involved in cancer cell apoptosis. *Cancer Gene Ther.* **21,** 416–426 (2014).

127. Sundaram, M. RTK/Ras/MAPK signaling. *WormBook* (2006). doi:10.1895/wormbook.1.80.1

128. Han, M. & Sternberg, P. W. let-60, a gene that specifies cell fates during C. elegans vulval induction, encodes a ras protein. *Cell* **63,** 921–931 (1990).

129. Chen, Z. & Cobb, M. H. Regulation of Stress-responsive Mitogen-activated Protein (MAP) Kinase Pathways by TAO2. *J. Biol. Chem.* **276,** 16070–16075 (2001).

130. Pearson, G. *et al.* Mitogen-Activated Protein (MAP) Kinase Pathways: Regulation and Physiological Functions. *Endocr. Rev.* **22,** 153–183 (2001).

131. O'neill, L. The Toll/interleukin-1 receptor domain: a molecular switch for inflammation and host defence. *Biochem. Soc. Trans.* **28,** 557–563 (2000).

132. Chen, Z., Hutchison, M. & Cobb, M. H. Isolation of the Protein Kinase TAO2 and Identification of Its Mitogen-activated Protein Kinase/Extracellular Signal-regulated Kinase Kinase Binding Domain. *J. Biol. Chem.* **274,** 28803–28807 (1999).

133. Hutchison, M., Berman, K. S. & Cobb, M. H. Isolation of TAO1, a Protein Kinase That Activates MEKs in Stress-activated Protein Kinase Cascades. *J. Biol. Chem.* **273,** 28625–28632 (1998).

134. Chen, H. H. *et al.* Novel Nrf2/ARE Activator, trans-Coniferylaldehyde, Induces a HO-1-Mediated Defense Mechanism through a Dual p38α/MAPKAPK-2 and PK-N3 Signaling Pathway. *Chem. Res. Toxicol.* **28,** 1681–1692 (2015).

135. Andrusiak, M. G. & Jin, Y. Context Specificity of Stress-activated Mitogen-activated Protein (MAP) Kinase Signaling: The Story as Told by Caenorhabditis elegans. *J. Biol. Chem.* **291,** 7796–7804 (2016).

136. Hers, I., Vincent, E. E. & Tavaré, J. M. Akt signalling in health and disease. *Cell. Signal.* **23,** 1515–1527 (2011).

137. Newton, A. C. & Trotman, L. C. Turning off AKT: PHLPP as a drug target. *Annu. Rev. Pharmacol. Toxicol.* **54,** 537–558 (2014).

138. Webb, A. E. & Brunet, A. FOXO flips the longevity SWItch. *Nat. Cell Biol.* **15,** 444–446 (2013).

139. Bansal, A. *et al.* Transcriptional regulation of Caenorhabditis elegans FOXO/DAF-16 modulates lifespan. *Longev. Heal.* **3,** 5 (2014).

140. Ogg, S. *et al.* The Fork head transcription factor DAF-16 transduces insulin-like metabolic and longevity signals in C. elegans. *Nature* **389,** 994–999 (1997).

141. Hung, W. L., Wang, Y., Chitturi, J. & Zhen, M. A Caenorhabditis elegans developmental decision requires insulin signaling-mediated neuron-intestine communication. *Dev. Camb. Engl.* **141,** 1767–1779 (2014).

142. Paradis, S. & Ruvkun, G. Caenorhabditis elegans Akt/PKB transduces insulin receptor-like signals from AGE-1 PI3 kinase to the DAF-16 transcription factor. *Genes Dev.* **12,** 2488–2498 (1998).

143. Paradis, S., Ailion, M., Toker, A., Thomas, J. H. & Ruvkun, G. A PDK1 homolog is necessary and sufficient to transduce AGE-1 PI3 kinase signals that regulate diapause in Caenorhabditis elegans. *Genes Dev.* **13,** 1438–1452 (1999).

144. Tissenbaum, H. A. & Ruvkun, G. An insulin-like signaling pathway affects both longevity and reproduction in Caenorhabditis elegans. *Genetics* **148,** 703–717 (1998).

145. Cai, B., Chang, S. H., Becker, E. B. E., Bonni, A. & Xia, Z. p38 MAP Kinase Mediates Apoptosis through Phosphorylation of BimEL at Ser-65. *J. Biol. Chem.* **281,** 25215–25222 (2006).

146. Gonzalez, M. & Li, F. DNA replication, RNAi and epigenetic inheritance. *Epigenetics* **7,** 14–19 (2012).

147. Brenner, S. The Genetics of CAENORHABDITIS ELEGANS. *Genetics* **77,** 71–94 (1974).

148. Kay, A. J. & Hunter, C. P. CDC-42 regulates PAR protein localization and function to control cellular and embryonic polarity in C. elegans. *Curr. Biol.* **11,** 474–481 (2001).

149. D'Amora, D. R., Hu, Q., Pizzardi, M. & Kubiseski, T. J. BRAP-2 promotes DNA damage induced germline apoptosis in C. elegans through the regulation of SKN-1 and AKT-1. *Cell Death Differ.* **25,** 1276–1288 (2018).

150. Timmons, L. & Fire, A. Specific interference by ingested dsRNA. *Nature* **395,** 854–854 (1998).

151. Rual, J.-F. *et al.* Toward Improving Caenorhabditis elegans Phenome Mapping With an ORFeome-Based RNAi Library. *Genome Res.* **14,** 2162–2168 (2004).

152. Timmons, L., Court, D. L. & Fire, A. Ingestion of bacterially expressed dsRNAs can produce specific and potent genetic interference in Caenorhabditis elegans. *Gene* **263,** 103–112 (2001).

153. Coolon, J. D., Jones, K. L., Todd, T. C., Carr, B. C. & Herman, M. A. Caenorhabditis elegans Genomic Response to Soil Bacteria Predicts Environment-Specific Genetic Effects on Life History Traits. *PLOS Genet.* **5,** e1000503 (2009).

154. Gracida, X. & Eckmann, C. R. Fertility and Germline Stem Cell Maintenance under Different Diets Requires nhr-114/HNF4 in C. elegans. *Curr. Biol.* **23,** 607–613 (2013).

155. MacNeil, L., Watson, E., Arda, H. E., Zhu, L. J. & Walhout, A. J. M. Diet-Induced Developmental Acceleration Independent of TOR and Insulin in C. elegans. *Cell* **153,** (2013).

156. Maier, W., Adilov, B., Regenass, M. & Alcedo, J. A Neuromedin U Receptor Acts with the Sensory System to Modulate Food Type-Dependent Effects on C. elegans Lifespan. *PLoS Biol.* **8,** (2010).

157. Pang, S. & Curran, S. P. Adaptive capacity to bacterial diet modulates aging in C. elegans. *Cell Metab.* **19,** 221–231 (2014).

158. Soukas, A. A., Kane, E. A., Carr, C. E., Melo, J. A. & Ruvkun, G. Rictor/TORC2 regulates fat metabolism, feeding, growth, and life span in Caenorhabditis elegans. *Genes Dev.* **23,** 496–511 (2009).

159. You, Y., Kim, J., Raizen, D. M. & Avery, L. Insulin, cGMP, and TGF-β Signals Regulate Food Intake and Quiescence in C. elegans: A Model for Satiety. *Cell Metab.* **7,** 249–257 (2008).

160. Xiao, R. *et al.* RNAi interrogation of dietary modulation of development, metabolism, behavior, and aging in C. elegans. *Cell Rep.* **11,** 1123–1133 (2015).

161. Tiwari, B. S., Belenghi, B. & Levine, A. Oxidative Stress Increased Respiration and Generation of Reactive Oxygen Species, Resulting in ATP Depletion, Opening of Mitochondrial Permeability Transition, and Programmed Cell Death. *Plant Physiol.* **128,** 1271–1281 (2002).

162. Housden, B. E. *et al.* Loss-of-function genetic tools for animal models: cross-species and cross-platform differences. *Nat. Rev. Genet.* **18,** 24–40 (2017).

163. Lawson, N. D. Reverse Genetics in Zebrafish: Mutants, Morphants, and Moving Forward. *Trends Cell Biol.* **26,** 77–79 (2016).

164. Schulte-Merker, S. & Stainier, D. Y. R. Out with the old, in with the new: reassessing morpholino knockdowns in light of genome editing technology. *Development* **141,** 3103–3104 (2014).

165. Lynn Shugene, Gurr Jia-Ran, Lai Hsien-Tsung & Jan Kun-Yan. NADH Oxidase Activation Is Involved in Arsenite-Induced Oxidative DNA Damage in Human Vascular Smooth Muscle Cells. *Circ. Res.* **86,** 514–519 (2000).

166. Smith, K. R., Klei, L. R. & Barchowsky, A. Arsenite stimulates plasma membrane NADPH oxidase in vascular endothelial cells. *Am. J. Physiol.-Lung Cell. Mol. Physiol.* **280,** L442–L449 (2001).

167. Bus, J. S. & Gibson, J. E. Paraquat: model for oxidant-initiated toxicity. *Environ. Health Perspect.* **55,** 37–46 (1984).

168. Clejan, L. & Cederbaum, A. I. Synergistic interactions between nadph-cytochrome P-450 reductase, paraquat, and iron in the generation of active oxygen radicals. *Biochem. Pharmacol.* **38,** 1779–1786 (1989).

169. Kato, R., Iwasaki, K. & Noguchi, H. Stimulatory effect of FMN and methyl viologen on cytochrome P-450 dependent reduction of tertiary amine N-oxide. *Biochem. Biophys. Res. Commun.* **72,** 267–274 (1976).

170. Awad, M. E., Abdel-Rahman, M. S. & Hassan, S. A. Acrylamide toxicity in isolated rat hepatocytes. *Toxicol. In Vitro* **12,** 699–704 (1998).

171. Calleman, C. J., Bergmark, E. & Costa, L. G. Acrylamide is metabolized to glycidamide in the rat: evidence from hemoglobin adduct formation. *Chem. Res. Toxicol.* **3,** 406–412 (1990).

172. Dixit, R., Mukhtar, H., Seth, P. K. & Krishna Murti, C. R. Conjugation of acrylamide with glutathione catalysed by glutathione-s-transferases of rat liver and brain. *Biochem. Pharmacol.* **30,** 1739–1744 (1981).

173. Dixit, R., Seth, P. K. & Mukjtar, H. Metabolism of acrylamide into urinary mercapturic acid and cysteine conjugates in rats. *Drug Metab. Dispos.* **10,** 196–197 (1982).

174. Dixit, R., Das, M., Seth, P. K. & Mukhtar, H. Interaction of acrylamide with glutathione in rat erythrocytes. *Toxicol. Lett.* **23,** 291–298 (1984).

175. Dybing, E. & Sanner, T. Risk Assessment of Acrylamide in Foods. *Toxicol. Sci.* **75,** 7–15 (2003).

176. Miller, M. J., Carter, D. E. & Sipes, I. G. Pharmacokinetics of acrylamide in Fisher-334 rats. *Toxicol. Appl. Pharmacol.* **63,** 36–44 (1982).

177. Sumner, S. C., MacNeela, J. P. & Fennell, T. R. Characterization and quantitation of urinary metabolites of [1,2,3-13C]acrylamide in rats and mice using 13C nuclear magnetic resonance spectroscopy. *Chem. Res. Toxicol.* **5,** 81–89 (1992).

178. Tong, G. C., Cornwell, W. K. & Means, G. E. Reactions of acrylamide with glutathione and serum albumin. *Toxicol. Lett.* **147,** 127–131 (2004).

179. Yousef, M. I. & El-Demerdash, F. M. Acrylamide-induced oxidative stress and biochemical perturbations in rats. *Toxicology* **219,** 133–141 (2006).

180. Zhu, Y.-J. *et al.* Effects of acrylamide on the nervous tissue antioxidant system and sciatic nerve electrophysiology in the rat. *Neurochem. Res.* **33,** 2310–2317 (2008).

181. Zhang, Z. *et al.* Electron transfer by domain movement in cytochrome bc 1. *Nature* **392,** 677–684 (1998).

182. Spencer, J. P. E. The interactions of flavonoids within neuronal signalling pathways. *Genes Nutr.* **2,** 257–273 (2007).

183. Ripple, M. O., Abajian, M. & Springett, R. Cytochrome c is rapidly reduced in the cytosol after mitochondrial outer membrane permeabilization. *Apoptosis Int. J. Program. Cell Death* **15,** 563–573 (2010).

184. Manning, B. D. & Cantley, L. C. AKT/PKB Signaling: Navigating Downstream. *Cell* **129,** 1261–1274 (2007).

185. Elena-Real, C. A. *et al.* Cytochrome c speeds up caspase cascade activation by blocking 14-3-3ε-dependent Apaf-1 inhibition. *Cell Death Dis.* **9,** 1–12 (2018).

186. Li, J., Tewari, M., Vidal, M. & Lee, S. S. The 14-3-3 protein FTT-2 regulates DAF-16 in Caenorhabditis elegans. *Dev. Biol.* **301,** 82–91 (2007).

187. López de Cerain, A., Marín, A., Idoate, M. A., Tuñón, M. T. & Bello, J. Carbonyl reductase and NADPH cytochrome P450 reductase activities in human tumoral versus normal tissues. *Eur. J. Cancer* **35,** 320–324 (1999).

188. Cheng, Q., Kalabus, J. L., Zhang, J. & Blanco, J. G. A conserved antioxidant response element (ARE) in the promoter of human carbonyl reductase 3 (CBR3) mediates induction by the master redox switch Nrf2. *Biochem. Pharmacol.* **83,** 139–148 (2012).

189. Rodrigues, E. G. *et al.* GSTO and AS3MT genetic polymorphisms and differences in urinary arsenic concentrations among residents in Bangladesh. *Biomarkers* **17,** 240–247 (2012).

190. Steinmaus, C. *et al.* Individual Differences in Arsenic Metabolism and Lung Cancer in a Case-Control Study in Cordoba, Argentina. *Toxicol. Appl. Pharmacol.* **247,** (2010).

191. Vahter, M. Mechanisms of arsenic biotransformation. *Toxicology* **181–182,** 211–217 (2002).

192. Flora, S. J. S. Arsenic-induced oxidative stress and its reversibility. *Free Radic. Biol. Med.* **51,** 257–281 (2011).

193. Abu-Remaileh, M. & Aqeilan, R. I. Tumor suppressor WWOX regulates glucose metabolism via HIF1α modulation. *Cell Death Differ.* **21,** 1805–1814 (2014).

194. O'Keefe, L. V. *et al.* Drosophila orthologue of WWOX, the chromosomal fragile site FRA16D tumour suppressor gene, functions in aerobic metabolism and regulates reactive oxygen species. *Hum. Mol. Genet.* **20,** 497–509 (2011).

195. Shaukat, Z. *et al.* Chromosomal instability causes sensitivity to metabolic stress. *Oncogene* **34,** 4044–4055 (2015).

196. Petriv, O. I. & Rachubinski, R. A. Lack of Peroxisomal Catalase Causes a Progeric Phenotype in Caenorhabditis elegans. *J. Biol. Chem.* **279,** 19996–20001 (2004).

197. Taub, J. *et al.* Retraction Note to: A cytosolic catalase is needed to extend adult lifespan in C. elegans daf-C and clk-1 mutants. *Nature* **421,** 764–764 (2003).

198. Islinger, M., Voelkl, A., Fahimi, H. D. & Schrader, M. The peroxisome: an update on mysteries 2.0. *Histochem. Cell Biol.* **150,** 443–471 (2018).

199. Fan, X. *et al.* SapTrap Assembly of *Caenorhabditis elegans* MosSCI Transgene Vectors. *G3amp58 GenesGenomesGenetics* **10,** 635–644 (2020).

200. Grimm, J. B. *et al.* A general method to improve fluorophores for live-cell and single-molecule microscopy. *Nat. Methods* **12,** 244–250 (2015).

201. Raiders, S. A., Eastwood, M. D., Bacher, M. & Priess, J. R. Binucleate germ cells in Caenorhabditis elegans are removed by physiological apoptosis. *PLOS Genet.* **14,** e1007417 (2018).

202. Colón-Ramos, D. A., Margeta, M. A. & Shen, K. Glia promote local synaptogenesis through UNC-6 (netrin) signaling in C. elegans. *Science* **318,** 103–106 (2007).

203. Heiman, M. G. & Shaham, S. Ancestral roles of glia suggested by the nervous system of Caenorhabditis elegans. *Neuron Glia Biol.* **3,** 55–61 (2007).

204. Shaham, S. Glia–neuron interactions in the nervous system of Caenorhabditis elegans. *Curr. Opin. Neurobiol.* **16,** 522–528 (2006).

205. Yoshimura, S., Murray, J. I., Lu, Y., Waterston, R. H. & Shaham, S. mls-2 and vab-3 control glia development, hlh-17/Olig expression and glia-dependent neurite extension in C. elegans. *Development* **135,** 2263–2275 (2008).

206. Wilson, M. A. *et al.* skn-1 is required for interneuron sensory integration and foraging behavior in Caenorhabditis elegans. *PLOS ONE* **12,** e0176798 (2017).

207. Hu, Q., D'Amora, D. R., MacNeil, L. T., Walhout, A. J. M. & Kubiseski, T. J. The Caenorhabditis elegans Oxidative Stress Response Requires the NHR-49 Transcription Factor. *G3 GenesGenomesGenetics* **8,** 3857–3863 (2018).

Appendix

Table 1. List of Worm Strains The Caenorhabditis Genetics Center (The University of Minnesota) and the National Bioresource Project (Tokyo, Japan) are the source for strains. Double mutants were created according to the standard single-worm PCR protocol.

Strains	Genotype
N2	Wild Type
CB648	*vab-3(e648)*
CL2166	*dvIS19(gst-4p::gfp)*
DR466	*him-5 (e1490)V*
YF15	*brap-2(ok1492)II*
YF67	*brap-2(ok1492)II; dvIS19(gst-4p::gfp)*
YF211	*brap-2(ok1492)II; vab-3(e648)*
YF212	*dvIS19(gst-4p::gfp); vab-3(e648)*

Table 2. Forward and Reverse Primers for SW-PCR

Gene	Allele	Name	T_m (°C)	Sequence
brap-2	ok1492	ok14925 ok14923B ok14925 ok1492N23	66.8 62.3 62.5 61.1	F: GTCAGCACCGAAAATGTGTCAG R: CAGACAACGTCGAATGATCTC F: GAGTGTATTCGAGTTTGATTCCC R: TTTGTTCTGCCTAGGAATAAGTG

Table 3. List of Forward and Reverse Primers for qRT-PCR

Name	T_m (°C)	Sequence
act-1	63.9 64.1	F: GTCGGTATGGGACAGAAGGA R: GCTTCAGTGAGGAGGACTGG
cdc-42	65.0 65.0	F: TCGACAATTACGCCGTCACA R: AGGCACCCATTTTTCTCGGA
ctl-1	68.4 65.0	F: GTGTCGTTCATGCCAAGGGA R: CCCAGTTACCCTCCTCGGTA
ctl-2	69.2 65.7	F: TCAACCCCGTCAATTCTGGG R: GAGCGAGCCTGTTTCTGGAT
dhs-8	64.2 65.4	F: AAAAGGATCGGGTGGGTACA R: AAACGACATGTGCTCCTGCT
gst-4	64.4 64.0	F: TGCTCAATGTGCCTTACGAG R: AGTTTTTCCAGCGAGTCCAA
gsto-2	66.6 65.5	F: TCCACCAGCTTCAGGAACCA R: TTCCCTCGTCGTGCTCTAGT
sdz-8	64.7 60.4	F: CTGCTGAGGTACGGAACGAA R: TCTGTAFFCGACAACTGGGA
ugt-13	65.0 65.0	F: CCGGATTCCTGGATCGACTG R:TTGTCGCAGTAGTTGGGACC